THE UNIVERSITY OF OKLAHOMA

GRADUATE COLLEGE

ISOTOPIC FRACTIONATION AND ANAEROBIC PHYSIOLOGY OF *n*-ALKANE DEGRADATION BY BACTERIAL ISOLATES AND MIXED COMMUNITIES

A DISSERTATION

SUBMITTED TO THE GRADUATE FACULTY

in partial fulfillment of the requirements for the

Degree of

DOCTOR OF PHILOSOPHY

By

BRANDON E. L. MORRIS
Norman, OK
2011

ISOTOPIC FRACTIONATION AND ANAEROBIC PHYSIOLOGY OF *n*-ALKANE DEGRADATION BY BACTERIAL ISOLATES AND MIXED COMMUNITIES

A DISSERTATION APPROVED FOR THE
DEPARTMENT OF BOTANY AND MICROBIOLOGY

BY

_____
Dr. Joseph M. Suflita, Chair

_____
Dr. Michael J. McInerney

_____
Dr. Paul A. Lawson

_____
Dr. Tyrrell Conway

_____
Dr. Paul F. Cook

Acknowledgements

First and foremost, I would like to gratefully acknowledge the guidance of my advisor Dr. Joseph Suflita and his role in my development as a scientific researcher. I hereby recognize my committee members, Dr. Michael McInerney, Dr. Paul Cook, Dr. Tyrrell Conway, and Dr. Paul Lawson for their support and thoughtful discussions throughout my graduate career at the University of Oklahoma. All of these admirable researchers were principle in helping me develop scientific judgment and the ability to carry out meaningful research. My colleagues in the Suflita lab past and present, including Dr. Lisa Gieg, Dr. Victoria Parisi, Dr. Irene Davidova, Dr. Deniz Aktas, Carolina Berdugo, Margarita Mendivelso, and Chris Lyles deserve recognition for their support and contribution to my skill set, including the ability to investigate anaerobic hydrocarbon degradation, cultivate anaerobic organisms, and develop analytical methods. Roughly two years of my graduate career was spent in collaboration with Dr. Amy Callaghan on annotation of the genome sequence for *Desulfatibacillum alkenivorans* AK-01, an incredibly challenging and rewarding experience. Many thanks to her for discussion and guidance during this endeavor are in order. I would like to express a special thank you to Neil Wofford for his assistance in developing laboratory methods and finding a way to resurrect old instrumentation. Dr. Fares Najar at the OU Advanced Center for Genome Technology assisted in the development of perl scripts to identify relevant information in large amounts of data, and in genome sequencing and

annotation of *Desulfoglaeba alkanexedens*. I would also like to recognize fellow graduate students in the Department of Botany & Microbiology for their camaraderie and scientific interaction during and after normal business hours.

The acknowledgements would not be complete without expressing gratitude to my advisor and mentor during one and a half years in Germany, Dr. Hans-Hermann Richnow. I brought to him knowledge regarding anaerobic physiology and cultivation, and he conferred upon me skills in isotope biogeochemistry and insight into the wonderful utility of isotopes during the study of intricate enzymatic mechanisms and the interplay between microorganisms in complex consortia. Members of the Departments of Isotope Biogeochemistry and Proteomics at the Helmholtz Centre for Environment Research also made me a part of their team and were tremendously helpful on a personal and professional level. Support of other German colleagues including, but not limited to, Dr. Anko Fischer, Dr. Carsten Vogt, Dr. Ivonne Nijenhuis, Dr. Lorenz Adrian, Dr. Martin von Bergen, Dr. Felipe Bastida, and Dr. Jana Seifert for collaboration, research discussion, and use of their lab space(s) is also acknowledged. Penultimately, I would like to thank our dear Dionex machine for many hours of frustration and labor that can only be described as a crash course on ion chromatography and modern instrumentation/software. Perhaps, I will one day put those skills to good use in a laboratory of my own. To conclude, I would like to express earnest recognition to my family for their understanding and *caritas* during the long hours and missed holidays while working towards the realization of this dream.

Table of Contents

List of Tables

List of Figures

Chapter 1 **Page**

Chapter 2

Chapter 3

.

PREFACE

One of the most exciting features of microorganisms is their ability to survive in anaerobic environments. The metabolic features, unique cofactors, and varied terminal electron acceptors used by these unique microorganisms demonstrate novel mechanisms for life and lead to new ideas about our understanding of 'hostile' environments. Indeed, bacteria have been found in areas ranging from the deepest reaches of the ocean to environments at temperatures above 100º C. We now have an understanding of their ability to use sulfurous-, metallic-, or nitrogenous-compounds as terminal electron acceptors. In fact, sulfur and metal chemistry is important for many human physiological processes as well. Nevertheless, the focus of this dissertation is to further characterize the ability of prokaryotic organisms to mineralize hydrocarbons in the absence of molecular oxygen, and to develop diagnostic indicators for this process that can be used to monitor *in situ* activity in the environment.

Hydrocarbons represent the main sources of energy for mankind, and are expected to retain this status for the foreseeable future despite the increasing relevance of alternative energy sources. The realization that bacteria are able to survive in the presence of hydrocarbons happened in the early 20th century, but the mineralization of these compounds was only thought to occur in the presence of oxygen. We now understand not only that anaerobic hydrocarbon biodegradation can occur, but also that this activity affects geochemical changes in petroliferous formations, alters the chemical profile of crude oil, and can increase the overall cost of energy production. Several anaerobic activation

mechanisms for hydrocarbons have been elucidated including addition of a hydrocarbon moiety across the double bond of fumarate, carboxylation, or direct methylation of the C-H bond. Recently, it has even been suggested that nitrite can act as both a terminal electron acceptor and a co-metabolite for *n*-alkane activation in a nitrate-reducing bacterium. Therefore, our understanding of anaerobic processes relating to hydrocarbon degradation and cycling is only in its infancy and new activation strategies may still be discovered. The ability to carry out fumarate addition to *n*-alkanes is dependent upon the presence of an enzyme known as alkylsuccinate synthase. The DNA sequence coding for this enzyme was recently characterized, and several proteins related to the process have been expressed in their inactive form. Questions remain however as to latter steps of the pathway, how these steps are catalyzed, and how anaerobic metabolism of *n*-alkanes affects the overall physiology of other cellular processes on an organismal and community level. These are the questions that I aim to address in this dissertation.

This work is comprised of three chapters, all related to the biodegradation of *n*-alkanes under anoxic conditions. The first chapter uses the concept of stable carbon and hydrogen isotope fractionation, in the context of the Rayleigh model, to compare *n*-alkane activation mechanisms under aerobic and anaerobic conditions. The model aerobic alkane-degrading organism *Pseudomonas putida* was compared to a model sulfate-reducing, alkane-degrading bacterium *Desulfoglaeba alkanexedens* strain ALDC. I found that enrichment factors (ε_{bulk}) during aerobic and anaerobic hydrocarbon mineralization were significantly

different and, when combined with ε_{bulk} values for hydrogen, provided a diagnostic pattern of compound specific isotope enrichment. In collaboration with Dr. Anko Fischer, enrichment factors developed from strain ALDC were used to model alkane biodegradation in a Chinese oil reservoir. I conducted this work in the laboratory of Dr. Hans-Hermann Richnow, at the Helmholtz Centre for Environmental Research (UFZ) in Leipzig, Germany. This chapter was written in the style required by *Applied and Environmental Microbiology*, where it has been submitted as a manuscript. The following chapters are also presented in this format for conformity. Chapter two investigates the physiology of *Desulfoglaeba alkanexedens* by comparing different protein expression profiles during metabolism of butyrate and hexane, respectively. This work was also done while in Germany, in collaboration with Dr. Martin von Bergen at the UFZ. I grew the cultures, extracted the proteins, and performed bioinformatics and data analysis. Dr. von Bergen's group operated the protein mass spectrometer. The genome sequence for strain ALDC was obtained at the OU Advanced Center for Genome Technology in collaboration with Dr. Fares Najar and annotated by myself, using the genome sequence of *Desulfatibacillum alkenivorans* (AK-01) as a scaffold. I was involved in the annotation of the latter organism with Dr. Amy Callaghan at OU. In the second chapter, I present information showing that strain ALDC differentially regulates proteins related to arginine biosynthesis in the presence of *n*-alkanes. Upon my return to the US, I found that amendments of arginine-family amino acids yielded increased rates of sulfate reduction during growth of ALDC on decane. The final chapter extends the information I learned from the

pure culture study of strain ALDC to a model hydrocarbon-degrading, methanogenic consortium. I grew the consortium in the presence of residual oil-bearing sandstone core and quartz sand, and examined the enrichment of ^{13}C in carbon dioxide and methane when grown on several straight-chain fatty acids and *n*-alkanes. Assistance from Dr. Felipe Bastida, at the UFZ, helped me extract proteins from the core and quartz sand respectively, and I compared the protein profiles of the community using ^{13}C-labeled substrates and bioinformatics. This work was conducted in collaboration with both Dr. Hans-Hermann Richnow and Dr. Martin von Bergen. Major findings from chapter 3 are related to the demonstration that carbon sharing is more even in the presence of alkanes than fatty acids, illustrating a greater degree of syntrophy than previously characterized. In fact, it seems that the three pathways for methanogenesis all contribute equally to the overall production of methane in this system. In addition, I found similar proteins related to arginine biosynthesis in ALDC to be differentially expressed in the methanogenic consortium. The implications of these findings in light of the larger anaerobic hydrocarbon degradation story are discussed.

ABSTRACT

In the first chapter, carbon and hydrogen isotope fractionation of *n*-alkanes was examined in order to compare aliphatic hydrocarbon biodegradation under oxic and anoxic conditions. *Desulfoglaeba alkanexedens*, a sulfate-reducing bacterium known to degrade n-alkanes, and *Pseudomonas putida* strain GPo1, an aerobic alkane degrading bacterium, were used as model organisms for the study. Hexane and octane were used as model substrates. Bulk isotope enrichment factors (ε_{bulk}) for carbon and hydrogen under anoxic conditions were respectively, -5.5 ± 0.2‰ and -43.1 ± 6.3‰ for hexane, and -5.2 ± 0.4‰ and -27.8 ± 4.2‰ for octane. The ε_{bulk} for carbon during aerobic hexane biodegradation was -4.3 ± 0.3‰, while hydrogen isotope fractionation was too low for quantification. The correlation of *n*-alkane carbon and hydrogen isotope fractionation ($\Lambda_{reactive}$) for sulfate-reducing conditions was between 9.12± 1.67 and 6.02± 1.37, while the comparable measure for aerobiosis was < 2. We compared our results to carbon and hydrogen isotope values from an oil reservoir and demonstrate how carbon and hydrogen isotope analysis can be used to garner an understanding of *in situ* microbial processes within oil formations and contaminated environments.

The second chapter characterizes a draft genome for *Desulfoglaeba alkanexedens* (strain ALDC) and 3,168,086 base pairs encoding a total of 2,856 protein open reading frames (ORFs) were identified. The G+C content of the sequenced genome is 60.12%. This information was used to conduct a

differential proteomics study of the strain grown separately on butyrate and *n*-decane in order to characterize the physiology of the organism with particular regard to anaerobic *n*-alkane biodegradation. Shotgun proteomics using nano high performance liquid chromatography coupled to an LTQ-Orbitrap mass spectrometer revealed 97 and 75 proteins expressed exclusively under the alkane- and butyrate-growth condition, respectively. Another 217 proteins were common to both growth conditions. The analysis revealed that alkylsuccinate synthase and the proteins associated with the arginine biosynthesis pathway were only expressed in the presence of *n*-alkanes. Higher rates of sulfate reduction were observed during *n*-decane mineralization by the bacterium in the presence of citrulline, ornithine, aspartate, and arginine, relative to the amino acid unamended control. In butyrate-grown cells, butyrate is likely activated to its CoA thioester using acetyl-CoA transferase and subsequently metabolized by a typical complement of β-oxidation proteins. Proteins comprising the flagellar basal body and motor were also differentially detected in butyrate-grown cells. Proteins common to both growth conditions included the sulfate-reducing metabolic machinery, the β-oxidation components, and essential cell-housekeeping complexes including ATP synthases, H^+/Na^+-pumping Rnf-type complexes, and heterodisulfide reductases. *D. alkanexedens* expresses more proteins related to oxygen stress when grown on decane compared to butyrate, apparently reflecting the oxygen-sensitive nature of glycyl-radical enzymes necessary for hydrocarbon metabolism. For example, rubrerythrin and desulfoferredoxin were detected only in alkane-grown cells, and are predicted to

have peroxidase and superoxide reductase activities respectively. The combination of shotgun proteomics coupled with draft genome sequence analysis provided greater insight on the general physiology and regulatory controls of *in situ* metabolic activity in this model *n*-alkane-using, sulfate-reducing bacterium.

The results from the second chapter were expanded to the third chapter to investigate methanogenic degradation of n-alkanes by a microbial enrichment. The contribution of complete and incomplete hydrocarbon mineralization to overall carbon cycling, as well as the role of different methanogenic pathways to overall methane production in these environments is unclear. Carbon flow in a model methanogenic consortium capable of *n*-alkane mineralization was investigated using a combination of proteomics, stable isotope probing, and the degree of $\delta^{13}C$ incorporation in mineralization end products. Results show that ^{13}C from uniformally labeled substrates was distributed evenly among consortium members in the presence of hydrocarbons, and used by a small portion of the community members when provided only in the form of fatty acids. Therefore, syntrophy plays a larger role during the mineralization of hydrocarbons. In addition, patterns of $\delta\ ^{13}C$ enrichment for methane and CO_2 in the presence and absence of hydrocarbons also suggest that complex microbial interactions occur during methanogenic hydrocarbon mineralization. For example, the $\Delta\delta\ ^{13}C$ of CO_2 was statistically identical in all incubations, but the $\Delta\delta\ ^{13}C$ for methane was greater in the presence of hydrocarbons compared to fatty acids alone. In all incubations, aceticlastic and hydrogenotrophic methanogens incorporated ^{13}C

into their proteomes to an equal extent, suggesting that one pathway is not dominant during methanogenic hydrocarbon decay by the model consortium. Stable isotope probing of proteins identified signature enzymes responsible for methanogenesis from CO_2 and acetate labeled with 78.0 ± 4.4 % and 73.3 ± 1.0 % ^{13}C, respectively. A protein capable of catalyzing fumarate addition to a hydrocarbon was not found, despite previous evidence for the presence of genes encoding these enzymes. Five proteins were identified only in the sole presence of hydrocarbons, including a polyphosphate kinase, CheA signal transduction histidine kinase, argininosuccinate lyase, cellulase, and a resolvase-like protein. Collectively, this study suggests that each organism in this enrichment culture fills a unique niche, and may contribute to the capacity for hydrocarbon degradation in ways that are previously unrecognized.

In conclusion, this dissertation provides enrichment factors for *n*-alkane biodegradation and reveals characteristic patterns of compound specific isotope enrichment for mineralized end products during methanogenic hydrocarbon degradation. Both can be used to monitor *in situ* biodegradation on *n*-alkanes without previous knowledge of bacterial species or biodegradation processes at a site of interest. Furthermore, information regarding the proteins expressed during anaerobic alkane mineralization by a model SRB provided new insight into the physiology of this process.

CHAPTER 1

Characterization of Aerobic and Anaerobic *n*-Alkane Biodegradation Using Stable Carbon and Hydrogen Isotope Analysis

Abstract

Carbon and hydrogen isotope fractionation of *n*-alkanes was examined in order to compare aliphatic hydrocarbon biodegradation under oxic and anoxic conditions. *Desulfoglaeba alkanexedens*, a sulfate-reducing bacterium known to degrade n-alkanes, and *Pseudomonas putida* strain GPo1, an aerobic alkane degrading bacterium, were used as model organisms for the study. Hexane and octane were used as model substrates. Bulk isotope enrichment factors (ε_{bulk}) for carbon and hydrogen under anoxic conditions were respectively, -5.5 ± 0.2‰ and -43.1 ± 6.3‰ for hexane, and -5.2 ± 0.4‰ and -27.8 ± 4.2‰ for octane. The ε_{bulk} for carbon during aerobic hexane biodegradation was -4.3 ± 0.3‰, while hydrogen isotope fractionation was too low for quantification. The correlation of *n*-alkane carbon and hydrogen isotope fractionation ($\Lambda_{reactive}$) for sulfate-reducing conditions was between 9.12± 1.67 and 6.02± 1.37, while the comparable measure for aerobiosis was < 2. We compared our results to carbon and hydrogen isotope values from an oil reservoir and demonstrate how carbon and hydrogen isotope analysis can be used to garner an understanding of *in situ* microbial processes within oil formations and contaminated environments.

Introduction

A better understanding of the physiology and biochemistry of anaerobic *n*-alkane degradation in aquifers and oil formations has led to renewed interest in developing quantitative indicators of microbial processes in these environments. Characterizing *in situ* biodegradation activities would not only be important for monitoring alkane loss due to natural attenuation processes at contaminated sites, but can also be used to evaluate the extent of alkane depletion and consequent 'heavy' oil formation in reservoirs (25). Despite the relatively inert chemical nature and highly reduced state of hydrocarbons, it is now clear that these compounds can be degraded under both oxic and anoxic conditions (46). Several enzyme systems have been identified that are capable of oxidizing alkanes under oxic conditions, including soluble and particulate methane monooxygenase (sMMO and pMMO, respectively), cytochrome P450, and alkane ω-monooxygenases. All of these systems catalyze the activation of dioxygen to form alkanols, however the mechanisms and cofactors involved in the reactions vary (61). *Pseudomonas putida* GPo1, previously known as *Pseudomonas oleovorans*, has been used extensively as a model for aerobic alkane degradation initiated by alkane hydroxylases (4, 63). The catalytic subunit of alkane hydroxylase, AlkB, facilitates the terminal oxidation of medium-chain length aliphatic hydrocarbons to primary alcohols while using NADH as a necessary cofactor (31). A wide range of hydrocarbon oxidation has been

observed during *in vivo* and *in vitro* assays (62), but the *n*-alkane substrate range is typically considered to be C_5 to C_{12} (63). However, Johnson and Hyman (28) showed that propane and butane could also be degraded by *P. putida* GPo1 when octane was provided as an additional carbon source.

Conversely, there are a number of strict anaerobes capable of hydrocarbon degradation under sulfate-reducing (1, 8), nitrate-reducing (6), iron(III)-reducing (35) and syntrophic growth conditions (1, 52). One such organism, *Desulfoglaeba alkanexedens*, was isolated from an oily-wastewater storage facility and is capable of degrading hexane, octane, decane, and dodecane completely to CO_2 under sulfate-reducing conditions (11). This organism is one of only eight known sulfate-reducing isolates capable of degrading *n*-alkanes (11, 67). *D. alkanexedens* was the primary member of an enrichment culture first shown to degrade n-alkanes via the fumarate addition mechanism while growing on *n*-dodecane (12, 32), a process characterized in few other sulfate-reducing organisms to date (8). Fumarate addition to a hydrocarbon to form a succinic acid derivative is now known to be a common activating mechanism in anoxic environments for diverse substrate classes including alkyl benzenes, PAHs, alicyclic and n-alkanes, and BTEX-related compounds (40, 68). The glycyl radical enzymes that catalyze the reaction with *n*-alkanes are alkylsuccinate synthases (9), also known as (1-methylalkyl)succinate synthases (24). Currently, researchers have not purified an alkylsuccinate synthase, although cloning and expression of the inactive form of the closely-related benzylsuccinate synthase was successful (33). Such efforts

are complicated in sulfate-reducing bacteria (SRB) due to slow growth rates, low biomass yields, and rapid loss of radical activity in purified extracts (38). Therefore, it would be useful to utilize techniques other than classic protein characterization to garner information about biodegradation rates and biochemical mechanisms of n-alkane activation in these organisms. One technique that has been used successfully to characterize biodegradation pathways and elucidate reaction mechanisms is compound specific stable isotope analysis (CSIA) (40).

CSIA has been used to describe biodegradation of contaminants in groundwater systems (15, 23, 40, 49, 55) and oil reservoirs (20, 56, 64, 69). The Rayleigh equation is applied to quantify the isotope fractionation process and correlate isotope enrichment to the extent of biodegradation (60). Laboratory experiments, where substrate loss is only due to bacterial metabolism, are conducted to quantify the isotopic enrichment during biodegradation by calculating bulk isotopic enrichment factors (ε_{bulk}) that might later be used as a parameter to quantify *in situ* biodegradation in the field. Isotopic fractionation is a result of variations in bond strength between ^{2}H and ^{1}H, and between ^{13}C and ^{12}C containing molecules, and leads to a preferential cleavage of bonds formed with 'light' isotopes and an accumulation of 'heavy' isotope-containing compounds in the residual unreacted substrate fraction over time. Bulk isotopic enrichment factors determined from *in vitro* studies can be applied to environmental samples to resolve rates of biodegradation, or to monitor the loss of substrates via *in situ* microbial activities (17). For the comparison of isotopic fractionation processes

for various compounds, the enrichment factors for the reactive position ($\varepsilon_{reactive}$) can be calculated from the ε_{bulk} values, corrected for 'dilution effects' of heavy isotopes located in non-reactive positions, and used to characterize reaction mechanisms (14). In addition, apparent kinetic isotope effects (AKIE) can be derived from position-specific enrichment values ($\varepsilon_{reactive}$) and compared to kinetic isotope effects (KIE) derived from theoretical modeling approaches (e.g. semi quantitative Steitwieser limits), or the biochemical literature, for the purpose of characterizing specific bond changes during different biochemical pathways (18).

Significant isotope effects are only observed when the primary irreversible step in a biological transformation process is rate limiting and isotopically sensitive (45). Lower AKIE values compared to KIE values from the literature may indicate that rate limiting processes occur prior to or after the isotopically sensitive step (45). Since aliphatic hydrocarbon solubility in water is seriously affected by chain-length, it is likely that bioavailability plays an important role in determining overall biodegradation kinetics, thus reducing the extent of isotopic enrichment in oil reservoirs or contaminated ground water systems in comparison to the isotopic fractionation of the pure biochemical bond cleavage. Bioavailability might also become a rate-limiting step during biodegradation, subsequently decreasing the extent of isotope fractionation (59). However, rate limitations associated with substrate partitioning into the aqueous phase should affect each element of a compound in a similar manner, and measurement of isotopic fractionation for two or more elements in the same compound is suggested to

characterize bond cleavage better than the isotope effect of one element. (14). Therefore, analysis of the carbon and hydrogen isotopic composition of a reactive molecular moiety in a compound might provide unique insight into the study of hydrocarbon degradation in the environment. This concept is called two-dimensional isotope fractionation analysis (TDIFA) and has previously been used to characterize biodegradation of such compounds as benzene, toluene and xylene in pure and mixed cultures (17, 26, 36, 37, 65), as well as methyl *tert*-butyl ether (13, 22, 27, 50).

We determined carbon and hydrogen isotopic fractionation during the biodegradation of hexane and octane by *D. alkanexedens*, and hexane by *P. putida* strain PGo1. Experimentally derived isotopic enrichment factors, AKIEs, and the correlation of *n*-alkane carbon and hydrogen isotope fractionation ($\Lambda_{reactive}$) are compared to other known metabolic pathways initiated by glycyl-radical enzymes and monooxygenases. The isotope data from this study is compared to carbon and hydrogen isotope values from field data to quantify hydrocarbon biodegradation in an oil reservoir using isotopic fractionation concepts.

Materials and Methods

Microorganisms and Media Preparation

Desulfoglaeba alkanexedens strain ALDC was grown anaerobically in an artificial seawater medium (pH 7.2) (66) amended with resazurin to serve as a

redox indicator (1mL of a 0.1% solution L^{-1}). The medium was prepared and dispensed anaerobically (3) into 60mL serum bottles with N_2:CO_2 (4:1) headspace, and sealed with Teflon-lined stoppers and aluminum crimp seals. After autoclaving, sodium bicarbonate (3.0g L^{-1} from a 10% autoclaved stock solution), and 10ml L^{-1} of a vitamin solution (58) were added and the bottles were reduced with cysteine-sulfide (0.05g of each per liter). Each bottle was then inoculated with a nitrogen-flushed syringe. The cultures were grown inverted at 30° C. Finally, hexane and octane were added neat at theoretical starting concentrations of 3mM via calibrated Hamilton™ syringe, although actual concentrations in the aqueous phase would be determined by solubility and incubation temperature. This alkane concentration was used to stoichiometrically monitor alkane degradation via sulfate depletion. Sulfate concentrations were determined by ion chromatography as described previously (7). The stoichiometry of alkane loss was calculated according to previously determined mass balance equations for the SRB used here (11):

$$C_6H_{14} - 4.75SO_4^{2-} + 3.5H^+ \rightarrow 6HCO_3^- + 4.75H_2S + H_2O \quad \text{(eq.1)}$$

$$C_8H_{18} - 6.25SO_4^{2-} + 4.5H^+ \rightarrow 8HCO_3^- + 6.25H_2S + H_2O \quad \text{(eq. 2)}$$

Three replicates were acidified (<pH 2) for each time point when alkane concentrations were at approximately 0, 70, 75, 80, 85, 90, 95, and 99 percent degradation, as calculated by the mass balance of sulfate loss.

Pseudomonas putida strain GPo1 was obtained from the culture collection at the Helmholtz Centre for Environmental Research – UFZ (Leipzig, Germany). Cultures were grown on an orbital shaker at 30℃ in Brunner mineral salt medium

(pH 6.9, DSMZ medium no. 457) supplemented with DSMZ vitamin solution SL-10 (5mL L^{-1}). The medium (30mL) was dispensed aerobically into 120mL serum bottles and closed with Teflon stoppers and aluminum crimp seals. After autoclaving, the headspace was flushed with nitrogen and oxygen (50:50), and the bottles were inoculated. Autoclaved hexane (>97% pure, Sigma-Aldrich, Germany) was added to a theoretical initial concentration of 1mM using a calibrated Hamilton™ syringe. Hexane concentrations were quantified by taking 10µL of headspace and injecting the sample into an Agilent (Agilent Technologies, USA) 7890 GC coupled to a model 5975 MS with an HP-5 column. The GC-MS program was 40℃ isocratic and a split of 1:20 was used. Time points during the degradation were sacrificed by acidifying the medium to below pH 2 with 100µL of 12N hydrochloric acid (Sigma-Aldrich, Germany), the bottles were stored at room temperature until IRMS analysis.

Analytical Instruments and Techniques

Carbon and hydrogen isotope ratios of hexane and octane were determined, by gas chromatography isotope ratio mass spectrometry (GC-IRMS) using a MAT 253 IRMS (Thermo Scientific, Bremen, Germany). The IRMS was coupled to an HP 6890 gas chromatograph (Agilent Technologies, USA) via combustion furnace (GC/C-III, Thermo Scientific, Bremen, Germany) or pyrolysis reactor (GC-pyrolysis, Thermo Scientific, Bremen, Germany) for carbon and hydrogen isotope analysis, respectively (16). Separation of hexane and octane was achieved on a CP-Porabond Q column (50m x 0.32mm x 0.5 μm, Varian

Analytical Instruments, Netherlands) held isocratically at 60° C, a split of 1:10, and a constant flow of helium at 2mL min^{-1}. For carbon and hydrogen isotope ratio analysis of hexane and octane, 10µL and 100µL headspace samples, respectively, were collected using a nitrogen-flushed Hamilton™ syringe and injected manually into the GC.

Delta notation ($\delta^{13}C$ and $\delta^{2}H$) was used to represent the per mil [‰] value for heavy carbon and hydrogen respectively, versus the international standards Vienna Pee Dee Belemnite (V-PBD) for carbon and Vienna Standard Mean Ocean Water (V-SMOW) for hydrogen (10, 21). The δ-values are calculated as:

$$\delta^{13}C_{sample} \quad \text{or} \quad \delta^{2}H_{sample}\ [‰] = \left(\frac{R_{sample} - R_{standard}}{R_{standard}} \right) \cdot 1000 \qquad \text{(eq. 3)}$$

The R_{sample} and $R_{standard}$ notations in equation 3 represent the $^{12}C/^{13}C$- or $^{1}H/^{2}H$-ratios in the sample versus the respective international standard. Uncertainty of analytical isotope measurements was better than 0.05‰ for carbon and 10‰ for hydrogen. Stable carbon isotope enrichment factors (ε_{bulk}) were calculated using the logarithmic form of the Rayleigh equation, such that:

$$\ln\left(\frac{1000 + \delta^{13}C_{o} + \Delta\delta^{13}C}{1000 + \delta^{13}C_{o}}\right) = \left(\frac{\epsilon}{1000}\right) \cdot \ln f \qquad \text{(eq. 4)}$$

where $\delta^{13}C_{o}$ is the initial $\delta^{13}C$ composition of the alkane at time zero in delta notation, and $\Delta\delta^{13}C$ is the change of $\delta^{13}C$ over time. The hydrogen isotopic composition was calculated analogously. The molar fraction of remaining alkane at any given time is represented by the variable f. Values of ε_{bulk} were obtained by calculating the slope of a linear regression line onto a plot comparing changes

in substrate concentration versus changes in isotope ratios. The error of the ε_{bulk} was given as 95% confidence intervals (CI) and determined using a regression analysis as described elsewhere (13).

To normalize the enrichment factor for 'dilution effects' of heavy isotopes in non-reacting positions, a position-specific enrichment factor ($\varepsilon_{reactive}$) can be estimated from the ε_{bulk} using the approximation in equation 5. Position-specific enrichment factors were calculated using the estimate outlined by Elsner *et al*. (14) with the following equation:

$$\epsilon_{reactive} \approx \frac{n}{x} \cdot \epsilon_{bulk} \qquad \text{(eq. 5)}$$

where n is the total number of elements in the molecule at x reactive positions. Hexane and octane have a total carbon number of 6 (n = 6) and of 8 (n = 8). The total hydrogen numbers are 14 for hexane (n =14) and 18 for octane (n =18). Aerobic degradation of *n*-alkanes usually starts by the monohydroxylation of a terminal methyl group (4, 63). Thus, 2 carbon and 6 hydrogen atoms can be expected to be in a reactive position during aerobic hexane and octane biodegradation (x = 2 for carbon, x = 6 for hydrogen). Previous evidence has shown that fumarate addition occurs at the subterminal carbon in larger aliphatic alkanes (32), but has also been shown to occur at the terminal position for propane (30). Therefore, we assume a subterminal fumarate addition for hexane and octane and use x equal to 2 and 4 for carbon and hydrogen, respectively. The uncertainty of $\varepsilon_{reactive}$ was estimated by error propagation:

$$\text{error of } \varepsilon_{\text{reactive}} = \left| \frac{\partial \varepsilon_{\text{reactive}}}{\partial \varepsilon_{\text{bulk}}} \right| \times \text{error of } \varepsilon_{\text{bulk}} \qquad \text{(eq. 6)}$$

For evaluation of reaction mechanisms, apparent kinetic isotope effects (AKIE) for each element (carbon and hydrogen) were calculated according to Elsner *et al*. (14) using the following equation:

$$AKIE = \left(\frac{1}{1 + z \cdot \frac{\epsilon_{reactive}}{1000}} \right) \qquad \text{(eq. 7)}$$

where z is the number of atoms that are in intramolecular competition for reactive positions, and $\varepsilon_{\text{reactive}}$ is the calculated position-specific enrichment factor from approximation 5. For aerobic and anaerobic hexane and octane degradation, all carbon and hydrogen atoms within the reactive positions can be expected to be in intramolecular competition. Hence, z = 2 for carbon and z = 6 for hydrogen was assumed for the terminal monohydroxylation of hexane and octane as well as z = 2 for carbon and z = 6 for hydrogen for the subterminal fumarate addition of hexane and octane. The uncertainty of AKIE was estimated by error propagation:

$$\text{error of AKIE} = \left| \frac{\partial \text{AKIE}}{\partial \varepsilon_{\text{reactive}}} \right| \times \text{error of } \varepsilon_{\text{reactive}} \qquad \text{(eq. 8)}$$

For comparison of reaction mechanisms for hexane and octane, a two-dimensional isotopic approach was carried out. For this purpose, a reactive-position specific value ($\Lambda_{\text{reactive}}$) was obtained that corresponds to the slope of the line from the plot of reactive-position specific changes in hydrogen isotope ratios ($\Delta\delta\ ^{2}H_{\text{reactive}}$) versus reactive-position specific changes in carbon isotope

ratios ($\Delta\delta\ ^{13}C_{reactive}$), using the following approximation based on reactive-position specific carbon and hydrogen isotope enrichment factors ($\varepsilon^{C}_{reactive}$, $\varepsilon^{H}_{reactive}$).

$$\Lambda_{reactive} \approx \frac{\varepsilon^{H}_{reactive}}{\varepsilon^{C}_{reactive}} \qquad \text{(eq. 9)}$$

This value ($\Lambda_{reactive}$) in essence is the isotopic fingerprint of carbon and hydrogen fractionation during alkane biodegradation, and is valuable for comparing the biochemistry of *n*-alkane activation by alkylsuccinate synthase to the activating mechanism of other glycyl radical enzymes, or to aerobic aliphatic hydrocarbon degradation. The uncertainty of $\Lambda_{reactive}$ was estimated by error propagation:

$$\text{error of } \Lambda_{reactive} = \left(\left|\frac{\partial\Lambda_{reactive}}{\partial\varepsilon^{H}_{reactive}}\right| \times \text{error of } \varepsilon^{H}_{reactive}\right) + \left(\left|\frac{\partial\Lambda_{reactive}}{\partial\varepsilon^{C}_{reactive}}\right| \times \text{error of } \varepsilon^{C}_{reactive}\right) \text{(eq. 10)}$$

Results

Carbon Isotope Fractionation

Enrichment factors for carbon isotope fractionation were calculated using the Rayleigh equation, and results are summarized in Table 1. Hexane and octane degradation both showed marked carbon isotope fractionation with ε_{bulk} values of -5.5 ± 0.2‰ and -5.2 ± 0.4‰, respectively, but were not significantly different from one another. $AKIE_c$ values for hexane and octane biodegradation by *D. alkanexedens* were 1.034 ± 0.001 and 1.043 ± 0.004, respectively. The large isotope effect here suggests that the C-H bond cleavage is not significant. Isotope fractionation of carbon was not detected in sterile abiotic controls (data

not shown) and demonstrates that the changes in isotope ratios observed for biotic microcosms are clearly based on biological processes. The Rayleigh equation provided a significant linear fit for the carbon isotope fractionation observed during hexane (N = 6, R^2 = 0.95, *P* value < 0.05) and octane (N = 6, R^2 = 0.99, *P* value < 0.01) biodegradation (Figure 1). Each time point is presented as the grand mean of three replicates, each injected three times, for a total of nine measurements.

Carbon isotope fractionation for *P. putida* GPo1 was investigated for aerobic hexane biodegradation and the bulk enrichment factor (ε_{bulk}) was -4.3 ± 0.3 ‰, resulting in an $AKIE_C$ value of 1.027 ± 0.002 (Table 1). Bouchard *et al*. (5) previously investigated the carbon isotope fractionation for lower molecular weight aliphatic alkanes, and their data has also been provided in Table 1 as a reference. While the bulk isotope enrichment factor calculated for *Pseudomonas putida* GPo1 was higher than most of those obtained from the enrichment culture used by Bouchard *et al*., the AKIE values are very similar to the values from this study and might suggest that the microbial enrichment culture used in their study utilizes a similar mechanism for alkane degradation as strain GPo1, known to degrade *n*-alkanes with alkane hydroxylases.

Hydrogen Isotope Fractionation

Hydrogen isotopic enrichment was calculated according to the Rayleigh equation. Hydrogen ε_{bulk} values for anaerobic hexane and octane degradation by *D. alkanexedens* were -43.1±6.3‰, and -27.8 ± 4.2‰, respectively (Table 1) and

were significantly different from one another. The observed difference in ε_{bulk} for hexane and octane might suggest that the extent of hydrogen isotope fractionation increases for aliphatic hydrocarbons as chain length decreases, as previously shown by others (29). The $AKIE_H$ for anaerobic hexane and octane degradation was 2.526 ± 0.564 and 1.999 ± 0.302 respectively, and is comparable to the $AKIE_H$ value previously observed for anaerobic toluene degradation initiated by fumarate addition (65).

It has been noted that hydrogen isotope fractionation is much stronger under anoxic conditions when compared to the equivalent aerobic degradation (17, 26, 47). To highlight the differences in hydrogen isotope fractionation between aerobic and anaerobic growth conditions, we grew cultures of *P. putida* strain GPo1 under oxic conditions with hexane as the sole energy and carbon source. Isotope fractionation for carbon and hydrogen can be found in Table 1. Hydrogen isotope fractionation observed for *P. putida* GPo1 was below detection limits. The concerted reaction mechanism proposed for alkane hydroxylases might mask hydrogen isotope effects and make isotope fractionation difficult to detect (71). It is also possible that hydrogen abstraction is not the rate-limiting step in aerobic alkane degradation and therefore significant isotope effects would not be expected (70, 71).

Two-dimensional Isotope Fractionation Analysis (TDIFA)

If bioavailability plays a role in determining achievable rates of aliphatic hydrocarbon degradation, it becomes important to quantify the extent of isotope

fractionation for carbon and hydrogen in the parent substrate. This approach would improve the evaluation of isotope effects for degradation pathways that may have been masked by abiotic partitioning behavior (17). The results from the TDIFA approach can be quantified using equation nine. The $\Lambda_{reactive}$ value for hexane and octane degradation by *Desulfoglaeba alkanexedens* under sulfate-reducing conditions was 9.12 ± 1.67 and 6.02 ± 1.37, respectively (Table 1). Since carbon isotope effects for the two substrates were not statistically different, the variability in the observed $\Lambda_{reactive}$ value must be due to the extent of hydrogen isotope fractionation or other factors. A $\Lambda_{reactive}$ value for *P. putida* GPo1 could not be calculated due to the lack of detectable hydrogen isotope fractionation. However, based on the error associated with the measurements and error propagation techniques, we can predict that the $\Lambda_{reactive}$ in this organism would be < 2.

Observed $\Lambda_{reactive}$ values for benzylsuccinate synthase (*bss*) containing organisms exhibited a wide range of variability. This has been interpreted to mean that the reaction mechanism or enzyme involved is slightly variable with respect to substrate binding (the enzyme on-rate) or that different reaction mechanisms exist for the primary step of the degradation pathway (26, 65). This may also be the case for anaerobic *n*-alkane biodegradation, as the hydrogen variability observed in this study for anaerobic hexane and octane decay supports this assumption. In addition, different substrate binding affinities or different degrees of hydrogen tunneling may result in different $\Lambda_{reactive}$ values. Based on the present knowledge, $\Lambda_{reactive}$ values less than two could be

diagnostic of aerobic n-alkane degradation processes and values greater than six could be indicative of anaerobic n-alkane biodegradation. Therefore, TDIFA might be a valuable tool for assessing *in situ* microbial degradation processes involving aliphatic hydrocarbons.

Discussion

Carbon isotope fractionation

Desulfoglaeba alkanexedens uses a fumarate-addition mechanism for the anaerobic activation of aliphatic alkanes (12, 32) and this pathway is initiated by the glycyl-radical containing enzyme alkylsuccinate synthase (9). Therefore, we compared isotopic enrichment factors calculated here to those reported in the literature for other glycyl-radical containing enzymes. Vieth and Wilkes (64) previously described a slightly lower carbon isotope enrichment factor for the nitrate-reducing, n-hexane degrading bacterium HxN1, with ε_{bulk} values of -2.3 ‰ quantified from laboratory incubations. Meckenstock *et al*. (41) first reported isotope enrichment factors for aromatic hydrocarbon degradation by the enzyme benzylsuccinate synthase (Bss), and several studies have subsequently published enrichment factors for the paralogous protein alkylsuccinate synthase (30, 39, 53). For comparing different benzyl- and alkylsuccinate reactions, we used the bulk enrichment factors (ε_{bulk}) to calculate AKIEs, normalized for isotopic atoms in non-reactive positions and intramolecular isotopic competition. The AKIEs from data reported by Morasch *et al.* (42, 43) and Meckenstock *et al*.

(41) revealed that Bss apparent kinetic isotope effects for toluene, xylene, and cresol were relatively close and ranged from 1.011 for *Desulfobacterium cetonicum* degrading *p*-cresol to a maximum of 1.028 for the same organism degrading m-cresol. Herrmann *et al*. (26) also reported $AKIE_C$ values for the same substrates between 1.006 and 1.046, the latter an usually high value seen during the co-metabolic transformation of toluene by a sulfate-reducing consortium. The $AKIE_C$ for anaerobic toluene degradation has previously been investigated under a variety of electron-accepting conditions (23, 42, 65) and found to be within a similar order of magnitude for all conditions. This can be taken to mean that the $AKIE_C$ for toluene is characteristic of the radical cleavage of a carbon-hydrogen bond by enzymes employing a glycyl radical mechanism to activate hydrocarbons. Toluene degradation represents the most-characterized anaerobic hydrocarbon degradation process with regard to isotopic fractionation and biochemical characterization to date, and may cover the range of variability for carbon isotope effects related to C-H bond cleavage for aromatic compounds. Several studies have quantified biologically-mediated carbon isotope fractionation of low molecular weight *n*-alkanes, activated by fumarate-addition, including propane, butane, and pentane (30, 53). Both studies identified metabolites associated with alkane activation via the fumarate-addition mechanism, and Kniemeyer *et al.* (30) noted a bulk enrichment factor (ε_{bulk}) of -5.9 ‰ during propane biodegradation by an enrichment culture, and the unprecedented observation of terminal fumarate addition to the n-alkane chain. Savage et al. demonstrated *n*-propane $\delta^{13}C$ enrichment of 6.7 ‰ and also

detected fumarate-addition products in an enrichment culture originating from a sulfidogenic spring (53).

Lack of detectable hydrogen isotope effects during aerobic n-alkane biodegradation

The lack of a detectable hydrogen isotope effect during aerobic hexane degradation would at first seem to contradict the literature with regard to the present knowledge about the mechanism of alkane monooxygenases (51). However, there is still no consensus on the mechanism of alkane ω-monooxygenases, and different hydrogen isotope effects and rates have been observed to be dependent upon the reacting substrate (2, 19). Knowledge about hydrogen isotopic fractionation comes from mechanistic studies of particulate and soluble methane di-iron, non-heme monooxygenases (pMMO and sMMO, respectively), mainly the 'Bath MMO system' from *Methylococcus capsulatus*, and the heme-containing cytochrome P450 (61). The majority of cases during aerobic alkane oxidation have yielded significant hydrogen isotope effects, however it is important to distinguish between intramolecular and intermolecular isotope effects before coming to a conclusion about our study. Intramolecular isotope effects are those only expressed during the bond cleavage process, while intermolecular isotope effects reflect the whole mechanism including rate-determining steps before the actual bond cleavage (44). There are several studies involving aerobic oxidation of *n*-alkanes and other hydrocarbons that have observed substantial hydrogen intramolecular isotope effects, and low to

non-existent intermolecular isotope effects (34, 48, 54). With our experimental setup, we can measure only intermolecular isotope effects. Therefore, since a significant carbon isotope effect was observed during aerobic alkane degradation with the subsequent lack of a hydrogen isotope effect, we assume that oxygen activation or binding of the activated oxygen species with the enzyme/substrate complex led to greater than expected carbon isotope fractionation. Significant isotope fractionation is only observed during a non-reversible, rate-determining step of an enzymatic reaction. In the case of pMMO, it is known that oxygen activation and not hydrogen abstraction is the rate-determining step during propane degradation (2). Therefore, we hypothesize that hydrogen abstraction is not the rate-limiting step during hexane degradation by *Pseudomonas putida* GPo1, and suggest that the rate-limiting step (oxygen activation or enzyme/substrate binding) contributes to the overall levels of carbon isotope fractionation observed in the course of this study.

Applications to Field Data

To investigate how our isotopic enrichment factors performed in a field scenario, we analyzed a data set consisting of carbon and hydrogen isotope composition of *n*-alkanes undergoing *in situ* biodegradation in a reservoir (57). In this case, oil degradation indicators such as the relative *n*-alkane abundance, the pristine/phytane ratios, the asphaltene percentages, changes in API gravity, along with other parameters of the crude oil were measured. API gravity is a measure defined by the American Petroleum Institute (API) and the National

Institute of Standards and Technology (NIST) used to describe the relative density of petroleum liquids. Carbon ($\delta^{13}C$) and hydrogen ($\delta^{2}H$) isotopic patterns of the whole oil and different *n*-alkane ranged from 14 to 29 carbons were used in an attempt to measure the level of biodegradation. Sun *et al*. (57) observed a maximum increase in $\delta^{13}C$-values of up to 3.8‰ for C_{17} and in $\delta^{2}H$-values of up to 36.9‰ for C_{22}, and concluded that isotopic signatures could be used to assess different levels of biodegradation. With respect to our reference experiments, the pronounced hydrogen isotope fractionation suggests that anaerobic processes govern the development of biodegradation in this reservoir. The percent biodegradation for an observation point (x) in terms of a starting point in time or space (0) can be calculated by

$$B[\%] = \left[1 - \left(\frac{\delta_x + 1000}{\delta_0 + 1000}\right)^{\left(\frac{1000}{\varepsilon}\right)}\right] \times 100 \quad \text{(eq. 11)}$$

Required data are the initial isotope ratio of an individual alkane at a starting point in time or space (δ_0) and the isotope ratio of the remaining individual alkane at a temporal or spatial observation point (δ_x). The initial isotope ratio (δ_0) was given by the carbon isotope signature at location ‘IS005’ (57). The isotope ratios of individual alkanes at the more degraded location ‘IS006‘ were chosen as δ_x values (57).

We first calculated the $\varepsilon_{reactive}$ values from the AKIE obtained from *D. alkanexedens* alkane biodegradation using equation 7 and used these $\varepsilon_{reactive}$ values to calculate ε_{bulk} values according to approximation 5 for the *n*-alkanes (C_{14} – C_{29}) investigated in the case study of Sun *et al*. (57) (Fig. 3). Bulk

enrichment factors are valid for specific substrates and chain lengths only, and this provided us with the information necessary to calculate *in situ* biodegradation of individual alkanes. We assumed that anaerobic alkane degradation was occurring via the fumarate-addition pathway within the reservoir investigated by Sun *et al*. (57). The results from the biodegradation calculations using equation 10 are illustrated in Figure 3. For individual compounds, we calculated a percentage of biodegradation of up to 60-68% for specific alkanes such as *n*-pentadecane, while taking the variability of isotope fractionation of our reference experiments into account. The lowest degradation was calculated for the *n*-C_{29} and was between 13% and 16%. We assume that rate limitations in the reservoir will be similar to rate limitations experienced during the *in vitro* degradation experiments for medium chain-length alkanes although lower bioavailability for higher alkanes was not taken into account (69); thus the numbers reflect the lower boundary for the extent of biodegradation. Although the error of overall calculations can be large and lead to a rough estimate of biodegradation in a particular system, we calculated that total alkane loss in the case study was between 41-48 ± 18.5 %. Predominately non-degraded oil from the source characterized by Sun *et al*. (57) had relative *n*-alkane percentages ranging from 77% in a site with little to no biodegradation to 45% in the most heavily degraded zones of this reservoir. This represents a loss of 32% of the total alkanes in the system, quantified by GC-MS. Our estimate of alkane loss ranging from 41-48 ± 18.5 % is in good accordance with alkane loss quantified by GC-MS (32%). The benefit of using isotope data and enrichment factors in the context of the

Rayleigh model is that baseline levels of expected biodegradation can be identified for individual *n*-alkanes and can be separated from compositional changes of oils related to abiotic loss mechanisms.

During thorough interrogation of oil reservoirs, CSIA could be part of a more extensive site characterization using multiple indicators of hydrocarbon biodegradation such a metabolite profiling, molecular biology tools and cultivation efforts. Once an appropriate isotope enrichment factor for the compound of concern has been developed, it can be applied to other molecules in the compound class, as demonstrated for alkanes in the case study above. The basis of isotopic studies in petroliferous formations rests on the stability of AKIE values for a given activation mechanism such as fumarate addition to the subterminal carbon of *n*-alkanes. As illustrated in figure 3, the ε_{bulk} value decreases with increasing alkane chain length but the $AKIE_c$ value is constant over the entire chain length range, from C_6 to C_{29}. It is therefore important to develop bulk enrichment factors from biochemically well-characterized strains in order to establish a sound basis for the extension of calculated isotopic enrichment factors to the environment.

Acknowledgments

We sincerely thank Ursula Günther and Dr. Matthias Gehre for technical support in the isotope laboratory, and Dr. Carsten Vogt for fruitful discussions. In addition, we thank Dr. John Groves for helpful comments and suggestions with

regard to data interpretation. B. E. L. Morris was supported by a European Union Marie Curie Early-Stage Training Fellowship (AXIOM, contract N°MEST-CT-2004-8332) and by a grant from the State Ministry of Science and Art (SMWK), in the Free State of Saxony, Germany (Fellowship N°4- 7531.50-04-840-09/5).

Literature Cited

1. **Aeckersberg, F., F. Bak, and F. Widdel.** 1991. Anaerobic oxidation of saturated hydrocarbons to CO2 by a new type of sulfate-reducing bacterium. Arch. Microbiol. **156:**5-14.

2. **Austin, R. N., K. Luddy, K. Erickson, M. Pender-Cudlip, E. M. Bertrand, D. Deng, R. S. Buzdygon, J. B. van Beilen, and J. T. Groves.** 2008. Cage escape competes with geminate recombination during alkane hydroxylation by the diiron oxygenase *AlkB*. Agnew. Chem. Int. Ed. **47:**5232-5234.

3. **Balch, W. E., G. E. Fox, L. J. Magrum, C. R. Woese, and R. S. Wolfe.** 1979. Methanogens: reevaluation of a unique biological group. Microb. Rev. **43:**260-296.

4. **Baptist, J. N., R. K. Gholson, and M. J. Coon.** 1963. Hydrocarbon oxidation by a bacterial enzyme system: I. Products of octane oxidation. Biochimica et Biophysica Acta **69:**40-47.

5. **Bouchard, D., D. Hunkeler, and P. Hoehener.** 2008. Carbon isotope fractionation during aerobic biodegradation of n-alkanes and aromatic compounds in unstaturated sand. Organ. Geochem. **39:**23-33.

6. **Burland, S. M., and E. A. Edwards.** 1999. Anaerobic Benzene Biodegradation Linked to Nitrate Reduction. Appl. Environ. Microbiol. **65:**529-533.

7. **Caldwell, M. E., R. M. Garrett, R. C. Prince, and J. M. Suflita.** 1998. Anaerobic biodegradtion of long-chain *n*-alkanes under sulfate-reducing conditions. Environ Sci Technol **32:**2191-2195.

8. **Callaghan, A. V., L. M. Gieg, K. G. Kropp, J. M. Suflita, and L. Y. Young.** 2006. Comparison of mechanisms of alkane metabolism under sulfate-reducing conditions among two bacterial isolates and a bacterial consortium. Appl. Environ. Microb. **72:**4274-4282.

9. **Callaghan, A. V., B. Wawrik, S. M. Ni Chadhain, L. Y. Young, and G. J. Zylstra.** 2008. Anaerobic alkane-degrading strain AK-01 contains two alkylsuccinate synthase genes. Biochem. Bioph. Res. Co. **366:**142-148.

10. **Coplen, T. B., W. A. Brand, M. Gehre, M. Groning, H. A. J. Meijer, B. Toman, and R. M. Verkouteren.** 2006. New guidelines for delta C-13 measurements. Anal. Chem. **78**.

11. **Davidova, I. A., K. E. Duncan, O. K. Choi, and J. M. Suflita.** 2006. *Desulfoglaeba alkanexedens* gen. nov., sp. nov., an *n*-alkane-degrading, sulfate-reducing bacterium. Int. J. Syst. Evol. Micr. **56:**2737-2742.

12. **Davidova, I. A., L. M. Gieg, M. A. Nanny, K. G. Kropp, and J. M. Suflita.** 2005. Stable isotope studies of *n*-alkane metabolism by a sulfate-reducing bacterial enrichment culture. Appl. Environ. Microb. **71:**8174-8182.

13. **Elsner, M., J. McKelvie, G. L. Couloume, and B. Sherwood-Lollar.** 2007. Insight into methyl tert-butyl ether (MTBE) stable isotope fractionation from abiotic reference experiments. Environ. Sci. Technol. **41:**5693-5700.

14. **Elsner, M., L. Zwank, D. Hunkeler, and R. P. Schwarzenbach.** 2005. A new concept linking observable stable isotope fractionation to transformation pathways of organic pollutants. Environ. Sci. Technol. **39:**6896-6916.

15. **Fischer, A., J. Bauer, R. U. Meckenstock, W. Stichler, C. Griebler, P. Maloszewski, M. Kastner, and H. H. Richnow.** 2006. A Multitracer Test Proving the Reliability of Rayleigh Equation-Based Approach for Assessing Biodegradation in a BTEX Contaminated Aquifer. Environmental Science & Technology **40:**4245-4252.

16. **Fischer, A., M. Gehre, J. Breitfeld, H. H. Richnow, and C. Vogt.** 2009. Carbon and hydrogen isotope fractionation of benzene biodegradation under sulfate-reducing condtions: A laboratory to field site approach. Rapid Comm. Mass Spec. **23**.

17. **Fischer, A., I. Herklotz, S. Herrmann, M. Thullner, S. A. B. Weelink, A. Stams, J. M., M. Schloemann, H.-H. Richnow, and C. Vogt.** 2008. Combined carbon and hydrogen isotope fractionation investigations for elucidating benzene biodegradation pathways. Environ. Sci. Technol. **42:**4356-4363.

18. **Fischer, A., S. Weber, A.-K. Reineke, J. Hollender, and H. H. Richnow.** 2010. Carbon and hydrogen isotope fractionation during anaerobic quinoline degradation. Chemosphere **81**.

19. **Fu, H., M. Newcomb, and C.-H. Wong.** 1991. Pseudomonas oleovorans monooxygenase catalyzed asymmetric epoxidation of allyl alcohol derivatives with hydroxylation of a hypersensitive radical probe with the radical ring opening rate exceeding the oxygen rebound rate. J. Am. Chem. Soc. **113:**5878-5880.

20. **George, S. C., C. J. Boreham, S. A. Minifie, and S. C. Teerman.** 2002. The effect of minor to moderate biodegradation on C5 to C9 hydrocarbons in crude oils. Organic Geochemistry **33:**1293-1317.

21. **Gonfiantini, R., W. Stichler, and K. Rozanski.** 1995. Standards and intercomparison materials for stable isotopes of light elements. International Atomic Energy Agency**:**13-29.

22. **Gray, J. R., G. Lacrampe-Couloume, D. Gandhi, K. M. Scow, R. D. Wilson, D. M. Mackay, and B. Sherwood Lollar.** 2002. Carbon and Hydrogen Isotopic Fractionation during Biodegradation of Methyl tert-Butyl Ether. Environmental Science & Technology **36:**1931-1938.

23. **Griebler, C., M. Safinowski, A. Vieth, H. H. Richnow, and R. U. Meckenstock.** 2003. Combined Application of Stable Carbon Isotope Analysis and Specific Metabolites Determination for Assessing In Situ Degradation of Aromatic Hydrocarbons in a Tar Oil-Contaminated Aquifer. Environmental Science & Technology **38:**617-631.

24. **Grundmann, O., A. Behrends, R. Rabus, J. Amann, T. Halder, J. Heider, and F. Widdel.** 2008. Genes encoding the candidate enzyme for anaerobic activation of *n*-alkanes in the denitrifying bacterium, strain HxN1. Environ. Microbiol. **10:**376-385.

25. **Head, I. M., D. M. Jones, and S. R. Larter.** 2003. Biological activity in the deep subsurface and the origin of heavy oils. Nature **426:**344-352.

26. **Herrmann, S., C. Vogt, A. Fischer, A. Kuppardt, and H. H. Richnow.** 2009. Characterization of anaerobic xylene biodegradtion by two-dimensional isotope fractionation analysis. Environ Microbiol Rep.

27. **Jechalke, S., M. Rosell, P. M. Martinez-Lavanchy, P. Perez-Leiva, T. Rohwerder, C. Vogt, and H. H. Richnow.** 2010. Linking low stable isotope fractionation to expression of the cytochrome P450 monooxygenase encoding *ethB* gene for proving MTBE biodegradation in aerated treatment pond systems. Appl Environ Micro **doi:10.1128/AEM.01698-10**.

28. **Johnson, E. L., and M. R. Hyman.** 2006. Propane and *n*-butane oxidation by *Pseudomonas putida* GPo1. Appl Environ Micro **72:**950-952.

29. **Kinnaman, F. S., D. L. Valentine, and S. C. Tyler.** 2007. Carbon and hydrogen isotope fractionation associated with the aerobic microbial oxidation of methane, ethane, propane, and butane. Geo. Cosmo. Acta **71:**271-283.

30. **Kniemeyer, O., F. Musat, S. M. Sievert, K. Knittel, H. Wilkes, M. Blumenberg, W. Michaelis, A. Classen, C. Bolm, S. B. Joye, and F. Widdel.** 2007. Anaerobic oxidation of short-chain hydrocarbons by marine sulphate-reducing bacteria. Nature **449:**898-902.

31. **Kok, M., R. Oldenhuis, M. P. G. van der Linden, P. Raatjes, J. Kingma, P. H. van Lelyveld, and B. Witholt.** 1989. The Pseudomonas oleovorans alkane hydroxylase gene. J. Biol. Chem. **264:**5435-5441.

32. **Kropp, K. G., I. A. Davidova, and J. M. Suflita.** 2000. Anaerobic oxidation of n-dodecane by an addition reaction in a sulfate-reducing bacterial enrichment culture. Appl. Environ. Microb. **66:**5393-5398.

33. **Li, L., D. P. Patterson, C. C. Fox, B. Lin, P. W. Coschigano, and E. N. G. Marsh.** 2009. Subunit structure of benzylsuccinate synthase. Biochemistry **48:**1284-1292.

34. **Liu, K. E., C. C. Johnson, M. Newcomb, and S. J. Lippard.** 1993. Radical clock substrate probes and kinetic isotope effect studies of the hydroxylation of hydrocarbons by methane monooxygenase. J. Am. Chem. Soc. **115:**939-947.

35. **Lovley, D. R., J. C. Woodward, and F. H. Chapelle.** 1994. Stimulated anoxic biodegradation of aromatic hydrocarbons using Fe(III) ligand. Nature **370:**128-131.

36. **Mancini, S. A., C. E. Devine, M. Elsner, M. E. Nandi, A. C. Ulrich, E. A. Edwards, and B. Sherwood Lollar.** 2008. Isotopic Evidence Suggests Different Initial Reaction Mechanisms for Anaerobic Benzene Biodegradation. Environmental Science & Technology **42:**8290-8296.

37. **Mancini, S. A., S. K. Hirschorn, M. Elsner, G. Lacrampe-Couloume, B. E. Sleep, E. A. Edwards, and B. Sherwood Lollar.** 2006. Effects of trace element concentration on enzyme controlled stable isotope fracationation during aerobic biodegredation of toluene. Environ. Sci. Technol. **40:**7675-7681.

38. **Marsh, E. N. G., M. S. Huhta, and A. Patwardhan.** 2004. S-Adenosylmethionine radical enzymes. Bioorg. Chem. **32:**326-340.

39. **Mastalerz, V., G. J. de Lange, and A. Daehlmann.** 2009. Differential aerobic and anaerobic oxidation of hydrocarbon gases discharged at mud volcanoes in the Nile deep-sea fan. Geo. Cosmo. Acta **73:**3849-3863.

40. **Meckenstock, R. U., B. Morasch, C. Griebler, and H. H. Richnow.** 2004. Stable isotope fractionation analysis as a tool to monitor biodegradation in contaminated acquifers. Journal of Contaminant Hydrology **75:**215-255.

41. **Meckenstock, R. U., B. Morasch, R. Warthmann, B. Schink, E. Annweiler, W. Michaelis, and H. H. Richnow.** 1999. 13C/12C isotope fractionation of aromatic hydrocarbons during microbial degradation. Environmental Microbiology **1:**409-414.

42. **Morasch, B., H. H. Richnow, B. Schink, and R. U. Meckenstock.** 2001. Stable Hydrogen and Carbon Isotope Fractionation during Microbial Toluene Degradation: Mechanistic and Environmental Aspects. Appl Environ Micro **67:**4842-4849.

43. **Morasch, B., H. H. Richnow, A. Vieth, B. Schink, and R. U. Meckenstock.** 2004. Stable Isotope Fractionation Caused by Glycyl Radical Enzymes during Bacterial Degradation of Aromatic Compounds. Appl Environ Micro **70:**2935-2940.

44. **Nelson, S. D., and W. F. Trager.** 2003. The use of deuterium isotope effects to probe the active site properties, mechanism of cytochrome P450-catalyzed reactions, and mechanisms of metabolically dependent toxicity. Drug Metab. Dispos. **31:**1481-1498.

45. **Northrop, D. B.** 1981. The expression of isotope effects on enzyme-catalyzed reactions. Ann. Rev. Biochem. **50:**103-131.

46. **Ollivier, B., and M. Magot (ed.).** 2005. Petroleum Microbiology. ASM Press.

47. **Pond, K. L., Y. Huang, Y. Wang, and C. F. Kulpa.** 2002. Hydrogen Isotopic Composition of Individual n-Alkanes as an Intrinsic Tracer for Bioremediation and Source Identification of Petroleum Contamination. Environmental Science & Technology **36:**724-728.

48. **Rataj, M. J., J. E. Kauth, and M. I. Donnelly.** 1991. Oxidation of deuterated compounds by high specific activity methane monooxygenase from *Methylosinus trichosporium*. J. Biol. Chem. **266:**18684-18690.

49. **Richnow, H. H., E. Annweiler, W. Michaelis, and R. U. Meckenstock.** 2003. Microbial in situ degradation of aromatic hydrocarbons in a contaminated aquifer monitored by carbon isotope fractionation. Journal of Contaminant Hydrology **65:**101-120.

50. **Rosell, M., D. Barcelo, T. Rohwerder, U. Breuer, M. Gehre, and H. H. Richnow.** 2007. Variations in 13C/12C and D/H Enrichment Factors of Aerobic Bacterial Fuel Oxygenate Degradation. Environmental Science & Technology **41:**2036-2043.

51. **Rozhkova-Novosad, E. A., J.-C. Chae, G. J. Zylstra, E. M. Bertrand, M. Alexander-Ozinskas, D. Deng, L. A. Moe, J. B. van Beilen, M. Danahy, J. T. Groves, and R. N. Austin.** 2007. Profiling mechanisms of alkane hydroxylase activity in vivo using the diagnostic substrate norcarane. Chem. Biochem. **14:**165-172.

52. **Safinowski, M., C. Griebler, and R. U. Meckenstock.** 2006. Anaerobic Cometabolic Transformation of Polycyclic and Heterocyclic Aromatic

Hydrocarbons: Evidence from Laboratory and Field Studies. Envron Sci Technol **40:**4165-4173.

53. **Savage, K. N., L. R. Krumholz, L. M. Gieg, V. A. Parisi, J. M. Suflita, J. Allen, R. P. Philp, and M. S. Elshahed.** 2010. Biodegrdation of low-molecular weight alkanes under mesophilic, sulfate-reducing conditions: metabolitic intermediates and community patterns. FEMS Microb. Ecol. **72:**485-495.

54. **Shimoda, M., and I. Okura.** 1992. Further study on the reaction mechanism of propane hydroxylation with *Methylosinus trichosporium*. J. Mol. Catal. **72:**263-267.

55. **Steinbach, A., R. Seifert, E. Annweiler, and W. Michaelis.** 2003. Hydrogen and Carbon Isotope Fractionation during Anaerobic Biodegradation of Aromatic Hydrocarbons: A Field Study. Environmental Science & Technology **38:**609-616.

56. **Strapoc, D., M. Mastalerz, C. Eble, and A. Schimmelmann.** 2007. Characterization of the origin of coalbed gases in southeastern Illinois Basin by compound-specific carbon and hydrogen stable isotope ratios. Organ. Geochem. **38:**267-287.

57. **Sun, Y., Z. Chen, S. Xu, and P. Cai.** 2005. Stable carbon and hydrogen isotopic fractionation of individual n-alkanes accompanying biodegradation: evidence from a group of progressively biodegraded oils. Organic Geochemistry **36:**225-238.

58. **Tanner, R. S.** 1997. Cultivation of bacteria and fungi, p. 52-60. *In* C. J. Hurst, G. R. Knudsen, M. J. McInerney, L. D. Stetzenbch, and M. V. Walter (ed.), Manual of Environmental Microbiology. American Society for Microbiology, Washington D.C.

59. **Thullner, M., M. Kampara, H. H. Richnow, H. Harms, and L. Y. Wick.** 2008. Impact of bioavailability restrictions on microbially induced stable isotope fractionation. 1. Theoretical calculation. Environ Sci Technol **42:**6544-6551.

60. **Thullner, M., H. H. Richnow, and A. Fischer.** 2009. Characterization and quantification of in situ biodegradation of groundwater contaminants using stable isotope fractionation analysis: Advantages and limitations, p. 41-81. *In* D. Gallo and R. Mancini (ed.), Environmental and Regional Air Pollution. Nova Science Publishers, Hauppauge, NY.

61. **van Beilen, J. B., and E. G. Funhoff.** 2007. Alkane hydroxylases involved in microbial alkane degradation. Appl Microbiol Biotechnol **74:**13-21.

62. **van Beilen, J. B., J. Kingma, and B. Witholt.** 1994. Substrate specificity of the alkane hydroxylase of Pseudomonas putida GPo1. Enzyme Microb. Technol. **16**.

63. **van Beilen, J. B., M. G. Wubbolts, and B. Witholt.** 1994. Genetics of alkane oxidation by *Pseudomonas oleovorans*. Biodegradation **5:**161-174.

64. **Vieth, A., and H. Wilkes.** 2006. Deciphering biodegradation effects on light hydrocarbons in crude oils using their stable carbon isotopic composition: A case study from the Gullfaks oil field, offshore Norway. Geo. Cosmo. Acta **70:**651-665.

65. **Vogt, C., E. Cyrus, I. Herklotz, D. Schlosser, A. Bahr, S. Herrmann, H.-H. Richnow, and A. Fischer.** 2008. Evaluation of toluene degradation pathways by two-dimensional stable isotope fractionation. Environ. Sci. Technol. **42:**7793-7800.

66. **Widdel, F., and F. Bak.** 1992. Gram-negative mesophilic sulfate-reducing bacteria, p. 3352-3378. *In* A. Balows, H. G. Trueper, M. Dworkin, W. Harder, and K. H. Schleifer (ed.), The Prokaryotes, vol. 4. Springer, New York.

67. **Widdel, F., and O. Grundmann.** 2010. Biochemistry of the anaerobic degradation of non-methane alkanes, p. 909-924. *In* K. N. Timmis, T. McGenity, J. R. van der Meer, and V. de Lorenzo (ed.), Handbook of Hydrocarbon and Lipid Microbiology. Springer-Verlag, Berlin.

68. **Widdel, F., and R. Rabus.** 2001. Anaerobic biodegradation of saturated and aromatic hydrocarbons. Curr. Op. Biotech. **12**.

69. **Wilkes, H., A. Vieth, and R. Elias.** 2008. Constraints on the quantitative assessment of in-reservior biodegradation using compound-specific stable carbon isotopes. Organ. Geochem. **39:**1215-1221.

70. **Yoshizawa, K.** 2002. Theoretical study on kinetic isotope effects in the C-H bond activation of alkanes by iron-oxo complexes. Coord. Chem. Rev. **226:**251-259.

71. **Yoshizawa, K.** 1998. Two-step concerted mechanism for alkane hydroxylation on the ferryl active site of methane monooxygenase. J. Biol. Inorg. Chem. **3:**318-324.

Table 1. Comparison of ε_{bulk} and AKIE for carbon and hydrogen stable isotope fractionation during aerobic and anaerobic biodegradation from this study, and to the literature

Substrate	Condition	Culture	ε^{C}_{bulk} (‰)	$AKIE_C$	ε^{H}_{bulk} (‰)	$AKIE_H$	$\Lambda_{reactive}$	Mechanism	Reference
n-hexane	Sulfate-reducing	*D. alkanexedens*	-5.5 ± 0.2	1.034 ± 0.001	-43.1 ± 6.3	2.526 ± 0.564	9.12 ± 1.67	fumarate addition	this study
n-octane	Sulfate-reducing	*D. alkanexedens*	-5.2 ± 0.4	1.043 ± 0.004	-27.8 ± 4.2	1.999 ± 0.302	6.02 ± 1.37	fumarate addition	this study
n-hexane	Aerobic	*P. putida*	-4.3 ± 0.3	1.027 ± 0.002	*not detected*	*n.a.*	< 2	alkane hydroxylase	this study
n-hexane	Nitrate-reducing	*strain HxN1*	-2.3*	*n.a.*	*n.m.*	*n.a.*	*n.a.*	fumarate addition	Vieth and Wilkes, 2006
n-butane	Aerobic	*enrichment*	-2.4 ± 1.1	*n.a.*	*n.m.*	*n.a.*	*n.a.*	*unknown*	Kinnaman *et al.,* 2007
n-propane	Aerobic	*enrichment*	-4.9 ± 1.1	*n.a.*	-15.1 ± 1.9	*n.a.*	*n.a.*	*unknown*	Kinnaman *et al.,* 2007
n-ethane	Aerobic	*enrichment*	-9.3 ± 1.1	*n.a.*	-61.9 ± 8.3	*n.a.*	*n.a.*	*unknown*	Kinnaman *et al.,* 2007
n-decane	Unsaturated Aerobic	*enrichment*	-0.2 ± 0.1	1.002	*n.m.*	*n.a.*	*n.a.*	*unknown*	Bouchard *et al*., 2008
n-octane	Unsaturated Aerobic	*enrichment*	-0.9 ± 0.1	1.007	*n.m.*	*n.a.*	*n.a.*	*unknown*	Bouchard *et al*., 2008
n-heptane	Unsaturated Aerobic	*enrichment*	-1.4 ± 0.1	1.010	*n.m.*	*n.a.*	*n.a.*	*unknown*	Bouchard *et al*., 2008
n-hexane	Unsaturated Aerobic	*enrichment*	-2.3 ± 0.6	1.013	*n.m.*	*n.a.*	*n.a.*	*unknown*	Bouchard *et al*., 2008
n-pentane	Unsaturated Aerobic	*enrichment*	-2.4 ± 0.2	*n.a.*	*n.m.*	*n.a.*	*n.a.*	*unknown*	Bouchard *et al*., 2008
n-butane	Unsaturated Aerobic	*enrichment*	-5.6 ± 0.1	1.022	*n.m.*	*n.a.*	*n.a.*	*unknown*	Bouchard *et al*., 2008
n-propane	Unsaturated Aerobic	*enrichment*	-10.8 ± 0.7	1.033	*n.m.*	*n.a.*	*n.a.*	*unknown*	Bouchard *et al*., 2008

n.a. not applicable
n.m. not measured
*Error of ε_{bulk} value unknown.

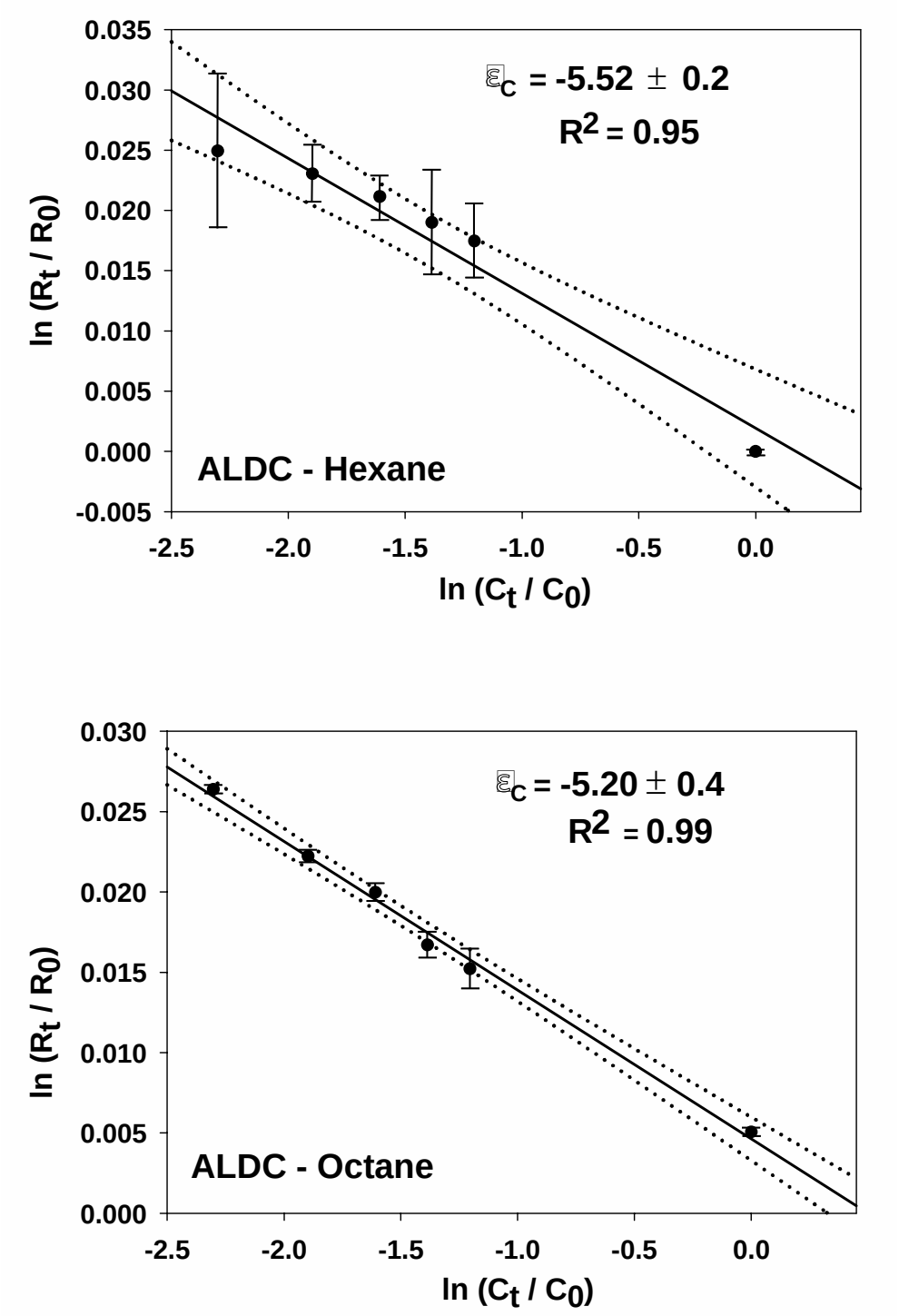

Figure 1. Rayleigh plots for carbon isotope fractionation of hexane and octane biodegradation by *Desulfoglaeba alkanexedens* (strain ALDC). The slope of the line represents the enrichment factor (ε_{bulk}), and the dotted lines show 95% confidence intervals of these data.

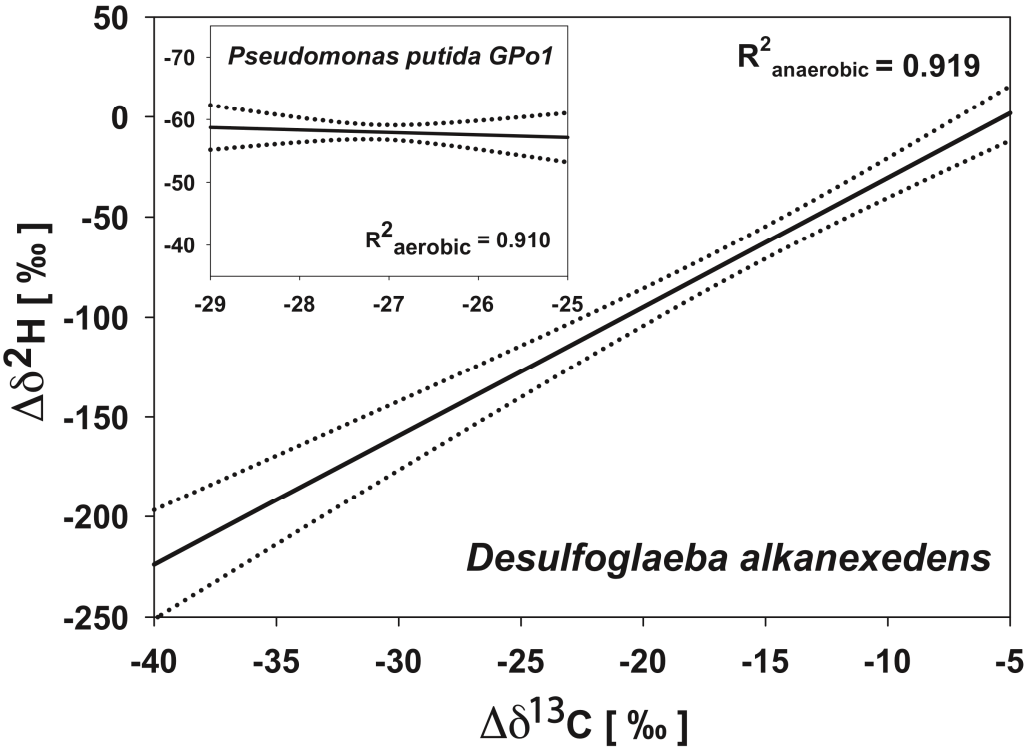

Figure 2. Two-dimensional $\Delta\ \delta\ ^{2}H$ and $\Delta\ \delta\ ^{13}C$ plot of anaerobic hexane degradation under sulfate-reducing conditions by *Desulfoglaeba alkanexedens* and aerobic hexane degradation by *Pseudomonas putida* strain GPo1. The dotted lines indicate 95% confidence intervals of these data.

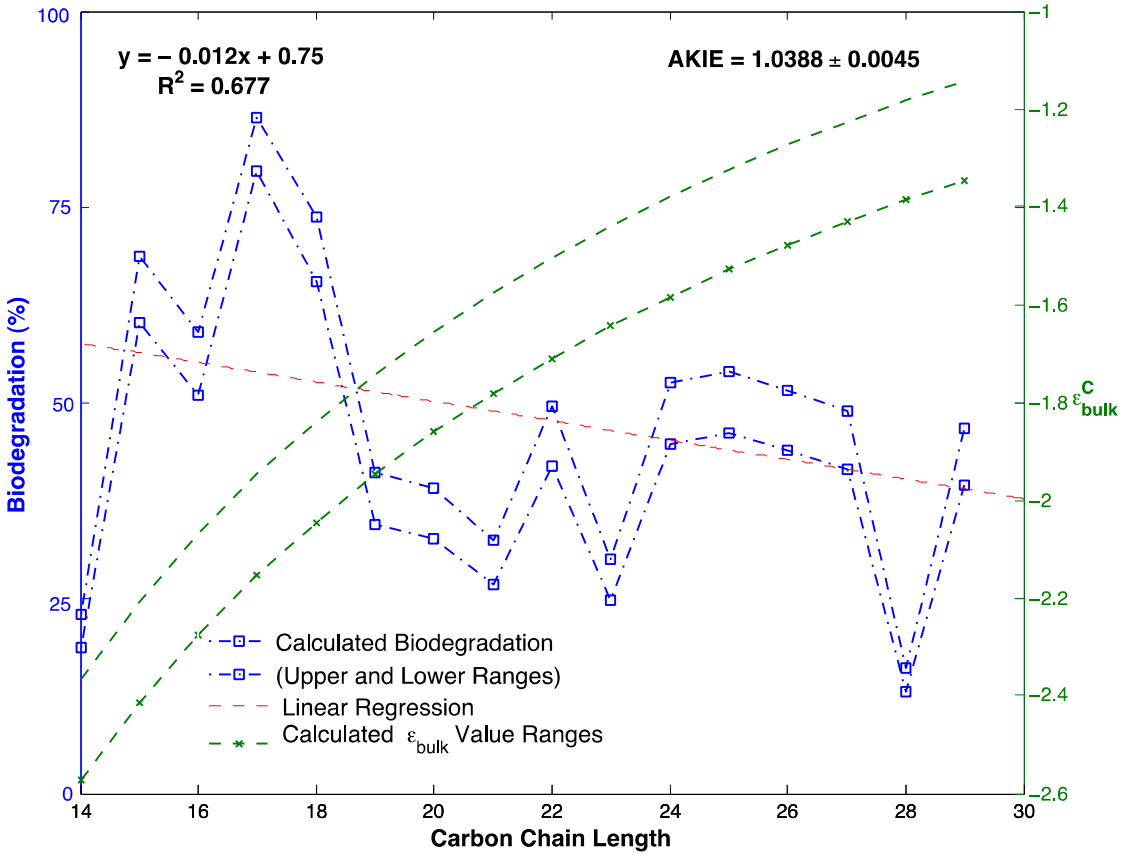

Figure 3. Calculated biodegradation and analysis of isotope data from Sun *et al*. (54). Upper and lower ε $_{bulk}$ values for carbon isotope fractionation were calculated using the *n*-hexane and *n*-octane AKIE values for anaerobic alkane degradation by *Desulfoglaeba alkanexedens*, respectively. The calculated ε $_{bulk}$ values given as green lines are represented on the right y-axis. The left y-axis depicts percent biodegradation for alkanes with carbon chain length values on the x-axis. The dashed red line represents a linear regression line for the

CHAPTER 2

Characterization of the Metabolism of *Desulfoglaeba alkanexedens*: A Differential Proteomics Study

Abstract

A draft genome was obtained for *Desulfoglaeba alkanexedens* strain ALDC^T and 3,168,086 base pairs encoding a total of 2,856 protein open reading frames (ORFs) were identified. The G+C content of the sequenced genome is 60.12%. This information was used to conduct a differential proteomics study of the strain grown separately on butyrate and *n*-decane in order to characterize the physiology of the organism with particular regard to anaerobic *n*-alkane biodegradation. Shotgun proteomics using nano high performance liquid chromatography coupled to an LTQ-Orbitrap mass spectrometer revealed 97 and 75 proteins expressed exclusively under the alkane- and butyrate-growth condition, respectively. Another 217 proteins were common to both growth conditions. The analysis revealed that alkylsuccinate synthase and the proteins associated with the arginine biosynthesis pathway were only expressed in the presence of *n*-alkanes. Higher rates of sulfate reduction were observed during *n*-decane mineralization by the bacterium in the presence of citrulline, ornithine, aspartate, and arginine, relative to the amino acid unamended control. In butyrate-grown cells, butyrate is likely activated to its CoA thioester using acetyl-

CoA transferase and subsequently metabolized by a typical complement of β-oxidation proteins. Proteins comprising the flagellar basal body and motor were also differentially detected in butyrate-grown cells. Proteins common to both growth conditions included the sulfate-reducing metabolic machinery, the β-oxidation components, and essential cell-housekeeping complexes including ATP synthases, H^+/Na^+-pumping Rnf-type complexes, and heterodisulfide reductases. *D. alkanexedens* expresses more proteins related to oxygen stress when grown on decane compared to butyrate, apparently reflecting the oxygen-sensitive nature of glycyl-radical enzymes necessary for hydrocarbon metabolism. For example, rubrerythrin and desulfoferredoxin were detected only in alkane-grown cells, and are predicted to have peroxidase and superoxide reductase activities respectively. The combination of shotgun proteomics coupled with draft genome sequence analysis provided greater insight on the general physiology and regulatory controls of *in situ* metabolic activity in this model *n*-alkane-using, sulfate-reducing bacterium.

Introduction

Desulfoglaeba alkanexedens strain $ALDC^T$ is a model sulfate-reducing bacterium isolated from an oily-wastewater storage facility (14). This organism was the primary member of an enriched bacterial consortium capable of complete *n*-alkane oxidation under sulfate-reducing conditions, and the first shown to use the fumarate-addition mechanism of alkane activation (30). This

process has also been associated with the anaerobic activation of many hydrocarbons including a variety of aliphatic, alicyclic, and alkylated aromatic compounds (see (84) for a review). Pure cultures of sulfate-reducing bacteria (SRB) can mineralize hydrocarbons in the presence of sulfate, but have also been implicated in the syntrophic bioconversion of petroleum constituents to methane (21, 84, 89). Indeed, SRB are thought to be key organisms in anaerobic hydrocarbon degradation in subsurface petroleum reservoirs and contaminated aquifers (2, 24, 26, 33, 46, 48, 59, 77). Sulfate-reducing prokaryotes also likely play a role in biocorrosion of oil pipelines and related infrastructure (17, 72, 75). Much of the molecular biology of *n*-alkane oxidation has come from the analysis of bacterial isolates and enrichments grown on straight-chain hydrocarbons (10, 22). In general, the subterminal carbon of the alkane is added across the double bond of fumarate to yield a succinic acid derivative. The resulting metabolite then undergoes carbon-skeleton rearrangement and decarboxylation by an unknown mechanism (15, 86). The resulting branched fatty acid is degraded via β-oxidation. Using stable isotopes, the co-metabolite fumarate was shown to be regenerated during the anaerobic degradation pathway for hexane (15). The exact mechanism for fumarate regeneration is currently unknown, but proposed to be similar to the reversible conversion of methylmalonyl-CoA to succinyl-CoA ((86), Callaghan *et al*., *in press*). Therefore, an improved understanding of anaerobic hydrocarbon metabolism, and the physiology of the requisite microorganisms, will lead to greater insights into the factors controlling this important process and on the cycling of carbon in anaerobic environments

Sulfate-reducing prokaryotes have long been associated with oil field systems (5), but recognition of their capacity for hydrocarbon metabolism has only been relatively recent (85). The metabolic activity of these and other bacteria generally serve to decrease oil quality and amplify the cost of hydrocarbon extraction and refining (26). However, the same metabolic processes also have beneficial biotechnological potential for the remediation of spilt hydrocarbons. However, relatively little is known about the organisms responsible for these important environmental processes. *Desulfoglaeba alkanexedens* ALDC^T is only the second *n*-alkane-degrading SRB that has been sequenced. *Desulfatibacillum alkenivorans* AK-01 also activates *n*-alkanes by fumarate-addition and its genome sequence has only recently been reported (Callaghan *et al., in press*). *Desulfococcus oleovorans* strain Hxd3 activates *n*-alkanes by an alternate mechanism (1, 10, 68) and its genome sequence will be subsequently reported. Insights provided by the genomic sequence of model strains help underpin the proteomic investigation presented herein.

Materials and Methods

Microorganisms and Media Preparation. Desulfoglaeba alkanexedens was grown in 20 L carboys containing a reduced marine mineral salts medium (83) and either *n*-decane (as an overlay) or butyrate (10mM) as the sole carbon and energy source. Specifically, NaCl (200g), MgCl▪6 H_20 (30g), $CaCl_2$▪2 H_20 (1.5g), $NaSO_4$ (35g), NH_4Cl (2.5g), KH_2PO_4, and KCl (5.0g) were added to an

acid-washed carboy and allowed to dissolve overnight in nanopure water. Next, 100mL of a trace metal solution (76) was added and the medium was adjusted to a pH of 7.2-7.4. The media was autoclaved for 60 min, and then sparged with N_2 for 3 h and N_2/CO_2 for 5 h during cooling. Once cool, 32g of autoclaved $NaHCO_3$ was aseptically added to the medium, the carboys were sealed with a rubber stopper (modified to contain a Balch tube and closure for ease of sampling) and held in place with wire. The medium in each carboy was reduced with 180mL of a cysteine-HCl/Na_2S stock solution containing 12.5g/L of each compound. A filter-sterilized vitamin solution (100mL, (76)) was added to each carboy. Lastly, 2 L of butyrate- or decane-grown cell suspensions that had been previously cultivated separately on the two substrates for at least six generations were inoculated into each carboy. For the hydrocarbon preparation, 20mL of autoclaved neat *n*-decane was added after inoculation. Cultures were incubated for six months at 30℃ in the dark.

The cultures were harvested using a Millipore™ Pellicon 2 tangential flow filtration system. The 0.45 µm Pellicon 2 (Millipore) cassettes measured 21cm x 17.8cm x 1.5cm (l x w x h). A coarse (C-type) screen and HVMP membrane were used as described at manufacturer's website (www.millipore.com/catalogue/module/c7840#1). Prior to culture harvesting, all tubes and membrane filters were reduced with an anaerobic flush solution consisting of anoxic 50mM phosphate buffer (3.05g $KHPO_4$ and 4.91g KH_2PO_4 per L, pH 7.3) containing 0.5% sodium thioglycollate. The concentrated cell suspension was transferred to an anoxic 1L Schott bottle. The culture was split

into 25mL aliquots while inside an anaerobic chamber and stored in 30mL Oak Ridge centrifuge tubes at 4℃ on dry ice for shipping , and until further analysis at the UFZ in Leipzig, Germany.

Protein Extraction. Concentrated biomass from each culture (100mL) was centrifuged for 15 minutes to form a cell pellet. The supernatant was discarded and 100µL of equilibration buffer containing trypsin was added to the pellet. The cells were disrupted using ultrasonication in a 37℃ wat er bath for five minutes. The cell lysate/trypsin mixture was then incubated overnight at 37℃. After digestion, the mixture was centrifuged for 10 minutes. The supernatant was carefully removed and dried using a vacuum centrifuge before storage at -20℃. Before mass spectral analysis, the peptides were redissolved in 30µL of 0.1% formic acid and purified two times using Zip-Tip purification and desalting according to manufacturer's directions (Millipore, Billerica, MA).

Mass Spectrometry. The reconstituted peptides were injected by autosampler and concentrated on a trapping column (nanoAcquity UPLC column, C_{18}, 180 µm x 2 cm x 5 µm) with a mobile phase consisting of 0.1% formic acid at 15 µl/min. After 8 min, the peptides were eluted onto a separation column (nanoAcquity UPLC column, C_{18}, 75 µm x 25 cm, 1.75 µm). Chromatography was performed with a 0.1% formic acid/acetonitrile mobile phase, using a gradient of either 6 or 8 – 40% acetonitrile over a 185 min elution time using a nano-HPLC system (nanoAcquity, Waters, Milford, MA, USA) coupled to an LTQ-

Orbitrap mass spectrometer (Thermo Fisher Scientific, Waltham, MA, USA). Continuous scanning of eluted peptide ions was carried out between 300 – 2000 Da, automatically switching to MS/MS collision induced dissociation mode on ions exceeding an intensity of 5000 Da. For MS/MS collision induced dissociation measurements, dynamic precursor exclusion was enabled for 3 minutes.

Amino Acid Amendments. Desulfoglaeba alkanexedens was grown in 60mL serum bottles containing anaerobic mineral salts, bicarbonate-buffered media as previously described (14). Vitamin and mineral solutions (10mL per liter (76)) were added. Medium pH was adjusted to 7.2. Bottles were closed with butyl rubber stoppers and aluminum crimp seals, and contained a N_2/CO_2 (80:20) headspace. Arginine-family amino acids (arginine, citrulline, ornithine, aspartate) were filter sterilized and added to an initial concentration of 1mM. Ammonium chloride (NH_4Cl) was excluded from experimental replicates and amended to the amino acid-free control at a concentration of 0.25g/L. Sulfate concentrations in the medium were periodically monitored by ion chromatography on a Dionex™ ICS-3000 running an AS-4A column and carbonate/bicarbonate eluent as previously described (30).

Data Analysis. Two replicates of $ALDC^T$ were analyzed for each growth substrate. A list of identified ORFs from the Proteome Discover™ results for each replicate were combined in Matlab (Mathworks, Version R2010b), and only those

ORFs identified in both replicates were used for further analysis. Therefore, screening took place in MASCOT and during *post hoc* analysis to create a conservative list of differentially expressed proteins. The identified ORF lists from butyrate and *n*-decane were then analyzed to create a Boolean list of proteins present with each substrate, or both respectively.

Results

Genome Analysis

A draft genome sequence was obtained for strain ALDC^T with predicted 9X coverage. Gap closing was not undertaken, and the genome is currently unclosed with a total of 42 contigs deposited with NCBI under the accession numbers XXXX-XXXX. General genome features are summarized in Table 1. The genome currently consists of 3,168,086 base pairs encoding a total of 2,856 proteins. The G+C content of the sequenced genome is 60.12 mol %, a value higher than previously reported for this organism (14), and among the highest seen for previously described alkane-degrading SRB which range from 40.9 mol % in strain BuS5 (29) to 54.5 mol % in strain AK-01 (Callaghan *et al, in press*). The organism does not contain any plasmids or mobile genetic elements. The Kyoto Encyclopedia of Genes and Genomes (KEGG) categories for the identified open reading frames in *Desulfoglaeba* can be found in Figure 1. Overall, 58% of the 2,856 identified proteins can be assigned to a KEGG category. Roughly 1200

proteins are hypothetical and cannot be attributed to particular cellular functions. With the limited number of genes and restricted nutritional capabilities, the genome size of strain ALDC^T (at 3.17 Mbp) is intermediate between fatty acid-degrading specialists like *Syntrophus aciditrophicus,* (at 2.81 Mbp), and SRB generalist such as *Desulfovibrio vulgaris* (3.66 Mbp). Strain ALDC^T can be considered a specialist, as general metabolic capabilities predicted by the genome are consistent with the narrow substrate range previously observed (14). Specifically, the cell metabolizes pyruvate, butyrate, hexanoic acid, 4-methyoctanoic acid, and C_6-C_{12} *n*-alkanes, using sulfate or thiosulfate as an electron acceptor under mesophilic conditions (14). *Desulfoglaeba* cannot grow on acetate, succinate, lactate, citrate, glucose, fructose, or benzoate. Strain ALDC^T was the first known sulfate-reducing bacterium capable of metabolizing *n*-alkanes syntrophically in the presence of the H_2/formate-utilizing *Methanospirillum hungatei* JF-1 (74). Although the molecular physiology of syntrophy is in the early stages of characterization, it seems that a unique Rnf-type complex, membrane-bound Fe-S region, and menaquinone are necessary for reverse electron transport (41, 67), and these features were detected in the *Desulfoglaeba* genome. Based on 16S homology, strain ALDC^T is closely related to a branch of organisms relying heavily on syntrophy as a major mode of existence (14). Since fatty-acid metabolism via β-oxidation represents a major life strategy for ALDC^T, it was expected that genes coding for these biochemical functions would be prevalent in the genome. Indeed, the genome contains all genes necessary for saturated fatty acid metabolism including four acyl-CoA

dehydrogenases; other related genes such as a thiolase(II)-type acetyl-CoA acetyltransferases, enoyl-Co hydratases, and AMP-dependent CoA ligases also seem to be present as multiple copies. The genome also contains one 3-hydroxyacyl-CoA dehydrogenase, but evidence for a 4-hydroxyacyl-CoA dehydrogenase could not be found in the current draft-sequence available.

A general feature of completely oxidizing sulfate-reducing bacteria is a mechanism for the oxidation of acetyl-CoA (52). Two common mechanisms exist for the oxidation of acetyl-CoA by SRB, either a reversal of the Wood-Ljungdahl pathway first observed in homoacetogenic bacteria (64) or via the TCA cycle. Citric acid cycle genes detected in *Desulfoglaeba* include those encoding a *Si*-type citrate synthase, aconitate hydratase, isocitrate dehydrogenase, 2-oxoglutarate dehydrogenase, succinate dehydrogenase, fumarate hydratase, malate dehydrogenase, and citrate lyase. The only apparent gene lacking for a complete TCA cycle seems to be succinyl-CoA synthetase, however 2-oxoglutarate synthase is present and therefore provides a route for succinyl-CoA generation from 2-oxoglutarate (8). It is also possible that succinyl-CoA is generated by CoA transfer from acetyl-CoA in a *Desulfobacter*-type process (65). In addition, phosphoenolpyruvate carboxylase and pyruvate:ferredoxin oxidoreductase were detected. The latter enzyme catalyzes the reductive carboxylation of acetyl-CoA to form pyruvate (56). The only gene apparently missing for an operative, traditional reductive TCA cycle is ATP citrate lyase. With the exception of *Desulfobacter* species, the absence of 2-oxoglutarate

dehydrogenase is common among SRB capable of complete carbon oxidation (52)

A key enzyme necessary for the Wood-Ljungdahl pathway is the bifunctional carbon monoxide (CO) dehydrogenase/acetyl-CoA synthetase (CODH/ACS). This protein complex uses ferredoxin as the electron donor to synthesize acetyl-CoA from enzyme bound CO and CoA (55), but the gene coding for this protein was not detected in strain ALDC^T. However, a monofunctional nickel carbon monoxide dehydrogenase is present. The monofunctional CODH physiologically functions in the direction of CO oxidation, but does not catalyze the production of acetyl-CoA from carbon dioxide (55). Overall, a large number of genes for the Eastern branch of the Wood-Ljungdahl pathway were detected (54), including methylenetetrahydrofolate dehydrogenase (NADP+) / methenyltetrahydrofolate cyclohydrolase, and the aforementioned pyruvate:ferredoxin oxidoreductase. Physiologically, the Eastern branch is involved in folate-dependent metabolism of C_1-compounds and is phylogenetically conserved (54). It has been widely observed that completely-oxidizing SRB have a limited capacity to use acetate as a carbon source, and this is also the case for strain ALDC^T (14), however the reason behind limited acetate utilization is not well understood (52). Taken together, the lack of a bifunctional carbon monoxide (CO) dehydrogenase/acetyl-CoA synthetase (CODH/ACS) and the observed inability of strain ALDC^T to grow chemolithoautotrophically on CO_2 and H_2 suggest that terminal acetate oxidation

does not occur via a reversal of the acetogenic Wood-Ljungdahl pathway but rather via a modified citric acid cycle similar to *Desulfobacter postgatei* (52, 65).

It was previously asserted that *n*-alkanes could not be metabolized in the absence of molecular oxygen, but this assertion is now known to be incorrect. For medium-chain length *n*-alkanes specifically, fumarate is added to the subterminal carbon of the hydrocarbon to form a substituted succinic acid derivative that can be subsequently metabolized (30, 69, 71). Terminal addition of fumarate has been observed for smaller *n*-alkanes such as ethane, and propane (29, 63). This process is catalyzed by a glycyl-radical enzyme known as alkylsuccinate synthase (*ass*, (11)), or (1-methylalkyl)succinate synthase (*mas*, (22)). This mode of activation has also been observed with other hydrocarbon classes and catalyzed by several *δ*- and *β-proteobacteria* (85). Recently, chromosomal regions containing the fumarate-addition genes have been characterized in a nitrate-reducing isolate (22) and the first genome sequence for a SRB capable of *n*-alkane biodegradation via this mechanism is available (Callaghan *et al., in press*). In fact, the availability of the AK-01 *ass* operon made it possible to describe some of the functionally comparable features of the alkylsuccinate synthase in *Desulfoglaeba*. The catalytic A-subunit of alkylsuccinate synthase contains a conserved subterminal glycine motif (I/V-R-I/V-X-G-F/W/Y), and central cysteine residues (11). This amino acid orientation is crucial for formation of the glycyl radical and hydrogen abstraction from the alkane substrate (12, 30, 53). In stain ALDC^T, the *assA* subunit contains 858 amino acids and is 75% identical on the amino acid level to the catalytic subunit

of AK-01 (9). Following alkane activation and thioesterification, it is proposed that carbon-skeleton rearrangement occurs via a B_{12} catalyzed mutase reaction similar to the reversible regeneration of succinyl-CoA from methylmalonyl-CoA in propionic acid bacteria (38, 86). Indeed, genes annotated as methylmalonyl-CoA mutases are commonly found in the alkylsuccinate operons ((22); Callaghan *et al., in press*). Two separate, complete methylmalonyl-CoA (large and small subunits) enzymes are present in the *Desulfoglaeba* genome. One set of methylmalonyl-CoA encoding genes is located in close proximity to the *ass* genes, while the other is located in a region related to fatty-acid metabolism. The complete alkylsuccinate synthase enzyme complex consists of eight subunits labeled AssABCDEFJK, and the majority of these subunit-coding genes were detected in the *Desulfoglaeba* genome. Specifically, *ass* subunits ACDEJ were detected based on BLAST homology to the *ass* operon in strain AK-01 and conserved cysteine residues in the C-, and E-subunits. It is possible that the B-subunit is present, but some of the conserved cysteines are missing and the BLAST e-value (0.054) to related genes in strain AK-01 is not high enough to make this conclusion at this time. The B-subunit is proposed to be involved in substrate concentration sensing through interaction with an unknown regulatory protein (35). Subunit C likely plays a role in stabilizing the catalytic site of *AssA* and contains the conserved cysteines indicative of Fe-S clusters in a homologous subunit of the toluene-activating complex of benzylsuccinate synthase (34, 35). Also contained in the strain $ALDC^T$ *ass* operon is the glycyl radical activase necessary for the creation of the active catalytic site on the A-

subunit. All glycyl radical enzymes of the *S*-adenosylmethionine family require similar activases (40).

Given the limited metabolic capability of *Desulfoglaeba*, the capability of mineralizing *n*-alkanes represents a compelling reason to undertake differential protein expression studies. In addition, the only other known sulfate-reducing bacterium capable of *n*-alkane activation by fumarate-addition has a genome size roughly twice that of strain ALDC^{T}. Therefore, *Desulfoglaeba* represents an ideal model organism to probe alkane metabolism and biochemistry due to its limited substrate range, known anaerobic alkane-activation strategy, and the compact size of the encoded proteome.

Functional Proteomics

After growth of *Desulfoglaeba* on either butyrate or *n*-decane, cells were harvested, concentrated, and subjected to protein extraction and trypsin digestion. A total of 30,083 Orbitrap MS/MS scans were obtained for the alkane replicates, and 29,196 for the butyrate replicates over a 185 minute run time. Reproducibility between replicates was excellent, and only identically charged peptides identified in both replicates, for each condition, were retained for further analysis. Single-hits and peptides without MS/MS spectra were discarded. Tryptic peptides were screened and searched, against a database of translated amino acid sequences for each open reading frame in the *Desulfoglaeba* draft genome, using MASCOT and Proteome Discover software (Thermo Scientific). A

total of 217 proteins were shared in both growth conditions, 97 were unique to alkane-grown cells, and 75 were unique to the butyrate-grown cells (Table 2).

Shared Proteins. Many proteins detected in butyrate- and alkane-grown cells are related to general respiratory processes such as chemiosmotic ATP generation and sulfate reduction. Both cultures used sulfate as a terminal electron acceptor and sulfate reduction biochemical machinery including the dissimilatory sulfite reductase B- and C- subunits, adenylylsulfate reductase, and sulfate adenylyltransferase were observed in all protein preparations. In addition, peptides coding for an entire F_0F_1 ATP synthase were also common among all samples. Butyrate is the smallest fatty acid capable of undergoing β-oxidation, yielding two acetyl-CoA subunits that can be further degraded by several mechanisms (64). This process is also integral to the mineralization of long-chain alkane substrates (69). Detected strain ALDC^T proteins related to fatty-acid metabolism include acyl-CoA oxidase, enoyl-CoA hydratase, acetyl-CoA acetyltransferase, and 3-hydroxyacyl-CoA dehydrogenase. Several heterodisulfide reductases, known to be involved in electron-cycling, were also observed along with the quinone-interacting membrane-bound oxidoreductase that supplies electrons essential for the reduction of adenosine-5'-phosphosulfate to sulfite during sulfate respiration (47). Two complete methylmalonyl-CoA (*mmc*) operons are encoded in the strain ALDC^T genome. One is contained in the *ass* operon, however a separate Mmc complex encoded elsewhere in the genome was detected that contained a B_{12}-binding site, epimerase subunit, and mutase subunit. As already suggested, *mmc*-related reactions are thought to be involved

in the B_{12}-dependent carbon skeleton rearrangement reactions of the proposed, fumarate-dependent *n*-alkane degradation pathway but also during general fatty acid metabolism (86). Finally, a cytoplasmic non-reducing F_{420} hydrogenase (MvhD) subunit associated with heterodisulfide reductase A (HdrA) was present in both samples, and has been proposed to function in electron bifurcation under low H_2 partial pressures to reduce ferredoxin (73). Overall, the proteins shared between both growth substrates were related to overall cell homeostasis, dissimilatory sulfate reduction, ATP generation, reducing equivalent production, and fatty acid metabolism.

Butyrate-Grown Cells. *Desulfoglaeba alkanexedens* was initially described as a sessile organism that tended to form clumps (14). However, the genes necessary for flagellum biosynthesis are present in the genome suggesting that the organism can be motile under certain conditions. The proteins related to flagellar structure were differentially expressed in butyrate-grown cells, including the flagellar protein (FliS), flagellar basal-body protein (FliL), and flagellar motor switch protein (FliN). Strain ALDC^T also has the capacity to detect changes in the environment (*i.e.* substrate concentrations, redox conditions) and respond accordingly. Signal transduction is required to transmit information about substrate-receptor binding to a flagellar motor switch that results in chemotaxis toward or away from an effector (7). A protein with prescribed chemotaxis sensory transducer function was noted in the butyrate-grown cells (Table 2). The detection of flagellar proteins and chemotaxis sensory transducers suggests that strain ALDC^T cell excitation occurs in the presence of butyric acid.

Curiously, class I and class II fumarate hydratases (also known as fumarases) were only detected in butyrate-grown cells. Amino acid homology between the two classes is very low (20). Fumarase class I and II differ in several aspects related to thermostability, molecular mass, and iron-sulfur content (23, 88). However, the two proteins classes are functionally related and catalyze the reversible hydration of fumarate to *L*-malate. Three genes are responsible for fumarase production, class I is produced by *fumA* and *fumB* while class II is produced by *fumC* (87, 88). In *Escherichia coli*, *fumA* and *fumB* were shown to be differentially expressed during aerobic or anaerobic growth, respectively (87). FumA in fact was highly upregulated during aerobiosis, and repressed by glucose and anoxic conditions, indicating its association with the citric acid cycle (87).

The physiology of short-chain fatty acid degradation by SRB has been studied in detail (27, 31, 44, 82). The two known, non-syntrophic butyrate degradation pathways proceed via β-oxidation, producing two acetyl-CoA subunits, and result in acetate and CO_2 production or CO_2 alone depending on the cell's ability for terminal oxidation of acetate (Acetyl-CoA) (4, 44). Butyrate is activated to butyryl-CoA via CoA transfer from acetyl-CoA (67). The protein catalyzing this process is acetyl-CoA transferase, and was detected in *Desulfoglaeba* only in the presence of butyrate (Table 2). Butyrate and higher fatty acids are transported via the proton-driven symporter FadL (73). Indeed, FadL was differentially expressed in the presence of butyrate.

Decane-Grown Cells. It was previously observed that *n*-alkanes induce the capacity for their utilization and alkylsuccinate synthase is differentially expressed (22, 30, 53). Several subunits of the strain ALDC^T alkylsuccinate synthase were detected in alkane-grown cells including the catalytic AssA subunit, a methylmalonyl-CoA mutase in the same operon as AssA, and a subunit of *ass* annotated to encode an MgmE/PrpD family protein (Table 1). This protein family is thought to be involved in propionyl-CoA metabolism, catalyzing an aconitase-like isomerization reaction (36). Glycyl-radical enzymes such as alkylsuccinate synthase are rapidly deactivated in the presence of molecular oxygen (34, 40, 70). Several sulfate-reducing bacteria are apparently genetically well suited to occupy niches at oxic/anoxic interfaces (Callaghan *et al., in press*). Indeed, a number of SRB have been isolated from permanent oxic zones or sediments and are aerotolerant (52, 60, 62). Strain ALDC^T has not been specifically characterized with regard to oxygen tolerance. However, several proteins with oxygen radical detoxification properties were identified in the presence of *n*-alkanes including desulfoferredoxin (rubredoxin oxidoreductase) and rubrerythrin (37, 39), and may be expressed differentially to ensure the integrity of oxygen-sensitive metabolism related to hydrocarbon mineralization. In *Desulfovibrio vulgaris* (strain Hildenborough), rubrerythrin was characterized and found to be a non-heme iron alternative to superoxide dismutase (39). While the differential expression of alkylsuccinate synthase was expected in *Desulfoglaeba*, it was not known *a priori* whether an off-gel based proteomics approach would be able to detect this phenomenon. However, no peptides

specific for the alkylsuccinate synthase protein complex were detected in the butyrate-grown culture of strain ALDC^T. Table 2 shows unique proteins identified in each growth condition, the presence of unique peptides for those proteins, the number of unique peptides, and the corresponding MOWSE score for the MASCOT search. The MOWSE score is a similarity index used in peptide mass fingerprinting, and represents the probability of matching a set of mass peaks by random chance (3). This index increases with the detection of more peptide mass peaks for a given protein, or of peaks that are determined to be rare.

A close examination of the proteins detected only in alkane-grown cells revealed insight into the relationship between nitrogen and carbon metabolism. Specifically, we detected the enzymes involved in the arginine biosynthetic pathway, including a bifunctional arginine biosynthesis protein (ornithine acetyltransferase, ArgJ), urease subunits UreG and UreE, and argininosuccinate synthetase (Table 2). There are two known routes for arginine biosynthesis in prokaryotes, each differing in the mechanism of acetyl group removal from *N*-(2)-acetyl-ornithine and in points of feedback inhibition control of metabolic intermediate production (13). The first type of pathway is linear, typically found in *Bacillus* species or *Enterobacteriaceae,* and characterized by *N*-(2)-acetyl-ornithine giving rise to ornithine via a hydrolytic reaction catalyzed by acetylornithinase (51). The feedback point of the linear pathway is the first enzyme, *N*-acetylglutamate synthetase, inhibited by arginine (80). Both pathways involve five steps leading from glutamate to ornithine, and three ancillary steps producing arginine from ornithine. The second type of pathway is

cyclical due to acetyl group recycling by transacetylation of glutamate and *N*-(2)-acetylornithine (25). This recycling mechanism provides an energetically less-demanding way to synthesize arginine (16, 78). Excess arginine causes feedback inhibition at the point of *N*-acetylglutamate 5-phosphotransferase, the second enzyme in the pathway (78, 79). The cyclical pathway is present in all three domains of life (13, 25, 42). The high-energy metabolite carbamoylphosphate is involved in the first step of the conversion of ornithine to arginine but is also involved in the production of pyrimidine bases cytosine, thiamine, and uracil. The detected strain ALDC^T protein annotated as a 'bifunctional arginine biosynthesis protein (ArgJ, Table 2) is the key enzyme in the cyclical pathway and catalyzes the first and fifth steps of the anabolic arginine process (61). The other genes necessary for the circular arginine biosynthesis pathway were detected in the *Desulfoglaeba* genome. In addition, the MASCOT algorithm identified a putative argininosuccinate synthetase protein, although not with unique peptides. This enzyme catalyzes the condensation of citrulline and aspartate into argininosuccinate in an ATP-dependent reaction (13). Arginine can then be liberated from argininosuccinate by a hydrolysis reaction catalyzed by argininosuccinate lyase, producing fumarate as a byproduct (19).

Amino Acid Amendments. Nitrogen assimilation is an essential biological process that must be tightly regulated with relation to growth rate and accessibility of a chemically preferred nitrogen source. For *Escherichia coli*, the preferred form of bioavailable nitrogen is ammonium (57), and this is also the case for many other forms of life. *E. coli* has been shown to exhibit chemotaxis

toward selected free *L*-amino acids including alanine, asparagine, cysteine, and glycine, but did not show chemotaxis toward arginine-related amino acids (43). On the other hand, several heterotrophic bacteria have been shown to prefer amino acids as a nitrogen source instead of ammonia (28). Therefore, we decided to explore the relationship between sulfate-reduction rates in the combined presence of *n*-alkane and dissolved free amino acids of the arginine family, to determine if increased rates of biodegradation could be achieved. Microbial activity was monitored by sulfate reduction rates (Figure 2). After 59 days, the residual sulfate concentration in the presence of *n*-decane and *L*-arginine was 9.63 ± 1.39 mM compared to 26.54 ± 2.64 mM in the replicates amended with *L*-arginine alone. *L*-citrulline and *L*-ornithine amended singly to *n*-decane cultures produced a similar effect in the presence of *n*-decane, with residual sulfate concentrations reduced to 11.25 ± 1.05 mM and 11.80 ± 0.53 mM, respectively. Mean sulfate concentrations for cultures with only *L*-citrulline were 19.53 ± 1.24 mM, and 18.69 ± 0.20 mM when only L-ornithine was provided. For *L*-aspartate, more sulfate was reduced when only the amino acid was provided as compared to the single amino acid and *n*-decane, with averages of 15.77 ± 1.61 mM and 20.93 ± 1.90 mM respectively. D-enantiomers for all of the amino acids mentioned above, did not stimulate sulfate reduction above the *n*-decane only controls (Figure 2).

Discussion

Genome sequencing and annotation, combined with proteomics, provided a better understanding of the physiology of the model alkane-degrading sulfate-reducing bacterium *Desulfoglaeba alkanexedens*. The genome sequence of strain ALDC^T furnished a picture of an organism especially well suited for an anaerobic lifestyle of dissimilatory sulfate respiration or syntrophy coupled to the mineralization of medium-length alkanes or small fatty acids. The metabolic range of strain ALDC^T predicted by the genome is very narrow, and supports previous experiments characterizing this strain (14). Carbon is completely oxidized to CO_2 using a modified citric acid cycle similar to *Desulfobacter* species (52). Alkanes can be activated via fumarate-addition in a reaction catalyzed by alkylsuccinate synthase encoded by the chromosome. Genes similar to methylmalonyl-CoA mutase were found close to the *ass* genes, and suggest that the carbon skeleton rearrangement seen during alkane mineralization is catalyzed in a similar fashion as the conversion of succinyl-CoA to methylmalonyl-CoA (58). Latter *n*-alkane metabolites are β-oxidized to acetyl-CoA which is further degraded to CO_2 (15).

Strain ALDC^T was grown separately on butyrate and *n*-decane under sulfate-reducing conditions to compare proteins expressed differentially in the presence of these two substrates. Proteins related to cell homeostasis, chemiosmotic energy generation, fatty acid metabolism, and sulfate reduction were shared in all replicates. For butyrate-grown cells, the picture that emerges is proton-driven transport of butyrate by the long-chain fatty acid transporter FadL and activation of butyrate to butyryl-CoA via CoA transfer from acetyl-CoA. It

seems that *Desulfoglaeba* has the ability to form flagella in response to redox or substrate concentration stimuli. Flagellar proteins were not detected in alkane-grown cells. It is possible that the flagellum is used for environmental sensing and not necessarily for cell locomotion (81). Strain ALDC^T has been observed to degrade hydrocarbons syntrophically in the absence of sulfate and the presence of a H_2/formate-utilizing *Archaeon* (74). It would be interesting to see if a flagellum is present under these circumstances, as the flagellar protein FliD alone has been shown to promote a close physical association between a bacterium and archaeon partners as well as induce the expression of methanogen genes required for syntrophic growth (66). The role that the *Desulfoglaeba* flagellum occupies in syntrophic relationships is unknown at this time.

The lack of fumarase detection in alkane-grown cells is intriguing. The ability of *Desulfoglaeba* strain ALDC^T to respire fumarate has not been tested at this time, but likely does not play a role in the life-strategy of this cell. Fumarase expression studies in *E. coli* suggest that *fumABC* encode cytoplasmic proteins (87, 88). Analysis of these genes in strain ALDC^T could not detect a membrane-insertion tag or membrane-bound region. The alkylsuccinate synthase and related benzylsuccinate synthase enzymes are also known to be cytoplasmic (9, 35). Therefore, cells might be expected to regulate the availability of cytoplasmic fumarate during *n*-alkane metabolism to ensure sufficient concentrations of this necessary co-metabolite. Under normal conditions, fumarate can be converted to *L*-malate and used as a substrate for malate dehydrogenase during the

production of NADH. However, strain ALDC^T can use other methods to reduce NAD^+ such as the sodium- or proton-pumping Rnf-type complex (41, 73). Indeed, this method for regeneration of reducing equivalents seems more likely as ALDC^T probably does not gain net ATP from substrate-level phosphorylation and would require a chemiosmotic set of reactions to achieve energy conservation (52). Therefore, future studies elucidating the role of fumarate regeneration during *n*-alkane metabolism and the source of the cellular fumarate reserve being used during the alkylsuccinate synthase reaction might help to determine the rate-limiting steps of this process.

Proteins from alkane-grown cells were analyzed for differential expression compared to strain ALDC^T growth on butyrate. We detected alkylsuccinate synthase only in the presence of decane, and affirm previous studies demonstrating the inducibility of related proteins only in the presence of hydrocarbons (22, 30, 53). Glycyl radical enzymes are extremely sensitive to inactivation by oxygen radicals or other oxidants (70), and we found proteins with oxygen radical detoxification properties in alkane-grown cells. In addition, the pathway for arginine biosynthesis was expressed differentially in alkane-grown cells. In general, amino acids are synthesized by transamination of α-ketoacids, in a reaction catalyzed by a family of enzymes known as transaminases (18). However, bacterial catabolism of arginine and downstream amino acids is much more complex than anabolism and may proceed via several different pathways (13). In general, the first step of arginine would involve hydrolysis to ornithine and urea (45). Strain ALDC^T does contain all the genes necessary for an active

urease. A survey of the *Desulfobacterium autotrophicum HRM2 and Desulfatibacillum alkenivorans* AK-01 genomes indicates that the latter organisms do not possess this feature. Whether the presence of urease in strain ALDC^T would explain the increase in sulfate reduction when amended with arginine-family amino acids is unknown. Future study will be needed to determine if strain ALDC^T prefers amino acids as a nitrogen source during growth on alkanes, or if the higher rates of sulfate reduction were due to increased carbon availability and co-metabolism of amino acids with alkanes. Several studies have however examined the arginase pathway in *Bacillus* species, and noted coordinate induction of pathway enzymes in the presence of arginine, citrulline, ornithine, and proline (6, 32). The sulfate reduction rates seen in strain ALDC^T were higher when amended singly with those same amino acids, *L*-arginine, *L*-citrulline, and *L*-ornithine, in the presence of *n*-alkanes (Figure 3). Taken together, these data imply that the arginase pathway is induced in the combined presence of *n*-alkanes and the amino acids of the arginine-family. The detection of arginine biosynthesis proteins in alkane-grown ALDC^T and the presumed activation of the arginase pathway garnered from sulfate-reduction rates suggests that this amino acid family may be more important during anaerobic hydrocarbon degradation than previously recognized. Sulfate-reducing bacteria are commonly known to be prototrophic with regard to amino acid biosynthesis (50). During the initial characterization of *Desulfoglaeba*, it was noted that co-factors or amino acids were not needed for growth, however small amounts of yeast extract stimulate biomass production (14). This effect has often

been reported for other SRB as well (56). *L*-Arginine, *L*-citrulline, and *L*-ornithine are likely components of yeast extract. Postgate also noted that these amino acids have a chelating function and increase the solubility of FeS (49). Enhanced iron availability could well play a role in the increased sulfate reduction in our experiments.

In conclusion, the combination of genome analysis and differential proteomics provided insight into the biochemical processes involved under different growth conditions for the model sulfate-reducing bacterium *Desulfoglaeba alkanexedens*. Information gleaned from this study will lead to a greater knowledge of preferred nitrogen sources during growth on hydrocarbons, and the source(s) of the fumarate pool during anaerobic alkane mineralization.

Literature Cited

1. **Aeckersberg, F., F. Bak, and F. Widdel.** 1991. Anaerobic oxidation of saturated hydrocarbons to CO2 by a new type of sulfate-reducing bacterium. Arch. Microbiol. **156:**5-14.

2. **Aitken, C. M., D. M. Jones, and S. R. Larter.** 2004. Anaerobic hydrocarbon biodegradation in deep subsurface oil reservoirs. Nature **431:**291-294.

3. **Baldwin, M. A.** 2004. Protein identification by mass spectrometry. Mol. Cell. Proteo. **3:**1-9.

4. **Banat, I. M., and D. B. Nedwell.** 1983. Mechanism of turnover of C2–C4 fatty acids in high-sulphate and low-sulphate anaerobic sediments. FEMS Microbiol. Lett. **17:**107-110.

5. **Bastin, E. S.** 1926. The presence of sulphate reducing bacteria in oil field waters. Science **63:**21-24.

6. **Baumberg, S., and C. R. Harwood.** 1979. Carbon and nitrogen repression or arginine catabolic enzymes in *Bacillus subtilis*. J. Bacteriol. **137:**189-196.

7. **Bollinger, J., C. Parki, S. Harayamao, and G. L. Hazelbauer.** 1984. Structure of the Trg protein: Homologies with and differences from other sensory transducers of *Escherichia coli*. P. Natl. Acad. Sci. USA **81:**3287-3291.

8. **Buchanan, B., and M. C. Evans.** 1965. The synthesis of alpha-ketoglutarate from succinate and carbon dioxide by a subcellular preparation of a photosynthetic bacterium. P. Natl. Acad. Sci. USA **54:**1212-1218.

9. **Callaghan, A. V., I. A. Davidova, K. Savage-Ashlock, V. A. Parisi, L. M. Gieg, J. M. Suflita, J. J. Kukor, and B. Wawrik.** 2010. Diversity of benzyl- and alkylsuccinate synthase genes in hydrocarbon-impacted environments and enrichment cultures. Environ. Sci. Technol. **44:**7287-7294.

10. **Callaghan, A. V., L. M. Gieg, K. G. Kropp, J. M. Suflita, and L. Y. Young.** 2006. Comparison of mechanisms of alkane metabolism under sulfate-reducing conditions among two bacterial isolates and a bacterial consortium. Appl. Environ. Microb. **72:**4274-4282.

11. **Callaghan, A. V., B. Wawrik, S. M. Ni Chadhain, L. Y. Young, and G. J. Zylstra.** 2008. Anaerobic alkane-degrading strain AK-01 contains two alkylsuccinate synthase genes. Biochem. Bioph. Res. Co. **366:**142-148.

12. **Cravo-Laureau, C., V. Grossi, D. Raphel, R. Matheron, and A. Hirschler-Rea.** 2005. Anaerobic n-alkane metabolism by a sulfate-reducing bacterium, *Desulfatibacillum aliphaticivorans* strain CV2803T. Appl. Environ. Microb. **71:**3458-3467.

13. **Cunin, R., N. Glansdorff, A. Pierard, and V. Stalon.** 1986. Biosynthesis and metabolism of arginine in Bacteria. Microbiol. Rev. **50:**314-352.

14. **Davidova, I. A., K. E. Duncan, O. K. Choi, and J. M. Suflita.** 2006. *Desulfoglaeba alkanexedens* gen. nov., sp. nov., an *n*-alkane-degrading, sulfate-reducing bacterium. Int. J. Syst. Evol. Micr. **56:**2737-2742.

15. **Davidova, I. A., L. M. Gieg, M. A. Nanny, K. G. Kropp, and J. M. Suflita.** 2005. Stable isotope studies of *n*-alkane metabolism by a sulfate-reducing bacterial enrichment culture. Appl. Environ. Microb. **71:**8174-8182.

16. **Degryse, E., N. Glansdorff, and A. Pierard.** 1976. Arginine biosynthesis and degradation in an extreme thermophile, strain ZO5. Arch. Int. Physiol. Biochim. **84:**599-601.

17. **Duncan, K. E., L. M. Gieg, V. A. Parisi, R. S. Tanner, S. G. Tringe, J. Bristow, and J. M. Suflita.** 2009. Biocorrosive thermophilic microbial communities in Alaskan North Slope oil facilities. Environ. Sci. Technol. **43:**7977-7984.

18. **Feldman, L. I., and I. C. Gunsalus.** 1950. Transaminases in Bacteria. J. Biol. Chem. **187:**821-830.

19. **Fulde, M., J. Willenborg, A. de Greeff, L. Benga, H. E. Smith, P. Valentin-Weigand, and R. Goethe.** 2011. ArgR is an essential local transcriptional regulator of the *arcABC* operon in *Streptococcus suis* and is crucial for biological fitness in an acidic environment. Microbiology **157:**572-582.

20. **Gerbod, D., V. P. Edgcomb, C. Noel, S. Vanacova, R. Wintjens, J. Tachezy, M. L. Sogin, and E. Viscogliosi.** 2001. Phylogenetic relationships of class II fumarase genes from *Trichomonad* species. Mol. Biol. Evol. **18:**1574-1584.

21. **Gieg, L. M., K. E. Duncan, and J. M. Suflita.** 2008. Bioenegy production via microbial conversion of residual oil to natural gas. Appl. Environ. Microb. **74:**3022-3029.

22. **Grundmann, O., A. Behrends, R. Rabus, J. Amann, T. Halder, J. Heider, and F. Widdel.** 2008. Genes encoding the candidate enzyme for anaerobic activation of *n*-alkanes in the denitrifying bacterium, strain HxN1. Environ. Microbiol. **10:**376-385.

23. **Guest, J. R., J. S. Miles, R. E. Roberts, and S. A. Woods.** 1985. The fumarase genes of *Escherichia coli:* location of the f*umB* gene and discovery of a new gene (*fumC)*. J. Gen. Microbiol. **131:**2971-2984.

24. **Head, I. M., D. M. Jones, and S. R. Larter.** 2003. Biological activity in the deep subsurface and the origin of heavy oils. Nature **426:**344-352.

25. **Hoare, D. S., and S. L. Hoare.** 1966. Feedback regulation of arginine biosynthesis in blue-green algae and photosynthetic bacteria. J. Bacteriol. **92:**375-379.

26. **Jones, D. M., I. M. Head, N. D. Gray, J. J. Adams, A. K. Rowan, C. M. Aitken, B. Bennett, H. Huang, A. Brown, B. F. J. Bowler, T. Oldenburg, M. Erdmann, and S. R. Larter.** 2008. Crude-oil biodegradation via methanogenesis in subsurface petroleum reserviors. Nature **451:**176-180.

27. **Jørgensen, B. B.** 1982. Mineralization of organic matter in the sea bed-the role of sulphate reduction. . Nature **296:**643-645.

28. **Kirchman, D. L., and R. G. Keil.** 1989. The effect of amino acids on ammonium utilization and regeneration by heterotrophlc bacteria In the subarctic Pacific. Deep Sea Res. **36:**1763-1776.

29. **Kniemeyer, O., F. Musat, S. M. Sievert, K. Knittel, H. Wilkes, M. Blumenberg, W. Michaelis, A. Classen, C. Bolm, S. B. Joye, and F. Widdel.** 2007. Anaerobic oxidation of short-chain hydrocarbons by marine sulphate-reducing bacteria. Nature **449:**898-902.

30. **Kropp, K. G., I. A. Davidova, and J. M. Suflita.** 2000. Anaerobic oxidation of n-dodecane by an addition reaction in a sulfate-reducing bacterial enrichment culture. Appl. Environ. Microb. **66:**5393-5398.

31. **Laanbroek, H. J., and N. Pfennig.** 1981. Oxidation of Short-Chain Fatty Acids by Sulfate-Reducing Bacteria in Freshwater and in Marine Sediments. Arch. Microbiol. **128:**330-335.

32. **Laishley, E. J., and R. W. Bernlohr.** 1968. Regulation of arginine and proline catabolism in *Bacillus licheniformis*. J. Bacteriol. **96:**322-329.

33. **Larter, S. R., I. M. Head, H. Huang, B. Bennett, M. Jones, A. C. Aplin, A. Murray, M. Erdmann, A. Wilhelms, and R. Di Primio.** 2005. Biodegradation, gas destruction and methane generation in deep

subsurface petroleum reservoirs: an overview. Geological Society, London, Petroleum Geology Conference Series **6:**633-639.

34. **Leuthner, B., C. Leutwein, H. Schulz, P. Horth, W. Haehnel, E. Schiltz, H. Schagger, and J. Heider.** 1998. Biochemical and genetic characterization of benzylsuccinate synthase from T*hauera aromatica*: a new glycyl radical enzyme catalysing the first step in anaerobic toluene metabolism. Mol. Microbiol. **28:**615-628.

35. **Li, L., D. P. Patterson, C. C. Fox, B. Lin, P. W. Coschigano, and E. N. G. Marsh.** 2009. Subunit structure of benzylsuccinate synthase. Biochemistry **48:**1284-1292.

36. **Lohkamp, B., B. Bäuerle, P. G. Rieger, and G. Schneider.** 2006. Three-dimensional structure of iminodisuccinate epimerase defines the fold of the MmgE/PrpD protein family. J. Mol. Biol. **362:**555-566.

37. **Lombard, M., M. Fontecave, D. Touati, and V. Niviere.** 2000. Reaction of the Desulfoferrodoxin from Desulfoarculus baarsii with Superoxide Anion. J. Biol. Chem. **275:**115-121.

38. **Ludwig, M. L., and M. R.G.** 1997. Structure-based perspectives on B12-dependent enzymes. Ann. Rev. Biochem. **66:**239-313.

39. **Lumppio, H. L., N. V. Shenvi, A. O. Summers, G. Voordouw, and D. M. J. Kurtz.** 2001. Rubrerythrin and Rubredoxin Oxidoreductase in Desulfovibrio vulgaris: a Novel Oxidative Stress Protection System. J. Bacteriol. **183:**101-108.

40. **Marsh, E. N. G., M. S. Huhta, and A. Patwardhan.** 2004. S-Adenosylmethionine radical enzymes. Bioorg. Chem. **32:**326-340.

41. **McInerney, M. J., L. Rohlin, H. Mouttaki, U. Kim, R. S. Krupp, L. Rios-Hernandez, J. Sieber, C. G. Struchtemeyer, A. Bhattacharyya, J. W. Campbell, and R. P. Gunsalus.** 2007. The genome of Syntrophus aciditrophicus: Life at the thermodynamic limit of microbial growth. P. Natl. Acad. Sci. USA **104:**7600-7605.

42. **Meile, L., and T. Leisinger.** 1984. Enzymes of the arginine biosynthesis in methanogneic bacteria. Experientia **40:**899-900.

43. **Mesibov, R., and J. Adler.** 1972. Chemotaxis toward amino acids in *Escherichia coli*. J. Bacteriol. **112:**315-326.

44. **Muyzer, G., and A. Stams, J. M.** 2008. The ecology and biotechnology of sulphate-reducing bacteria. Nat. Rev. Microbiol. **8:**441-454.

45. **Ottow, J. C. G.** 1974. Arginine dihydrolase activity in species of the genus *Bacillus* revealed by thin-layer chromatography. J. Gen. Microbiol. **84:**209-213.

46. **Parisi, V. A., G. R. Brubaker, M. J. Zenker, R. C. Prince, L. M. Gieg, M. L. B. da Silva, P. J. J. Alvarez, and J. M. Suflita.** 2009. Field metabolomics and laboratory assessments of anaerobic intrinsic bioremediation of hydrocarbons at a petroleum-contaminated site. Microb. Biotechnol. **2:**202-212.

47. **Pereira, P. M., Q. He, F. M. Valente, A. V. Xavier, J. Zhou, I. A. C. Pereira, and R. O. Louro.** 2008. Energy metabolism in *Desulfovibrio vulgaris* Hildenborough: Insights from transcriptome analysis. A. van Leeuw **93:**347-362.

48. **Pham, V. D., L. L. Hnatow, S. Zhang, R. D. Fallon, S. C. jackson, J.-F. Tomb, E. F. DeLong, and S. J. Keeler.** 2009. Characterizing microbial diversity in petroleum wather from an Alaskan mesothermic petroleum reservior with two independent molecular methods. Environ. Microbiol. **11:**176-187.

49. **Postgate, J. R.** 1965. Recent advances in the study of sulfate-reducing bacteria. Bacteriol. Rev. **29:**425-441.

50. **Postgate, J. R.** 1984. The sulphate-reducing bacteria. 2nd ed., 2nd ed. Cambridge University Press, Cambridge, U.K.

51. **Prozesky, O. W.** 1967. Arginine synthesis in *Proteus mirabilis*. J. Gen. Micro. **49:**325-334.

52. **Rabus, R., T. A. Hansen, and F. Widdel.** 2006. Dissimilatory Sulfate- and Sulfur-Reducing Prokaryotes, p. 659-768, The Prokaryotes.

53. **Rabus, R., H. Wilkes, A. Behrends, A. Armstroff, T. Fischer, A. J. Pierik, and F. Widdel.** 2001. Anaerobic initial reaction of n-alkanes in a denitrifying bacterium: Evidence for (1-methylpentyl)succinate as initial product and for involvement of an organic radical in n-hexane metabolism. J. Bacteriol. **183:**1707-1715.

54. **Ragsdale, S. W.** 1997. The Eastern and Western branches of the Wood/Ljungdahl pathway: how the East and West were won. BioFactors **9:**1-9.

55. **Ragsdale, S. W.** 2008. Enzymology of the Wood-Ljungdahl pathway for acetogenesis. Ann. NY Acad. Sci. **1125:**129-136.

56. **Ragsdale, S. W.** 2003. Pyruvate:ferrodoxin oxidoreductase and its radical intermediate. Chem. Rev. **103:**2333-2346.

57. **Reitzer, L.** 2003. Nitrogen assimilation and global regulation in *Escherichia coli*. Ann. Rev. Microbiol. **57:**155-176.

58. **Retey, J.** 1982. Methymalonyl-CoA mutase, p. 357-379. *In* D. Dolphin (ed.), B_{12} Biochemistry and Medicine. John Wiley and Sons, New York.

59. **Rios-Hernandez, L. A., L. M. Gieg, and J. M. Suflita.** 2003. Biodegradation of an alicyclic hydrocarbon by a sulfate-reducing enrichment from a gas condensate-contaminated aquifer. Appl. Environ. Microb. **69:**434-443.

60. **Risatti, J. B., W. C. Capman, and D. A. Stahl.** 1994. Community structure of a microbial mat: the phylogenetic dimension. P. Natl. Acad. Sci. USA **91:**10173-10177.

61. **Sakanyan, V., D. Charlier, C. Legrain, A. Kochikyan, I. Mett, A. Pierard, and N. Glansdorff.** 2003. Primary structure, partial purification and regulation of key enzymes of the acetyl cycle of arginine biosynthesis in *Bacillus stearothermophilus*: dual function of ornithine acetyltransferase. . J. Gen. Micro. **139:**393-402.

62. **Sass, H., M. Berchtold, J. Branke, H. Konig, H. Cypionka, and H.-D. Babenzien.** 1998. Psychrotolerant sulfate-reducing bacteria from an oxic freshwater sediment, description of *Desulfovibrio cuneatus* sp. nov. and *Desulfovibrio litoralis* sp. nov. Syst. Appl. Microbiol. **21:**212-219.

63. **Savage, K. N., L. R. Krumholz, L. M. Gieg, V. A. Parisi, J. M. Suflita, J. Allen, R. P. Philp, and M. S. Elshahed.** 2010. Biodegrdation of low-molecular weight alkanes under mesophilic, sulfate-reducing conditions: metabolitic intermediates and community patterns. FEMS Microb. Ecol. **72:**485-495.

64. **Schauder, R., A. Preuss, M. Jetten, and G. Fuchs.** 1989. Oxidative and reductive acetyl CoA/carbon monoxide dehydrogenase pathway in *Desulfobacterium autotrophicum*. Arch. Microbiol. **151:**84-89.

65. **Schauder, R., F. Widdel, and G. Fuchs.** 1987. Carbon assimilation pathways in sulfate-reducing bacteria II. Enzymes of a reductive citric acid cycle in the autotrophic *Desulfobacter hydrogenophilus*. Arch Microbiol **148:**218-225.

66. **Shimoyama, T., S. Kato, S. i. Ishii, and K. Watanabe.** 2009. Flagellum mediates symbiosis. Science **323:**1574.

67. **Sieber, J. R., D. R. Sims, C. Han, E. Kim, A. Lykidis, A. L. Lapidus, E. McDonnald, L. Rohlin, D. E. Culley, R. Gunsalus, and M. J. McInerney.** 2010. The genome of Syntrophomonas wolfei: new insights

into syntrophic metabolism and biohydrogen production. Environ. Microbiol. **12:**2289-2301.

68. **So, C. M., C. D. Phelps, and L. Y. Young.** 2003. Anaerobic transformation of alkanes to fatty acids by a sulfate-reducing bacterium, strain Hxd3. Appl. Environ. Microbiol. **69:**3892-3900.

69. **So, C. M., and L. Y. Young.** 1999. Initial Reactions in Anaerobic Alkane Degradation by a Sulfate Reducer, Strain AK-01. Appl. Environ. Microb. **65:**5532-5540.

70. **Sofia, H. J., G. Chen, B. G. Hetzler, J. F. Reyes-Spindola, and N. E. Miller.** 2001. Radical SAM, a novel protein superfamily linking unresolved steps in familiar biosynthetic pathways with radical mechanisms: functional characterization using new analysis and information visualization methods. Nucl. Acid Res. **29:**1097-1106.

71. **Spormann, A. M., and F. Widdel.** 2000. Metabolism of alkylbenzenes, alkanes, and other hydrocarbons in anaerobic bacteria. Biodegradation **11:**85-105.

72. **Stevenson, B. S., H. S. Drilling, P. A. Lawson, K. E. Duncan, V. A. Parisi, and J. M. Suflita.** 2011. Microbial communities in bulk fluids and biofilms of an oil facility have similar composition but different structure. Environ. Microbiol. **13:**1078-1090.

73. **Strittmatter, A. W., H. Liesegang, R. Rabus, I. Decker, J. Amann, S. Andres, A. Henne, W. F. Fricke, R. Martinez-Arias, D. Bartels, A. Goesmann, L. Krause, A. Pühler, H.-P. Klenk, M. Richter, M. Schüler, F. O. Glöckner, A. Meyerdierks, G. Gottschalk, and R. Amann.** 2009. Genome sequence of *Desulfobacterium autotrophicum* HRM2, a marine sulfate reducer oxidizing organic carbon completely to carbon dioxide. Environ. Microbiol. **11:**1038-1055.

74. **Suflita, J. M., I. A. Davidova, L. M. Gieg, M. A. Nanny, and R. C. Prince.** 2004. Anaerobic hydrocarbon biodegradation and the prospects for microbial enhanced energy production p. 283-306. *In* R. Vazquez-Duhalt and R. Quintero-Ramirez (ed.), Petroleum Biotechnology, Developments and Perspectives. Studies of Surface Science and Catalysis, vol. 151. Elsevier Science.

75. **Suflita, J. M., T. J. Phelps, and B. Little.** 2008. Carbon dioxide corrosion and acetate: a hypothesis on the influence of microorganisms. Corrosion **64:**854-859.

76. **Tanner, R. S.** 1997. Cultivation of bacteria and fungi, p. 52-60. *In* C. J. Hurst, G. R. Knudsen, M. J. McInerney, L. D. Stetzenbch, and M. V.

Walter (ed.), Manual of Environmental Microbiology. American Society for Microbiology, Washington D.C.

77. **Townsend, G. T., R. C. Prince, and J. M. Suflita.** 2003. Anaerobic oxidation of crude oil hydrocarbons by the resident microorganimss of a contaminted anoxic aquifer. Environ. Sci. Technol. **37:**5213-5218.

78. **Udaka, S.** 1966. Pathway-specific pattern of control of arginine biosynthesis in bacteria. J. Bacteriol. **91:**617-621.

79. **Udaka, S., and S. Kinoshita.** 1958. Studies on L-ornithine fermentation. II. The change of fermentation product by a feedback type mechanism. J. Gen. Appl. Microbiol. **4:**283-288.

80. **Vyas, S., and W. K. Maas.** 1963. Feedback inhibition of acetylglutamate synthetase by arginine in *Escherichia coli*. Arch. Biochem. Biophys. **100:**542-546.

81. **Wang, Q., A. Suzuki, S. Mariconda, S. Porwollik, and R. M. Harshey.** 2005. Sensing wetness: a new role for the bacterial flagellum. EMBO J. **24:**2034–2042.

82. **Widdel, F.** 1988. Microbiology and ecology of sulfate- and sulfur- reducing bacteria., p. 469–483. *In* A. J. B. Zehnder (ed.), Biology of Anaerobic Microorganisms. Wiley- Liss, New York.

83. **Widdel, F., and F. Bak.** 1992. Gram-negative mesophilic sulfate-reducing bacteria, p. 3352-3378. *In* A. Balows, H. G. Trueper, M. Dworkin, W. Harder, and K. H. Schleifer (ed.), The Prokaryotes, vol. 4. Springer, New York.

84. **Widdel, F., A. Boetius, and R. Rabus.** 2006. Anaerobic Biodegradation of Hydrocarbons Including Methane, p. 1028-1049. *In* M. Dworkin, S. Falkow, E. Rosenberg, K.-H. Schleifer, and E. Stackebrandt (ed.), The Prokaryotes, vol. Vol 2: Ecophysiology and Biochemistry. Springer, New York.

85. **Widdel, F., and O. Grundmann.** 2010. Biochemistry of the anaerobic degradation of non-methane alkanes, p. 909-924. *In* K. N. Timmis, T. McGenity, J. R. van der Meer, and V. de Lorenzo (ed.), Handbook of Hydrocarbon and Lipid Microbiology. Springer-Verlag, Berlin.

86. **Wilkes, H., R. Rabus, T. Fischer, A. Armstroff, A. Behrends, and F. Widdel.** 2002. Anaerobic degradation of *n*-hexane in a denitrifying bacterium: Further degradation of the initial intermediate (1-methylpentyl)succinate via C-skeleton rearrangement. Arch. Microbiol. **177:**235-243.

87. **Woods, S. A., and J. R. Guest.** 1987. Differential roles of the *Escherichia coli* fumarases and *fnr*-dependent expression of fumarase B and aspartase. FEMS Microbiol. Lett. **48:**219-244.

88. **Woods, S. A., S. D. Schwartzbach, and J. R. Guest.** 1988. Two biochemically distinct classes of fumarase in *Escherichia coli*. BBA - Protein Struct. M. **954:**14-26.

89. **Zengler, K., H. H. Richnow, R. Rossello-Mora, W. Michaelis, and F. Widdel.** 1999. Methane formation from long-chain alkanes by anerobic microorganisms. Nature **401:**266-269.

Table 1. General Information for the *Desulfoglaeba alkanexedens* draft genome.

description	calculation
DNA, total	3,168,086
Predicted genome coverage	9 X
Number of plasmids	0
G+C content (mol %)	60.12
Genes (open reading frames)	
Protein coding genes	2856 (99.05%)
Protein coding genes with predicted function	1626 (56.93%)
Hypothetical protein coding genes	1203 (42.12%)

Table 2. Selected proteins differentially expressed by *Desulfoglaeba* grown on butyrate and decane. The MOWSE score is a similarity index used in peptide mass fingerprinting, and represents the probability of matching a set of mass peaks by random chance.

growth condition	protein name	sequence ref.	unique peptides	# of peptides	% coverage	MOWSE Score‡
Alkane	arginine biosynthesis bifunctional protein (ArgJ)	YP_845329.1	yes	2	6.7	46.72
Alkane	urease accessory protein UreG [uncultured bacterium]	ABW80928.1	yes	4	22.78	181.16
Alkane	urease accessory protein UreE [Pseudomonas putida KT2440]	YP_001268159	yes	3	17.6	96.82
Alkane	argininosuccinate synthetase	YP_844199.1	no	2	3.7	45.38
Alkane	Alkylsuccinate synthase, alpha subunit (AssA1)	YP_002430896.1	yes	46	48.45	1641.69
Alkane	methylmalonyl-CoA mutase, large subunit (Ass operon)	YP_002430890.1	yes	4	22.38	77.38
Alkane	putative MmgE/PrpD family protein (Ass operon)	YP_002430892.1	yes	3	11.28	66.59
Alkane	desulfoferrodoxin	YP_002953138.1	yes	2	15.32	44.54
Alkane	rubrerythrin	YP_847328.1	yes	7	40.24	178.82
Butyrate	acetyl CoA-transferase	YP_039692.1	yes	3	12.08	69.89
Butyrate	fumarate hydratase, class II (FumC)	YP_846220.1	yes	2	6.84	85.00
Butyrate	fumarate hydratase, class I (FumB)	YP_002607625.1	yes	2	11.96	35.45
Butyrate	flagellar protein FliS	YP_002514046.1	yes	6	9.96	163.28
Butyrate	flagellar basal body-associated protein FliL	ZP_06402498.1	no	4	9.73	64.40
Butyrate	flagellar motor switch protein FliN	ZP_06232475.1	yes	3	17.83	77.62
Butyrate	chemotaxis sensory transducer	ZP_01289130.1	yes	2	4.82	58.30
Butyrate	FadL, long-chain fatty acid transporter	YP_002605158.1	yes	3	6.05	63.70

Both	ATP synthase F1, epsilon subunit	YP_846694.1	yes	5	12.32	93.00
Both	F0F1 ATP synthase subunit beta	YP_846695.1	yes	52	46.49	2078.38
Both	ATP synthase F1, gamma subunit	YP_846696.1	yes	4	23.61	131.72
Both	F0F1 ATP synthase subunit alpha	YP_846697.1	yes	45	44.27	1259.17
Both	F0F1 ATP synthase subunit delta	YP_846698.1	yes	8	35.11	200.65
Both	H+-transporting two-sector ATPase, B/B' subunit	YP_846699.1	yes	10	36.52	325.78
Both	dissimilatory sulfite reductase subunit B	CAC36213.1	yes	28	28.53	372.05
Both	DsrC family protein	YP_848146.1	yes	2	14.29	39.09
Both	adenylylsulfate reductase	YP_845177.1	yes	207	66.41	5998.74
Both	adenylylsulfate reductase, beta subunit	YP_845176.1	yes	9	39.19	279.19
Both	sulfate adenylyltransferase	YP_845175.1	yes	33	52.44	775.98
Both	urea ABC transporter, ATP-binding protein UrtD	YP_003009326.1	yes	4	35.41	191.37

‡The score is calculated by MASCOT and represents the significance of the match against the ALDC^{T} genome.

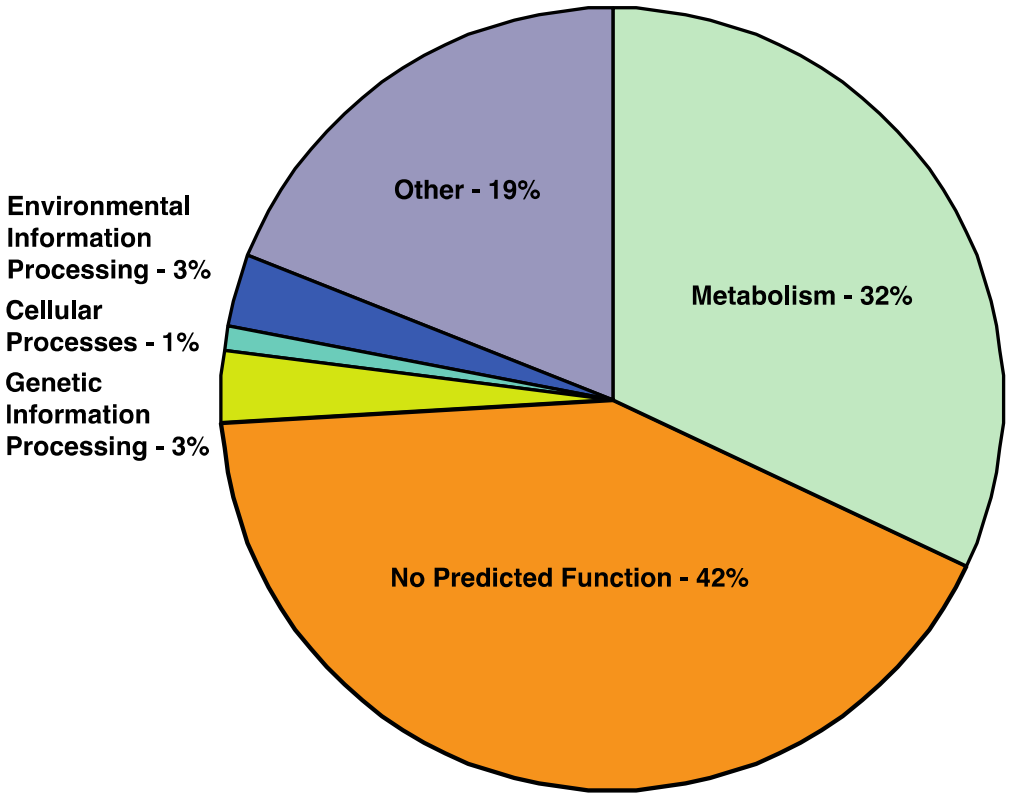

Figure 1. Functional gene categories from the Kyoto Encyclopedia of Genes and Genomes (KEGG) database for the *Desulfoglaeba alkanexedens* draft genome. A total of 2856 open reading frames (ORFs) were identified, and 56% of these have predicted function. ORFs identified as 'No Predicted Function' include proteins with BLAST hits against hypothetical proteins. The 'Cellular Processes' category includes proteins related to transport, cellular communication, cell motility, and cell growth. 'Genetic Information Processing' includes DNA replication and transcription, protein translation, and protein folding. 'Metabolism' includes all pathways related to carbon metabolism, energy metabolism, amino acid degradation, and alkane oxidation. The 'Other' category was used for identified proteins with annotated and predicted function not belonging to any previous category.

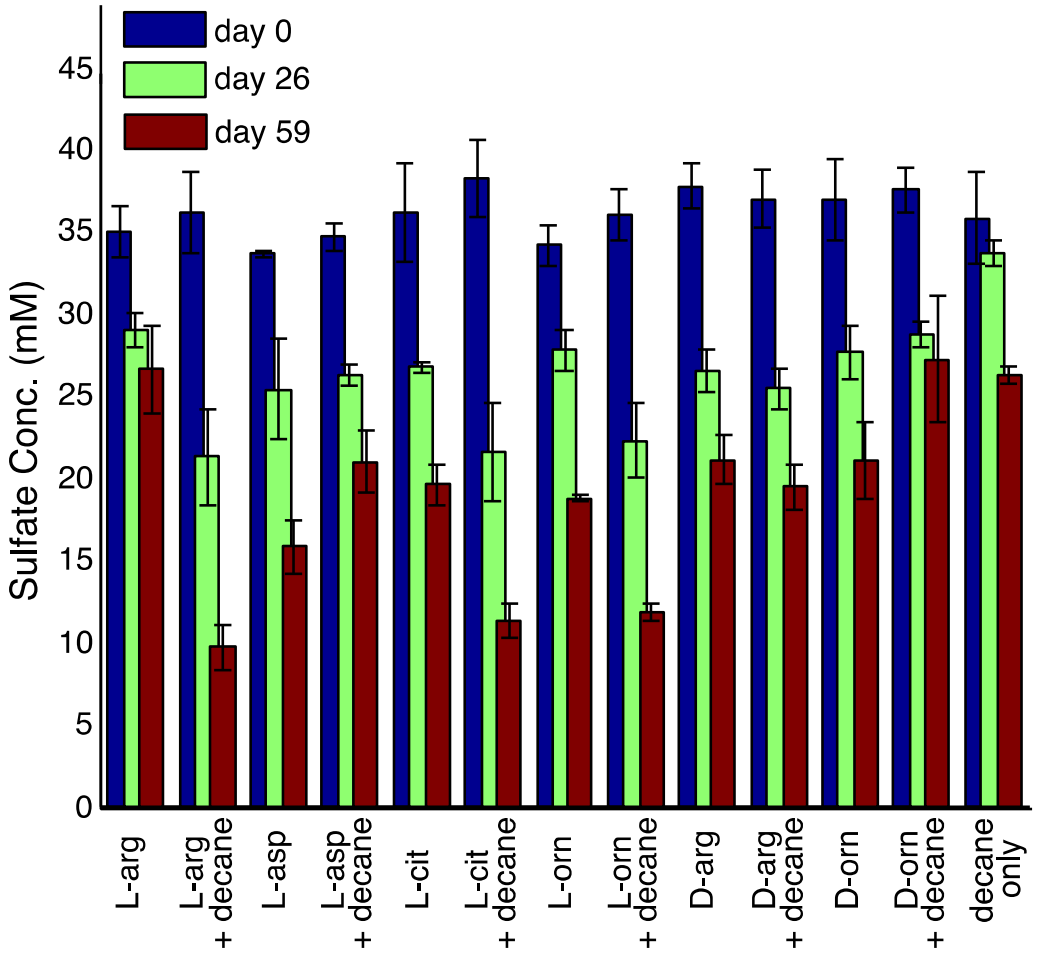

Figure 2. Sulfate reduction in *Desulfoglaeba* strain ALDC^{T} cultures in the presence and absence of *n*-decane and amended with selected amino acids (1mM). Abbreviations are *L*-arginine (*L-arg*), *L*-aspartate (*L-asp*), *L*-citrulline (*L-cit*), *L*-ornithine (*L-orn*), *D*-arginine (*D-arg*), and *D*-ornithine (*D-orn*).

CHAPTER 3

Investigating Carbon Sharing and Isotopic Enrichment in a Methanogenic, Hydrocarbon-Degrading Community

Abstract

Methanogenic hydrocarbon degradation can occur in petroleum-contaminated aquifers. However, the contribution of complete and incomplete hydrocarbon mineralization to overall carbon cycling, as well as the role of different methanogenic pathways to overall methane production in these environments is unclear. Carbon flow in a model methanogenic consortium capable of *n*-alkane mineralization was investigated using a combination of proteomics, stable isotope probing, and the measure of $\delta^{13}C$ enrichment in mineralization end products. Results show that ^{13}C from uniformally labeled substrates was distributed evenly among consortium members in the presence of oil, and used by a small majority of the community members when provided only in the form of fatty acids. Therefore, syntrophy plays a larger role during the mineralization of hydrocarbon compounds. In addition, patterns of $\delta\ ^{13}C$ enrichment for methane and CO_2 in the presence and absence of oil also suggests that complex microbial interactions occur during methanogenic hydrocarbon mineralization. For example, the $\Delta\delta\ ^{13}C$ of CO_2 was statistically identical in all incubations irrespective of oil presence, but the $\Delta\delta\ ^{13}C$ for methane

was greater in the presence of oil compared to fatty acids alone. In all incubations, aceticlastic and hydrogenotrophic methanogens incorporated ^{13}C into their proteomes to an equal extent, suggesting that one pathway is not dominant during methanogenic hydrocarbon decay in this model consortium. Stable isotope probing of proteins identified signature enzymes responsible for methanogenesis from CO_2 and acetate labeled with 78.0 ± 4.4 % and 73.3 ± 1.0 % ^{13}C, respectively. A protein capable of catalyzing fumarate addition to a hydrocarbon was not found. Five proteins were identified only in the sole presence of hydrocarbons, including a polyphosphate kinase, CheA signal transduction histidine kinase, argininosuccinate lyase, cellulase, and a resolvase-like protein. Collectively, this study suggests that each organism in this enrichment culture fills a unique niche, and may contribute to the capacity for methanogenic hydrocarbon mineralization in ways that are previously unrecognized.

Introduction

Much of the Earth's biosphere is anoxic and the anaerobic cycling of organic matter is known to involve a stepwise biodegradation of labile substrates to acetate, propionate, butyrate, CO_2, and hydrogen (10, 52). In the presence of exogenous electron acceptors, this process will usually be sulfidogenic. Methanogenesis represents the terminal electron-accepting process in the absence of oxygen or other electron acceptors and plays an essential function in

removal of acetate, CO_2, and H_2 (4, 76). Anaerobic hydrocarbon decay coupled to sulfate reduction or methanogenesis has received considerable attention due to 'weathering' of crude oil and consequences for energy recovery and processing (39). Beneficially, it has been proposed to use microorganisms as biocatalysts for the recovery of marginal hydrocarbon reserves, or for remediation of spilt contaminants (3, 9, 33, 34, 56, 67). The detection of anaerobic hydrocarbon-degrading bacteria and methanogenic archaea in petroleum reserves is now common (21, 32, 50, 60), yet the nature of signaling and electron flow between these organisms is unresolved.

Early evidence for the involvement of anaerobic prokaryotes in the degradation of hydrocarbons came from the recognition that sulfate-reducing bacteria were present in formation waters of oil fields and that oils were being altered by their activities (6, 48). This observation is now widely documented (see (72) for a review). Geologists have recognized that natural gas can be distinguished as either thermogenic or biogenic based on the $\delta^{13}C$ composition of formation gases (71). Methane $\delta^{13}C$ composition from -120 to -50 ‰ VPDB is diagnostic of a bacterial origin for the gases (55). A large deuterium kinetic isotope effect (KIE) has also been observed during microbially-mediated methanogenesis (70). In 1999, Zengler *et al*. (75) provided the first evidence of a microbial enrichment performing methanogenic hydrocarbon decay under laboratory conditions. Methanogenic hydrocarbon degradation has now been studied in some detail (2, 33, 69, 73). At least five possible routes for hydrocarbon conversion to methane can be postulated, ranging from the

complete oxidation of alkanes to CO_2 and hydrogen, with methane being produced only by CO_2 reduction, to incomplete oxidation of hydrocarbons to acetate with the involvement of syntrophic acetate oxidation or aceticlastic methanogens (20). Several modeling and experimental studies have concluded that syntrophic acetate oxidation does occur under *in situ* conditions in petroleum reservoirs (4, 20, 51).

A model methanogenic enrichment culture was chosen for this study based on its capacity for hydrocarbon degradation. The microbial consortium has been shown to degrade several hydrocarbon classes including alkylbenzenes, saturated and aromatic hydrocarbons, alicyclic hydrocarbons, and crude oil constituents under both sulfate reducing and methanogenic conditions (24, 34, 35, 62, 69). Interestingly, carbon substrates are more efficiently utilized by this consortium in the presence of a solid growth matrix (33). The chief interest of this study lay in identifying upstream and downstream metabolism of fatty acids during methanogenic hydrocarbon decay. Under anaerobic conditions, hydrocarbons are activated to fatty acids and subsequently degraded via β-oxidation (73). Therefore, this study was undertaken to, (a) identify the dominant hydrocarbon activation strategy in the consortium, (b) identify the proportion of complete and incomplete carbon mineralization to overall carbon throughput, and (c) elucidate the principal pathway for methanogenesis in the presence and absence of hydrocarbons. Oil-containing or oil-free sand grounds were supplied to the methanogenic consortium, each amended with an unlabeled and ^{13}C labeled model straight-chain fatty acid or *n*-

alkane. Primary characterization of overall carbon metabolism was achieved by measuring the $\delta^{13}C$ for carbon dioxide and methane gas in the presence or absence of oil. Better resolution of the kinetics of carbon fluxes was realized by monitoring ^{13}C incorporation into proteomes of consortium members using a pseudo-metagenome. Principal pathways for methanogenesis were elucidated using stable isotope probing (SIP) of proteins. This technique was recently introduced and has been used to demonstrate activity of individual members in anoxic microbial consortia (41, 43).

Materials and Methods

Microorganisms and Media Preparation

A model hydrocarbon-degrading methanogenic consortium was enriched from a gas condensate-contaminated aquifer as previously described (34). The culture was cultivated in the presence of crushed oil-bearing sandstone core material prior to the start of the experiments (67) and maintained by repeated transfer (10% v/v) to a reduced, sulfate-free, anaerobic minimal-salts medium (33) containing resazurin, trace metals, and a vitamin solution (68). The sandstone core was extracted from a depth of approximately 200m in a mature oil field in Nowata County, Oklahoma. Residual oil saturation of the sandstone averaged 0.013 g of oil per gram of core (33). Previous studies have show that the methanogenic consortium metabolizes substrates more effectively in the presence of a solid matrix (33). Therefore, the ground sandstone core or white

quartz sand (VWR, Darmstadt, Germany) in oil-free controls was supplied to the cultures to fulfill this requirement. The quartz sand was autoclaved and allowed to reduce in an anaerobic chamber prior to use.

The solid materials were amended with either ^{12}C- or uniformly ^{13}C-labeled hexadecane, palmitate, or stearate. The unlabeled replicates were used to measure $\delta^{13}C$ composition of mineralized end products (*i.e*. CO_2 and CH_4). The ^{13}C-labeled replicates were used for protein-SIP and community carbon-sharing studies. The amended chemicals (50 mg) were first dissolved in carriers (4 mL of hexane, in the case of hexadecane, or diethyl ether for the fatty acids) and added dropwise to the sandstone or quartz solids to ensure even distribution. The carriers were then volatilized under a stream of N_2 and the solids allowed to reduce in an anaerobic chamber. Prior to inoculation, 5 g of the amended sandstone material or quartz was added to 10 mL of sterile, reduced medium (33) and sealed with butyl rubber stoppers and aluminum crimp seals. The culture headspace was aseptically exchanged with N_2/CO_2 (80:20). The sandstone or quartz mixtures were then inoculated with a typical transfer and incubated at room temperature (25 ± 2º C) in the dark.

Protein Extraction

Proteins were extracted from the incubations using the method developed by Benndorf *et al*. to separate cells from sediments (7). At the completion of the experiment, the incubations were vortexed and placed in an ultrasonication water bath at 37º C for 10 min. The aqueous phase was removed and centrifuged (10

min; 13,000 X g; 4º C) to concentrate cells. The supernatant was replaced back onto the incubation solids and the process was repeated a total of 4 times. The combined cell pellet was suspended in 20mM Tris/HCl (pH 7.5). Cell lysis and protein extraction occurred by ultrasonication on ice for a period of 5 min (50% amplitude, Ultrasonic 250, Danbury, CT, USA). The cell lysate was centrifuged for 10 min at 10,000 X g at 4 º C. The pellets were mixed with 1mL of nanopure water containing 10 g of crystalline phenol, and shaken at 20 º C for 1 h to extract and purify proteins. The phenol phase was collected via centrifugation (10 min at 13.000 X g), and the proteins were precipitated using 5-fold volumes of 0.1 M ammonium acetate dissolved in methanol at -20 º C for 1 h. The precipitated proteins were collected by centrifugation (10 min at 13.000 X g at 4º C) and the resulting pellet was rehydrated in 0.1 M ammonium acetate in methanol, and incubated for 15 min at -20º C. This pellet was successively washed in 0.1 M ammonium acetate in methanol, 80% acetone, and 70% ethanol with each washing step including a 15 min incubation and centrifugation.

The protein pellet was digested overnight at 37℃ usin g trypsin. After digestion, the mixture was centrifuged for 10 minutes. The supernatant was carefully removed and dried using a vacuum centrifuge before storage at -20℃. Before mass spectral analysis, the peptides were redissolved in 30µL of 0.1% formic acid and purified two times using Zip-Tip purification and desalting according to manufacturer's instructions (Millipore, Billerica, MA).

Analytical Instruments and Techniques

Carbon isotope ratios of methane and carbon dioxide were determined by gas chromatography isotope ratio mass spectrometry (GC-IRMS) using a MAT 253 IRMS (Thermo Scientific, Bremen, Germany). The IRMS was coupled to an HP 6890 gas chromatograph (Agilent Technologies, USA) via combustion furnace (GC/C-III, Thermo Scientific, Bremen, Germany). Separation of methane and carbon dioxide was achieved on a CP-Porabond Q column (50m x 0.32mm x 0.5 μm, Varian Analytical Instruments, Netherlands) held isocratically at 60° C, using a split injection mode of 1:10, and a constant flow of helium at 2mL min^{-1}. For carbon isotope ratio analysis of methane and carbon dioxide, 10μL headspace samples were collected using a sterile, nitrogen-flushed Hamilton™ syringe and injected manually into the GC.

Protein Mass Spectrometry

The reconstituted peptides were injected by autosampler and concentrated on a trapping column (nanoAcquity UPLC column, C_{18}, 180 µm x 2 cm x 5 µm) with a mobile phase consisting of 0.1% formic acid at 15 µl/min. After 8 min, the peptides were eluted onto a separation column (nanoAcquity UPLC column, C_{18}, 75 µm x 25 cm x 1.75 µm). Chromatography was performed with a 0.1% formic acid/acetonitrile mobile phase, using a gradient of either 6 or 8 – 40% acetonitrile over a 185 min elution time using a nano-HPLC system (nanoAcquity, Waters, Milford, MA, USA) coupled to an LTQ-Orbitrap mass spectrometer (Thermo Fisher Scientific, Waltham, MA, USA). Continuous scanning of eluted peptide ions was carried out between 300 – 2000

m/z and peaks with a relative abundance exceeding 5000 units were analyzed by MS/MS in the collision induced dissociation mode, with the dynamic precursor exclusion feature enabled for 3 min.

Data Analysis

Protein identities were ascertained from peptide fragment sequences using Mascot and Proteome Discoverer (Thermo Scientific). A custom pseudo-metagenomic database was built for this study, based upon a previously published 16S clone library of the methanogenic enrichment (33). The database contained the amino acid sequences for every open reading frame (ORF) in the following genomes: *Anaeromyxobacter dehalogenans* 2CP-1, *Chloroflexus aggregans*, *Clostridium cellulolyticum* H10, *Clostridium thermocellum* ATCC 27405, *Desulfatibacillum alkenivorans* AK-01, *Desulfoglaeba alkanexedens* ALDC, *Desulfobulbus propionicus* Lindhorst, *Desulfotomaculum reducens* MI-1, *Desulfovibrio desulfuricans* G20, *Desulfovibrio vulgaris* Hildenborough, *Methanoculleus marisnigri* JR1, *Methanosaeta thermophila* PT, *Methanosarcina barkeri* fusaro, *Methanospirillum hungatei* JF-1, and *Syntrophus aciditrophicus* SB. A Boolean basis was used to assess differentially expressed proteins identified by comparing all identified ORFs in both oil-free and oil-containing replicates.

The intensity of aggregate ^{13}C-label incorporation into the pseudo-metaproteome was calculated using a method based on the peptide 'half decimal place rule' (28). The rule describes characteristic patterns of decimal masses for

trypsin-digested peptides. The slope of the linear relationship between peptide mass and decimal residual is proportional to the degree of ^{13}C contained in the peptide. A total of 100 peptides must be identified for significance levels of $P < 0.05$. This rule is also useful for detecting non-peptide contaminants in protein samples (28).

Results

Isotopic enrichment of mineralized end products

In order to investigate the principal methanogenic processes in the hydrocarbon-degrading consortium, the $\delta^{13}C$ signature of the culture headspace gases was analyzed. The stable carbon isotope content of methane and carbon dioxide were measured during the methanogenic biodegradation of fatty acids in both the presence and absence of oil. It is known that the $\delta^{13}C$ for methane produced via CO_2 reduction is more negative (contains less ^{13}C) than that produced during aceticlastic methanogenesis. Further, carbon stable isotope fractionation is high during CO_2 reduction and low during aceticlastic methanogenesis (*i.e*. equal to $\delta^{13}C$ of 75‰ versus $\delta^{13}C$ of 10‰, respectively (15, 57)). Signature patterns of mineralized end products were evident during the anaerobic biodegradation of fatty acids or hexadecane depending on the availability of residual oil (Figure 1A-1D). When the model inoculum was incubated (49 d) in the presence of residual oil and amended with hexadecane, the $\delta^{13}C$ of methane and CO_2 increased from -85.11 ± 9.98‰ to -48.39 ± 2.13‰

and from -21.34 ± 1.58‰ to -11.10 ± 0.56‰, respectively (Figure 1C). Similarly, the $\delta^{13}C$ of methane increased from -74.59 ± 22.18‰ and -84.06 ± 11.39‰ to -45.09 ± 4.81‰ and -48.39 ± 2.13‰ in the palmitate- and stearate-amended incubations in the presence of oil, respectively (Figure 1D). The comparable $\delta^{13}C$ of CO_2 in the C_{16} and C_{18} fatty acid-amended incubations increased from -16.77 ± 0.64‰ to -7.84 ± 0.59‰ and -17.89 ± 0.11‰ to -12.01 ± 0.15‰, respectively (Figure 1D). Therefore, the overall $\Delta\delta^{13}C$ increase in the presence of residual-oil bearing core amended with either fatty-acids or hexadecane was 33.96 ± 3.90‰ and 8.53 ± 2.24‰ for CH_4 and CO_2 respectively.

A much different stable carbon isotope pattern for CH_4 and CO_2 was evident when the same fatty-acid amendments were metabolized by the model inoculum in the absence of oil (Fig. 1B). Since the inoculum performed better in the presence of a solid matrix (26), the sandstone material was replaced with sterile quartz sand of similar grain size. Over the course of the incubation, the $\delta^{13}C$ of CH_4 remained relatively stable in both of the fatty acid-amended incubations, ranging from -56.65 ± 0.06‰ to -53.59 ± 3.35‰ in the presence of stearate and from -44.72 ± 0.41‰ to -46.44 ± 2.00‰ in the presence of palmitate (Figure 1B). While the $\delta^{13}C$ signature for methane was statistically identical when only fatty acids were present as a carbon source, the $\delta^{13}C$ signature for CO_2 increased from -14.71 ± 0.47‰ and -14.27 ± 0.07‰ to -8.54 ± 0.23‰ and -8.32 ± 0.04‰, in the palmitate and stearate-amended incubations, respectively (Figure 1B). Thus, a $\Delta\delta^{13}C$ for methane during fatty acid biodegradation was not observed and was similar to the values observed during residual-oil

biodegradation in the case of CO_2 ($\Delta\delta\ ^{13}C$ 6.06 ± 0.16‰). On the other hand, incubations containing only hydrocarbons in the form of oil or hexadecane exhibited a $\Delta\delta\ ^{13}C$ increase averaging 33.96 ± 3.90‰ (Figure 1C). The $\delta\ ^{13}C$ for carbon dioxide was relatively constant during this portion of the experiment, increasing on the order of 3 ‰ over the inoculum only control. The large $\Delta\delta\ ^{13}C$ for methane in the presence of hydrocarbons minimally suggests that multiple pathways of methanogenesis are involved during biodegradation processes. It is assumed that the light $\delta\ ^{13}C$ methane signature ranging from -93 to -73 ‰ observed during early methanogenesis (*e.g*. 0-20 days) arises from hydrogenotrophic methanogenesis. Carbon $\delta^{13}C$ values in this range are diagnostic of CO_2 reduction coupled to biomethanation (14). The $\Delta\delta\ ^{13}C$ for methane and CO_2 in the inoculum only control were small, with values of 13.68 ± 9.67‰ and 5.46 ± 3.86‰, respectively (Figure 1A).

Protein labeling in the methanogenic consortium

After approximately 90% of the amended fatty acid substrates were biodegraded (based on the stoichiometrically expected amount of methane produced - data not shown), proteins were extracted, enzymatically-digested with trypsin, and analyzed by LTQ-Orbitrap mass spectrometry. Bacterial and archaeal members of the enrichment were previously identified using clone library analysis (33). Based on this information, a pseudo-metagenome was constructed using the closest known organisms with an available complete genome sequence. In addition, a draft genome sequence of *Desulfoglaeba*

alkanexedens (see Chapter 2) and a complete genome sequence of the *n*-alkane degrading, sulfate-reducing bacterium (SRB) *Desulfatibacillum alkenivorans* AK-01 (Callaghan *et al., in press*) were included as alkane-degrading representatives. Other members of the pseudo-metagenome used for protein identification included incomplete-oxidizing SRB such as *Desulfovibrio vulgaris* and *Desulfovibrio desulfuricans*, fatty-acid oxidizing specialists such a *Syntrophus aciditrophicus* strain SB, *Clostridales*, and representative methanogenic *Archaea* capable of hydrogenotrophic, methylotrophic, and aceticlastic methanogenesis (76).

The overall ^{13}C incorporation into the proteome of each organism represented in the pseudo-metagenome was calculated and is illustrated in Figure 2. Consistent with the patterns of $\delta\ ^{13}C$ incorporation into methane and CO_2 as a function of the availability of oil, different degrees of stable isotope incorporation into the aggregate proteomes was observed (Figure 2). The carbon distribution among the community members is more uniform when the residual oil is present versus when a fatty acid was provided as a carbon source alone. In the presence of palmitate and oil, the overall incorporation of ^{13}C into labeled members of the community was 74 ± 5.36% and homogeneous among labeled constituents (Figure 2). In the presence of stearate and oil, the ^{13}C incorporation was 63 ± 6.36%, however the values ranged from 53% in *Anaeromyxobscter dehalogenans* to 73% in *Clostridium cellulolyticum* and might suggest a slight dominance of *Clostridia*-like organisms under these conditions. It is common for hydrocarbon-degrading SRB to have a narrow hydrocarbon

substrate range (19, 72), one notable exception being the nitrate-reducing strain HdN1 with an alkane substrate range of C_6 to C_{30} (74). Therefore, the slightly higher labeling in *C. cellulolyticum* may suggest that fermentative organisms such as *Clostridiales* play a bigger role in the degradation of long-chain fatty acids, although it has been suggested that they are capable of hydrocarbon degradation as well (49). Proteins belonging to *Syntrophus aciditrophicus*-like organisms were only labeled in the palmitate-amended core samples. The genus *Syntrophus* contains organisms that syntrophically degrade saturated and aromatic fatty acids in the presence of a hydrogen-utilizing SRB or methanogen (53). Related 16S sequences are commonly found in hydrocarbon-laden environments (32, 33, 44, 75) and our data reveal that cooperative metabolism is a more important process in the presence of residual-oil. Interestingly, in the lone presence of the fatty acid stearate, community labeling only occurred in the incompletely oxidizing SRB *Desulfovibrio vulgaris* and in both aceticlastic and hydrogenotrophic methanogens (Figure 2). This, along with the protein labeling patterns in the oil-free sample would suggest that the fatty acid is degraded by rapidly-growing SRB to acetate, the acetate is used to make methane by obligate aceticlastic *Archaea*, and the residual CO_2 is further reduced to methane by hydrogenotrophic methanogens.

It has been suggested that crude-oil biodegradation in the subsurface proceeds mainly via acetogenic alkane degradation and syntrophic acetate oxidation coupled to hydrogenotrophic methanogenesis, with a preferential removal of *n*-alkanes (44, 51). During a previous study with the enrichment,

preferential alkane utilization from the residual oil was observed (33). Archaeal 16S sequences were predominantly associated with the obligate aceticlastic genus *Methanosaeta*, although *mcrA* sequences from H_2/formate utilizing-species could be recovered after addition of H_2 and CO_2 to the headspace (33). In the present study, the labeling of methanogenic species differed depending on the availability of oil in the system (Figure 2). In the oil-containing, palmitate-amended sample, the hydrogenotrophic methanogens closely related to *Methanoculleus marisnigri* and *Methanospirillum hungatei* were labeled to a similar extent (75% and 72%, respectively), and the aceticlastic *Methanosaeta thermophila*-like organisms had 77% ^{13}C incorporation into their proteome. In addition, the methanogenic generalist *Methanosarcina barkeri*, capable of aceticlastic, hydrogenotrophic, and methylotrophic methane production (29), had an aggregate ^{13}C level of 69%. However, in the stearate-amended oil-containing samples, labeling for the methanogenic community was observed in hydrogenotrophic species, and generalists similar to *Methanosarcina barkeri*.

Protein-based stable isotope probing

An important aspect of microbial ecology is to link natural, microbially-driven processes to specific members of a community (54). Protein-based stable isotope probing (proteinSIP) was recently introduced and represents a sensitive method for determining bacterial growth and metabolic carbon flow in complex microbial consortia (40, 42, 43). Therefore, this method was chosen to further characterize the carbon flow in the system, and to elucidate the type of

methanogenesis active during hydrocarbon decay. The methanogenic pathways are very similar, although they differ in key reactions generating either methyl-tetrahydrosarcinapterin (CH_3-H_4SPT) in the case of aceticlastic, or methyl-tetrahydromethanopterin (CH_3-H_4MPT) in the case of hydrogenotrophic methanogenesis (26, 27, 76). The two main pathways also differ in the source of electrons used during the exergonic reduction of the heterodisulfide (CoM-S-S-CoB) to coenzyme M (HS-CoM) and coenzyme B (HS-CoB) (45). During aceticlastic methanogenesis the electrons come from the carbonyl group of acetate (27), or come from the oxidation of hydrogen in the CO_2 reduction pathway (26, 76). Specifically, two subunit heterodisulfide reductases (HdrDE) catalyze the terminal electron transport in the aceticlastic pathway, and three subunits heterodisulfide reductases (HdrABC) catalyze the reaction in obligate CO_2 reducers. In addition, for aceticlastic methanogens, there are two ways that acetate can be activated, exemplified by the *Methanosaeta* model using AMP-forming acetyl-CoA synthetase or the *Methanosarcina* mechanism using the combined action of acetate kinase and phosphotransacetylase (63). Therefore, aggregate protein stable isotope incorporation into proteins that catalyze the formation of these signature intermediates for each methanogenic pathway was determined, in the presence or absence of residual-oil (Table 1).

In the palmitate-amended, oil-containing sample, evidence for the activity of all three methanogenic pathways was found, *i.e.* hydrogenotrophic, methylotrophic, and aceticlastic (Table 1). Four unique peptides from the N^5, N^{10}-methylenetetrahydromethanopterin (CH_2=H_4MPT) reductase related to

Methanoculleus marisnigri were identified and had an average ^{13}C incorporation of 78 ± 4.4%. This value agrees with the labeling intensity seen in the proteome of related-organism (Figure 2). The CH_2=H_4MPT reductase catalyzes an intermediate step during hydrogenotrophic methanogenesis, reducing CH_2=H_4MPT to CH_3-H_4MPT (46). Evidence for aceticlastic methanogenesis came from the identification of two unique peptides associated with *Methanosaeta thermophila* and containing 73.3 ± 1.0% ^{13}C. Lastly, tetrahydromethanopterin S-methyltransferase (subunit A) was identified from *Methanospirillum hungatei* and contained 68.9 ± 0.34% heavy carbon. This enzyme catalyzes the first step of the oxidative branch of methylotrophic methanogenesis, transferring the methyl group from coenzyme M to tetrahydromethanopterin (66). This finding supports the overall labeling intensity throughout the community (Figure 2) and suggests that all three types of methanogenesis are active in the sample containing palmitate and oil.

In the stearate-amended oil-containing and oil-free samples, proteins related to methanogenesis were labeled, but signature proteins attributable to specific pathways could not be detected with absolute certainty. There was more evidence for active methanogenesis in the oil-free stearate sample, as two separate gamma subunits of methyl-coenzyme M reductase were detected with labeling intensities of 59.4 ± 0.6% and 59.0 ± 2.7% (Table 1). Methyl-CoM reductase catalyzes the terminal step of biogenic methane production and is considered to be a diagnostic indication of methanogenesis (23, 38). In addition, two unique peptides from a Na^+-transporting ATPase related to *Methanosaeta*

thermophila were detected. The average ^{13}C labeling calculated for this protein was 57.8 ± 2.3%. The growth of methanogenic *Archaea* is dependent upon the presence of Na^+ ions at a concentration greater than 1mM (36, 58, 59), and is required for all substrates except methanol (8). Methanol is not an expected metabolite of anaerobic hydrocarbon degradation and methanogenesis is expected to be Na^+-dependent in our system. However, methylotrophic-related proteins were detected in the oil-containing palmitate sample, possibly suggesting the formation and use of methylated-compounds (*e.g.,* methylamines) from the residual-oil constituents.

Differentially expressed proteins

Very few differences in protein expression patterns could be identified in the oil-containing and oil-free replicates. Part of the motivation in this study lay in elucidating the hydrocarbon activation strategies used by this microbial consortium. No proteins capable of catalyzing fumarate addition to a hydrocarbon moiety could be detected. However, a CheA signal transduction histidine kinase was detected in hydrocarbon-only samples. This protein subunit holds a key function in bacterial chemotaxis, accepting a signal from a methyl-accepting chemotaxis protein, autophosphorylating, and signaling downstream for flagellum rotation (30, 31). Polyphosphate kinase was also detected. The biological role of long and short polyphosphates is still under debate, but may be involved in energy storage or biofilm formation (12). Interestingly, a key enzyme involved in the liberation of fumarate during biogenesis of arginine-family amino

acids was detected only in the presence of hydrocarbons. Recently, this phenomenon was also observed during *n*-alkane biodegradation by *Desulfoglaeba alkanexedens* strain ALDC^{T} (see Chapter 2). Lastly, cellulase and resolvase-like proteins were also detected solely in the presence of hydrocarbons.

Discussion

The δ^{13}C enrichment of carbon dioxide and methane was examined during the methanogenic biodegradation of fatty acids in the presence and absence of oil. Signature patterns of δ^{13}C were apparent when δ^{13}C ‰ of methane was plotted against that measured for carbon dioxide (Figure 1). The δ^{13}C ‰ signatures for methane in the fatty acid-amended oil-free incubations are stable and suggest that one dominating mechanism is primarily responsible for producing the bulk of the methane over the course of the incubation (Figure 1B). It is assumed that the fatty acids are biodegraded to acetate by incompletely oxidizing SRB and aceticlastic methanogens produce a major portion of the methane under these conditions. However, the incorporation of ^{13}C into the proteome of *Methanospirillum*-like organisms suggested a role for hydrogen- or formate-utilizing methanogens in the enrichment culture as well.

Identified proteins attributable to specific members of the pseudo-metagenome were binned and ^{13}C enrichment was calculated using the method described by Fetzer *et al.* (28). The carbon labeling was distributed in a relatively

uniform manner amongst the organisms in the palmitate-amended, oil-containing samples. However, when stearate was amended to the oil-containing sand, no ^{13}C labeling was found in SRB generalists or known alkane-degrading organisms. The overall distribution of the label was more narrow, and existed only in *Anaeromyxobacter-, Chloroflexus-,* and *Clostridium-like* bacteria, and in methanogenic archaea with the collective capacity for methylotrophic, hydrogenotrophic, and aceticlastic methanogenesis (Figure 2). This might suggest that fermentative organisms play a greater role in the degradation of higher molecular weight fatty acids. Some evidence for this proposition exists, as several model SRB cannot degrade compounds larger than C_{18} (5, 18, 47, 65) possibly due to transport issues, substrate binding, or solubility limitations.

All known bacterial isolates with the capacity for hydrocarbon activation via fumarate-addition exhibit very narrow *n*-alkane substrate ranges, including *Betaproteobacteria* and *Deltaproteobacteria*. For example, *Desulfoglaeba alkanexedens* ALDC^T has an alkane substrate range of *n*-C_6-C_{12}, *Desulfatibacillum alkenivorans* has a substrate range of *n*-C_{13}-C_{18}, *n*-C_6-C_8 for the denitrifying *Azoarcus* strain HxN1, and *n*-C_{13}-C_{18} for strain CV2803 (11, 16-18, 22, 37, 61, 65). Bacterial isolates with other anaerobic alkane activation strategies exhibit much greater ranges; from *n*-C_{12}-C_{20} in *Desulfococcus oleovorans* strain Hxd3 to *n*-C_6-C_{30} in the denitrifying strain OcN1 (1, 64, 74). With regard to the methanogenic consortium used in this study, *n*-alkane loss was measured by GC-MS for molecules extending from *n*-C_{12}-C_{34} (33). No proteins related to alkylsuccinate synthase or benzylsuccinate synthase could be

detected during the experiment described herein. Taken together with the fact that signature fumarate-addition metabolites have never been detected in this enrichment (unpublished observation), it is postulated that hydrocarbon activation occurs via an alternative mechanism.

ProteinSIP was used to elucidate the carbon flow into different methanogenic members of the consortium and to determine the predominant pathways by targeting key enzymes. Overall, the majority of identified proteins in the palmitate-amended oil-containing samples could be attributed to methanogens, and specifically to hydrogenotrophic methanogens. Labeling in aceticlastic archaea, and labeled peptides attributable to the aceticlastic pathway including the AMP-forming acetyl-CoA synthetase (Table 1) were detected. The activity of aceticlastic methanogens was confirmed by detecting ^{13}C incorporation into *Methanosaeta thermophila*-like organisms.

The cooperative degradation of terrestrial organic matter relies upon the coordinated activities of four groups of microorganism, (*i*) hydrolytic and fermenting bacteria, (*ii*) homoacetogenic bacteria, (*iii*) proton-reducing bacteria (*i.e.* syntrophs), and (*iv*) methanogenic archaea (13). It can be expected that the methanogenic mineralization of hydrocarbons be accomplished in a similar manner. In fact, syntrophic species are routinely detected in hydrocarbon-impacted environments along with fermentative organisms, aceticlastic, and hydrogenotrophic methanogens (21, 32, 33, 44, 60, 75). However, interest has focused on identifying the dominant methanogenic pathway in subsurface environments, as research into the feasibility of increasing the recovery of

entrenched natural gas from hydrocarbons continues (20, 33, 39, 44). The subsurface methanogenic process has been modeled using Rayleigh-type isotope fractionation (see (25) for a review) and investigated in several oil reservoirs (44). The current consensus is that hydrogenotrophic methanogenesis and syntrophic acetate oxidation are coupled to hydrocarbon mineralization to acetate and hydrogen gas (44, 51). Our enrichment was derived from a gas condensate-contaminated aquifer on the interior Great Plains of the central United States (34). The overall methanogenic conversion in this enrichment culture should share fundamental similarities with other subsurface-derived enrichments. A degree of syntrophic acetate oxidation would explain several observations in this study. First, the distribution of ^{13}C throughout a syntrophic community would be expected to be more uniform, as observed for palmitate-amended, oil-containing incubations (Figure 2). Second, the $\delta^{13}C$ values for methane should remain below -60 ‰, as little free CO_2 is converted to methane under this scenario and $\delta\ ^{13}C$ values for methane would be close to those seen during aceticlastic methanogenesis (57). Measurements show that $\delta^{13}C$ for methane was below -60 ‰, although not until the latter stage of methane production (*i.e.* after 20 days, Figure 1C-1D). Initial methane $\delta\ ^{13}C$ was above -70 ‰ and characteristic of carbon dioxide reduction. It is likely that initial methanogenesis occurs via CO_2 reduction coupled with complete hydrocarbon mineralization to carbon dioxide. Syntrophs are slow-growing organisms and may have trouble competing for substrates during early phases of anaerobic carbon flow (53). However, as degradation proceeds, labile carbon substrates are

depleted and syntrophy becomes more important to the overall methanogenic process. Stoichiometric methane production accounted for 90% of the fatty acids amended to the incubations. Approximately 35% of the amended alkane was degraded during the same time frame. It is therefore possible that our endpoint-study missed the carbon incorporation into other members of the community, and that time points sampled during the course of biodegradation would provide better resolution of carbon flow in this community. A comparison of a U-^{13}C-hexadecane-amended incubation to the U-^{13}C-fatty acid samples was intended, but low protein yields resulted in low responses on the LTQ-Orbitrap and precluded this possibility. However, a shift in the methane production pattern occurred in this incubation after approximately 20 days, from hydrogenotrophic to aceticlastic methanogenesis (Figure 1C). In addition, this study demonstrated that the distribution of ^{13}C-label is more even in the presence of oil compared to fatty acids alone, in all likelihood due to syntrophic metabolism. In conclusion, methanogenesis can play an important part during anaerobic hydrocarbon degradation, but there is no overwhelming thermodynamic reason to expect one mode of methanogenesis to be active over another. This study provides evidence for simultaneous methane production via hydrogenotrophic and aceticlastic mechanisms during the biodegradation of oil and fatty acids.

Literature Cited

1. **Aeckersberg, F., F. Bak, and F. Widdel.** 1991. Anaerobic oxidation of saturated hydrocarbons to CO2 by a new type of sulfate-reducing bacterium. Arch. Microbiol. **156:**5-14.

2. **Anderson, R. T., and D. R. Lovley.** 2000. Hexadecane decay by methanogenesis. Nature **404:**722-723.

3. **Atlas, R. M.** 1995. Bioremediation of petroleum pollutants. Int. Biodeterior. Biodegrad. **35:**317-327.

4. **Balch, W. E., G. E. Fox, L. J. Magrum, C. R. Woese, and R. S. Wolfe.** 1979. Methanogens: reevaluation of a unique biological group. Microb. Rev. **43:**260-296.

5. **Balk, M., M. Altinbas, W. I. C. Rijpstra, J. S. S. Damste, and A. Stams, J. M.** 2008. *Desulfatirhabdium butyrativorans* gen. nov., sp. nov., a butyrate-oxidizing, sulfate-reducing bacterium isolated from an anaerobic bioreactor. Int. J. Syst. Evol. Micr. **58:**110-115.

6. **Bastin, E. S.** 1926. The presence of sulphate reducing bacteria in oil field waters. Science **63:**21-24.

7. **Benndorf, D., C. Vogt, N. Jehmlich, Y. Schmidt, H. Thomas, G. Woffendin, A. Shevchenko, H.-H. Richnow, and M. von Bergen.** 2009. Improving protein extraction and separation methods for investigating the metaproteome of anaerobic benzene communities within sediments. Biodegradation **20:**737-750.

8. **Blaut, M., and G. Gottschalk.** 1984. Coupling of ATP synthesis and methane formation from methanol and molecular hydrogen in *Methanosarcina barkeri*. Eur. J. Biochem. **141:**217-222.

9. **Bragg, J. R., R. C. Prince, E. J. Harner, and R. M. Atlat.** 1994. Effectiveness of bioremediation for the *Exxon Valdez* oil spill. Nature **368:**413-418.

10. **Bryant, M. P.** 1976. The microbiology of anaerobic degradation and methanogenesis with special reference to sewage, p. 107-117. *In* H. G. Schlegel and J. Barnea (ed.), Microbial energy conversion. Goltze KG, Goettingen.

11. **Callaghan, A. V., L. M. Gieg, K. G. Kropp, J. M. Suflita, and L. Y. Young.** 2006. Comparison of mechanisms of alkane metabolism under

sulfate-reducing conditions among two bacterial isolates and a bacterial consortium. Appl. Environ. Microb. **72:**4274-4282.

12. **Chen, W., R. J. Palmer, and H. K. Kuramitsu.** 2002. Role of polyphosphate kinase in biofilm formation by *Porphyromonas gingivalis*. Infect. Immun. **70:**4708-4715.

13. **Conrad, R.** 1989. Control of methane production in terrestrial ecosytems, p. 39-58. *In* M. O. Andreae and D. S. Schimel (ed.), Exchange of Trace Gases Between Terrestrial Ecosystems and the Atmosphere, vol. Dahlem Workshop Reports. Wiley, Chichester, UK.

14. **Conrad, R., M. Klose, P. Claus, and A. Enrich-Prast.** 2010. Methanogenic pathway, 13C isotope fractionation, and archaeal community composition in the sediment of two clear-water lakes of Amazonia. Limnol. Oceanogr. **55:**689-702.

15. **Conrad, R., M. Noll, P. Claus, M. Klose, W. R. Bastos, and A. Enrich-Prast.** 2011. Stable carbon isotope discrimination and microbiology of methane frormation in tropical anoxic lake sediments. Biogeosciences **8:**795-814.

16. **Cravo-Laureau, C., V. Grossi, D. Raphel, R. Matheron, and A. Hirschler-Rea.** 2005. Anaerobic n-alkane metabolism by a sulfate-reducing bacterium, *Desulfatibacillum aliphaticivorans* strain CV2803T. Appl. Environ. Microb. **71:**3458-3467.

17. **Cravo-Laureau, C., R. Matheron, J.-L. Cayol, C. Joulian, and A. Hirschler-Rea.** 2004. Desulfatibacillum aliphaticivorans gen. nov., sp. nov., an n-alkane- and n-alkene-degrading, sulfate-reducing bacterium. Int J Syst Evol Microbiol **54:**77-83.

18. **Davidova, I. A., K. E. Duncan, O. K. Choi, and J. M. Suflita.** 2006. *Desulfoglaeba alkanexedens* gen. nov., sp. nov., an *n*-alkane-degrading, sulfate-reducing bacterium. Int. J. Syst. Evol. Micr. **56:**2737-2742.

19. **Davidova, I. A., and J. M. Suflita.** 2005. Enrichment and isolation of anaerobic hydrocarbon-degrading bacteria. Methods Enzymol. **397:**17-34.

20. **Dolfing, J., S. R. Larther, and I. M. Head.** 2008. Thermodynamic constraints on methanogenic crude oil biodegradation. ISME **2:**442-452.

21. **Duncan, K. E., L. M. Gieg, V. A. Parisi, R. S. Tanner, S. G. Tringe, J. Bristow, and J. M. Suflita.** 2009. Biocorrosive thermophilic microbial communities in Alaskan North Slope oil facilities. Environ. Sci. Technol. **43:**7977-7984.

22. **Ehrenreich, P., A. Behrends, J. Harder, and F. Widdel.** 2000. Anaerobic oxidation of alkanes by newly isolated denitrifying bacteria. Archives of Microbiology **173:**58-64.

23. **Ellerman, J., R. Hedderich, R. Bocher, and R. K. Thauer.** 1988. The final step in methane formation. Investigations with highly purified methyl-CoM reductase (component C) from *Methanobacterium thermoautotrophicum* (strain Marburg). Eur. J. Biochem. **172:**669-677.

24. **Elshahed, M. S., L. M. Gieg, M. J. McInerney, and J. M. Suflita.** 2001. Signature metabolites attesting to the *in situ* attenuation of alkylbenzenes in anaerobic environments. Environ Sci Technol **35:**682-689.

25. **Elsner, M., L. Zwank, D. Hunkeler, and R. P. Schwarzenbach.** 2005. A new concept linking observable stable isotope fractionation to transformation pathways of organic pollutants. Environ. Sci. Technol. **39:**6896-6916.

26. **Ferry, J. G.** 1999. Enzymology of one-carbon metabolism in methanogenic pathways. FEMS Microbiol. Rev. **23:**13-38.

27. **Ferry, J. G.** 1992. Methane from acetate. J Bacteriol **174:**5489-5495.

28. **Fetzer, I., N. Jehmlich, C. Vogt, H. H. Richnow, J. Seifert, H. Harms, M. von Bergen, and F. Schmidt.** 2010. Calculation of partial isotope incorporation into peptides measured by mass spectrometry. BMC Res Notes **24:**178.

29. **Galagan, J. E., C. Nusbaum, A. Roy, M. G. Endrizzi, P. Macdonald, W. FitzHugh, S. Calvo, R. Engels, S. Smirnov, D. Atnoor, A. Brown, N. Allen, J. Naylor, N. Stange-Thomann, K. DeArellano, R. Johnson, L. Linton, P. McEwan, K. McKernan, J. Talamas, A. Tirrell, W. Ye, A. Zimmer, R. D. Barber, I. Cann, D. E. Graham, D. A. Grahame, A. M. Guss, R. Hedderich, C. Ingram-Smith, H. C. Kuettner, J. A. Krzycki, J. A. Leigh, W. Li, J. Liu, B. Mukhopadhyay, J. N. Reeve, K. Smith, T. A. Springer, L. A. Umayam, O. White, R. H. White, E. C. de Macario, J. G. Ferry, K. F. Jarrell, H. Jing, A. J. L. Macario, I. Paulsen, M. Pritchett, K. R. Sowers, R. V. Swanson, S. H. Zinder, E. Lander, W. W. Metcalf, and B. Birren.** 2002. The Genome of *M. acetivorans* reveals extensive metabolic and physiological diversity. Genome Res. **12:**532-542.

30. **Gegner, J. A., and F. W. Dahlquist.** 1991. Signal transduction in bacteria: CheW forms a reversible complex with the protein kinase CheA. Proceedings of the National Academy of Sciences **88:**750-754.

31. **Gegner, J. A., D. R. Graham, A. F. Roth, and F. W. Dahlquist.** 1992. Assembly of an MCP receptor, CheW, and kinase CheA complex in the bacterial chemotaxis signal transduction pathway. Cell **70:**975-982.

32. **Gieg, L. M., I. A. Davidova, K. E. Duncan, and J. M. Suflita.** 2010. Methanogenesis, sulfate reduction and crude oil biodegradation in hot Alaskan oilfields. Environ.Microbiol. **12:**3074-3086.

33. **Gieg, L. M., K. E. Duncan, and J. M. Suflita.** 2008. Bioenegy production via microbial conversion of residual oil to natural gas. Appl. Environ. Microb. **74:**3022-3029.

34. **Gieg, L. M., R. V. Kolhatkar, M. J. McInerney, R. S. Tanner, S. H. Harris, K. L. Sublette, and J. M. Suflita.** 1999. Intrinsic bioremediation of petroleum hydrocarbons in a gas condensate-contaminated aquifer. Environ. Sci. Technol. **33:**2550-2560.

35. **Gieg, L. M., and J. M. Suflita.** 2002. Detection of anaerobic metabolites of saturated and aromatic hydrocarbons in petroleum-contaminated aquifers. Environ. Sci. Technol. **36**.

36. **Gottschalk, G., and R. K. Thauer.** 2001. The Na+-translocating methyltransferase complex from methanogenic archaea. BBA - Bioenergetics **1505:**28-36.

37. **Grundmann, O., A. Behrends, R. Rabus, J. Amann, T. Halder, J. Heider, and F. Widdel.** 2008. Genes encoding the candidate enzyme for anaerobic activation of *n*-alkanes in the denitrifying bacterium, strain HxN1. Environ. Microbiol. **10:**376-385.

38. **Hallam, S. J., P. R. Girguis, C. M. Preston, P. M. Richardson, and E. F. DeLong.** 2003. Identification of methyl coenzyme M reductase A (mcrA) genes associated with methane-oxidizing archaea. Appl. Environ. Microbiol. **69:**5483-5491.

39. **Head, I. M., D. M. Jones, and S. R. Larter.** 2003. Biological activity in the deep subsurface and the origin of heavy oils. Nature **426:**344-352.

40. **Jehmlich, N., F. Schmidt, M. Hartwich, M. von Bergen, H.-H. Richnow, and C. Vogt.** 2008. Incorporation of carbon and nitrogen atoms into proteins measured by protein-based stable isotope probing (Protein-SIP). Rapid Comm. Mass Spec. **22:**2889-2897.

41. **Jehmlich, N., F. Schmidt, M. Taubert, J. Seifert, F. Bastida, M. von Bergen, H.-H. Richnow, and C. Vogt.** 2010. Protein-based stable isotope probing. Nat Protoc **5:**1957-1966.

42. **Jehmlich, N., F. Schmidt, M. Taubert, J. Seifert, M. von Bergen, H.-H. Richnow, and C. Vogt.** 2009. Comparison of methods for simultaneous identification of bacterial species and determination of metabolic activity by protein-based stable isotope probing (Protein-SIP) experiments. Rapid Comm. Mass Spec. **23:**1871-1878.

43. **Jehmlich, N., F. Schmidt, M. von Bergen, H.-H. Richnow, and C. Vogt.** 2008. Protein-based stable isotope probing (Protein-SIP) reveals active species within anoxic mixed cultures. ISME **2:**1122-1133.

44. **Jones, D. M., I. M. Head, N. D. Gray, J. J. Adams, A. K. Rowan, C. M. Aitken, B. Bennett, H. Huang, A. Brown, B. F. J. Bowler, T. Oldenburg, M. Erdmann, and S. R. Larter.** 2008. Crude-oil biodegradation via methanogenesis in subsurface petroleum reserviors. Nature **451:**176-180.

45. **Kaster, A.-K., J. Moll, K. Parey, and R. K. Thauer.** 2011. Coupling of ferredoxin and heterodisulfide reduction via electron bifurcation in hydrogenotrophic methanogenic archaea. P Natl. Acad. Sci. USA **108:**2981-2986.

46. **Kesen, M. A., and R. K. Thauer.** 1990. Purification and properties of N 5 , N 10-methylenetetrahydromethanopterin reductase from *Methanobacterium thermoautotrophicum* (strain Marburg). Eur. J. Biochem. **191:**187-193.

47. **Khelifi, N., V. Grossi, M. Hamdi, A. Dolla, J.-L. Tholozan, B. Ollivier, and A. Hirschler-Rea.** 2010. Anaerobic oxidation of fatty acids and alkenes by the hyperthermophilic sulfate-reducing Archaeon *Archaeoglobus fulgidus*. Appl. Environ. Micro. **76:**3057-3060.

48. **Krejci-Graf, K.** 1932. Rule of density in oils. Bull. Am. Assoc. Petrol. Geol. **16**.

49. **Kunapuli, U., T. Lueders, and R. U. Meckenstock.** 2007. The use of stable isotope probing to identify key iron-reducing microorganisms involved in anaerobic benzene degradation. ISME **1:**643-653.

50. **Magot, M.** 2005. Indigenous microbial communities in oil fields. *In* B. Ollivier and M. Magot (ed.), Petroleum Microbiology. ASM Press, Washington, D. C.

51. **Mayumi, D., H. Mochimaru, H. Yoshioka, S. Sakata, H. Maeda, Y. Miyagawa, M. Ikarashi, M. Takeuchi, and Y. Kamagata.** 2011. Evidence for syntrophic acetate oxidation coupled to hydrogenotrophic methanogenesis in the high-temperature petroleum reservoir of Yabase oil field (Japan). Environ. Microbiol. **13:**DOI: 10.1111/j.1462-2920.2010.02338.x.

52. **McInerney, M. J., and M. P. Bryant.** 1981. Basic principles of bioconversions in anaerobic digestion and methanogenesis, p. 277-296. *In* S. S. Sofer and O. R. Zaborsky (ed.), Biomass Conversion Processes for Energy and Fuels. Plenum.

53. **McInerney, M. J., L. Rohlin, H. Mouttaki, U. Kim, R. S. Krupp, L. Rios-Hernandez, J. Sieber, C. G. Struchtemeyer, A. Bhattacharyya, J. W. Campbell, and R. P. Gunsalus.** 2007. The genome of Syntrophus aciditrophicus: Life at the thermodynamic limit of microbial growth. P. Natl. Acad. Sci. USA **104:**7600-7605.

54. **Neufeld, J. D., M. Wagner, and J. C. Murrell.** 2007. Who eats what, where and when? Isotope-labelling experiments are coming of age. ISME **1:**103-110.

55. **Pallasser, R. J.** 2000. Recognising biodegradation in gas/oil accumulations through the d13C compositions of gas components. Organ. Geochem. **31:**1363-1373.

56. **Parisi, V. A., G. R. Brubaker, M. J. Zenker, R. C. Prince, L. M. Gieg, M. L. B. da Silva, P. J. J. Alvarez, and J. M. Suflita.** 2009. Field metabolomics and laboratory assessments of anaerobic intrinsic bioremediation of hydrocarbons at a petroleum-contaminated site. Microb. Biotechnol. **2:**202-212.

57. **Penning, H., P. Claus, P. Casper, and R. Conrad.** 2006. Carbon isotope fractionation during acetoclastic methanogenesis by *Methanosaeta concilii* in culture and a lake sediment. Appl. Environ. Micro. **72:**5648-5652.

58. **Perski, H.-J., J. Moll, and R. K. Thauer.** 1981. Sodium Dependence of Growth and Methane Formation in *Methanobacterium thermoautotrophicum*. Arch. Microbiol. **130:**319-321.

59. **Perski, H.-J., P. Schoenheit, and R. K. Thauer.** 1982. Sodium dependence of methane formation in methanogenic bacteria. FEBS Lett. **143:**323-326.

60. **Pham, V. D., L. L. Hnatow, S. Zhang, R. D. Fallon, S. C. jackson, J.-F. Tomb, E. F. DeLong, and S. J. Keeler.** 2009. Characterizing microbial diversity in petroleum wather from an Alaskan mesothermic petroleum reservior with two independent molecular methods. Environ. Microbiol. **11:**176-187.

61. **Rabus, R., H. Wilkes, A. Behrends, A. Armstroff, T. Fischer, A. J. Pierik, and F. Widdel.** 2001. Anaerobic initial reaction of n-alkanes in a denitrifying bacterium: Evidence for (1-methylpentyl)succinate as initial product and for involvement of an organic radical in n-hexane metabolism. J. Bacteriol. **183:**1707-1715.

62. **Rios-Hernandez, L. A., L. M. Gieg, and J. M. Suflita.** 2003. Biodegradation of an alicyclic hydrocarbon by a sulfate-reducing enrichment from a gas condensate-contaminated aquifer. Appl. Environ. Microb. **69:**434-443.

63. **Smith, K. S., and C. Ingram-Smith.** 2007. *Methanosaeta*, the forgotten methanogen? Trends. Microbiol. **15:**150-155.

64. **So, C. M., C. D. Phelps, and L. Y. Young.** 2003. Anaerobic transformation of alkanes to fatty acids by a sulfate-reducing bacterium, strain Hxd3. Appl. Environ. Microbiol. **69:**3892-3900.

65. **So, C. M., and L. Y. Young.** 1999. Initial Reactions in Anaerobic Alkane Degradation by a Sulfate Reducer, Strain AK-01. Appl. Environ. Microb. **65:**5532-5540.

66. **Spring, S., C. Scheuner, A. L. Lapidus, S. Lucas, T. Glavina Del Rio, H. Tice, A. Copelane, J.-F. Cheng, F. Chen, M. Nolan, E. Saunders, S. Pitluck, K. Liolios, N. Ivanova, K. Mavromatis, A. Lykdis, A. Pati, A. Chen, K. Palaniappan, M. Land, L. Hauser, Y.-J. Chang, C. D. Jeffries, L. Goodwin, J. C. Detter, T. Brettin, M. Rohde, M. Goeker, T. Woyke, J. Bristow, J. A. Elsen, V. Markowitz, P. Hugenholtz, N. C. Kyrpides, and H.-P. Kienk.** 2010. The genome sequence of *Methanohalophilus mahii* SLPT reveals differences in the energy metabolism among members of the *Methanosarcinaceae* Inhabiting freshwater and saline environments. Archaea **2010:**16 pages.

67. **Suflita, J. M., I. A. Davidova, L. M. Gieg, M. A. Nanny, and R. C. Prince.** 2004. Anaerobic hydrocarbon biodegradation and the prospects for microbial enhanced energy production p. 283-306. *In* R. Vazquez-Duhalt and R. Quintero-Ramirez (ed.), Petroleum Biotechnology, Developments and Perspectives. Studies of Surface Science and Catalysis, vol. 151. Elsevier Science.

68. **Tanner, R. S.** 1997. Cultivation of bacteria and fungi, p. 52-60. *In* C. J. Hurst, G. R. Knudsen, M. J. McInerney, L. D. Stetzenbch, and M. V. Walter (ed.), Manual of Environmental Microbiology. American Society for Microbiology, Washington D.C.

69. **Townsend, G. T., R. C. Prince, and J. M. Suflita.** 2003. Anaerobic oxidation of crude oil hydrocarbons by the resident microorganimss of a contaminted anoxic aquifer. Environ. Sci. Technol. **37:**5213-5218.

70. **Whiticar, M.** 1999. Carbon and hydrogen isotope systematics of bacterial formation and oxidation of methane. Chem. Geol. **161:**291-314.

71. **Whiticar, M. J.** 1994. Correlation of natural gases with their sources, p. 261-283. *In* L. B. Magoon and W. G. Dow (ed.), The Petroleum System from Source to Trap. AAPG Memoir 60.

72. **Widdel, F., A. Boetius, and R. Rabus.** 2006. Anaerobic Biodegradation of Hydrocarbons Including Methane, p. 1028-1049. *In* M. Dworkin, S. Falkow, E. Rosenberg, K.-H. Schleifer, and E. Stackebrandt (ed.), The

Prokaryotes, vol. Vol 2: Ecophysiology and Biochemistry. Springer, New York.

73. **Widdel, F., and O. Grundmann.** 2010. Biochemistry of the anaerobic degradation of non-methane alkanes, p. 909-924. *In* K. N. Timmis, T. McGenity, J. R. van der Meer, and V. de Lorenzo (ed.), Handbook of Hydrocarbon and Lipid Microbiology. Springer-Verlag, Berlin.

74. **Zedelius, J., R. Rabus, O. Grundmann, I. Werner, D. Brodkorb, F. Schreiber, P. Ehrenreich, A. Behrends, H. Wilkes, M. Kube, R. Reinhardt, and F. Widdel.** 2011. Alkane degradation under anoxic conditions by a nitrate-reducing bacterium with possible involvement of the electron acceptor in substrate activation. Environmental Microbiology Reports **3:**125-135.

75. **Zengler, K., H. H. Richnow, R. Rossello-Mora, W. Michaelis, and F. Widdel.** 1999. Methane formation from long-chain alkanes by anerobic microorganisms. Nature **401:**266-269.

76. **Zinder, S. H.** 1993. Physiological ecology of methanogens, p. 128-208. *In* J. G. Ferry (ed.), Methanogenesis. Ecology, Physiology, Biochemistry and Genetics. Chapman & Hall, New York.

Table 1. Relative isotope abundance (RIA) of select proteins.

Sample	GI number	protein name (organism)	peptide sequence	charge	molecular formula	m/z ^{12}C		RIA (%)
Oil - Palmitate	126178507	5,10-methylenetetrahydromethanopterin reductase	AVLGIGPGDLSTLPK	+2	$C_{65}H_{114}N_{16}O_{20}$	718.9176		77.1
			GIPVYIGAQGPK	+2	$C_{56}H_{92}N_{14}O_{15}$	599.8408		72.2
			LLAGEEVKK	+2	$C_{44}H_{81}N_{11}O_{14}$	493.2949		81.3
			LLAGEEVK	+2	$C_{38}H_{69}N_9O_{13}$	429.2474		81.4
		(*Methanoculleus marisnigri* JR1)					protein avg.	78.0 ± 4.4
Oil - Palmitate	116754497	acetyl-CoA synthetase (AMP-forming)	DKDGYWWIQGR	+2	$C_{66}H_{92}N_{18}O_{18}$	711.8392		73.0
			TPWPSMLR	+2	$C_{45}H_{72}N_{12}O_{11}S$	493.7550		74.4
		(*Methanosaeta thermophila* PT)					protein avg.	73.3 ± 1.0
Oil - Palmitate	88603420	tetrahydromethanopterin S-methyltransferase, subunit A	VIANVISNPNIR	+2	$C_{57}H_{102}N_{18}O_{17}$	654.8798		68.9
		(*Methanospirillum hungatei* JF-1)					protein avg.	*n.a.*
Oil - Palmitate	116753885	methyl-coenzyme M reductase, beta subunit	SDKIDIYSDR	+2	$C_{51}H_{84}N_{14}O_{20}$	605.7963		77.4
			QLLVQIPSAR	+2	$C_{50}H_{91}N_{15}O_{14}$	562.3406		80.8
		(*Methanosaeta thermophila* PT)					protein avg.	79.1 ± 2.4
Oil - Stearate	219849222	primosome, DnaD subunit	WAANGR	+2	$C_{29}H_{45}N_{11}O_8$	336.8612		63.1
		(*Chloroflexus aggregans* DSM 9485)					protein avg.	*n.a.*

Oil-free Stearate	88603394	methyl-coenzyme M reductase, gamma subunit (*Methanospirillum hungatei* JF-1)	LAEDGMMFDMLQR	+2	$C_{65}H_{107}N_{17}O_{21}S_3$	778.3406		58.9
			IVTPTDGAK	+2	$C_{39}H_{70}N_{10}O_{14}$	450.7469		59.8
							protein avg.	59.4 ± 0.6
Oil-free Stearate	126178564	methyl-coenzyme M reductase, gamma subunit (*Methanoculleus marisnigri* JR1)	LAENGMMFDMLQR	+2	$C_{65}H_{108}N_{18}O_{20}S_3$	777.8511		58.5
			SVLGEDGIVR	+2	$C_{44}H_{79}N_{13}O_{16}$	522.2814		61.9
			NQIGEPLDR	+2	$C_{43}H_{74}N_{14}O_{16}$	520.5572		56.5
							protein avg.	59.0 ± 2.7
Oil-free Stearate	116754898	Na-transporting two-sector ATPase (*Methanosaeta thermophila* PT)	TVmQQTLSK	+2	$C_{43}H_{80}N_{12}O_{15}S$	517.6123		59.4
			SIVYANTSNMPVAAR	+2	$C_{68}H_{114}N_{20}O_{22}S$	796.9029		56.2
							protein avg.	57.8 ± 2.3
Oil-free Stearate	125972667	phosphopyruvate hydratase (*Clostridium thermocellum* ATCC 27405)	VNQIGTLTETLDAIEMANR	+3	$C_{87}H_{151}N_{25}O_{32}S$	696.3520		1.2
							protein avg.	*n.a.*

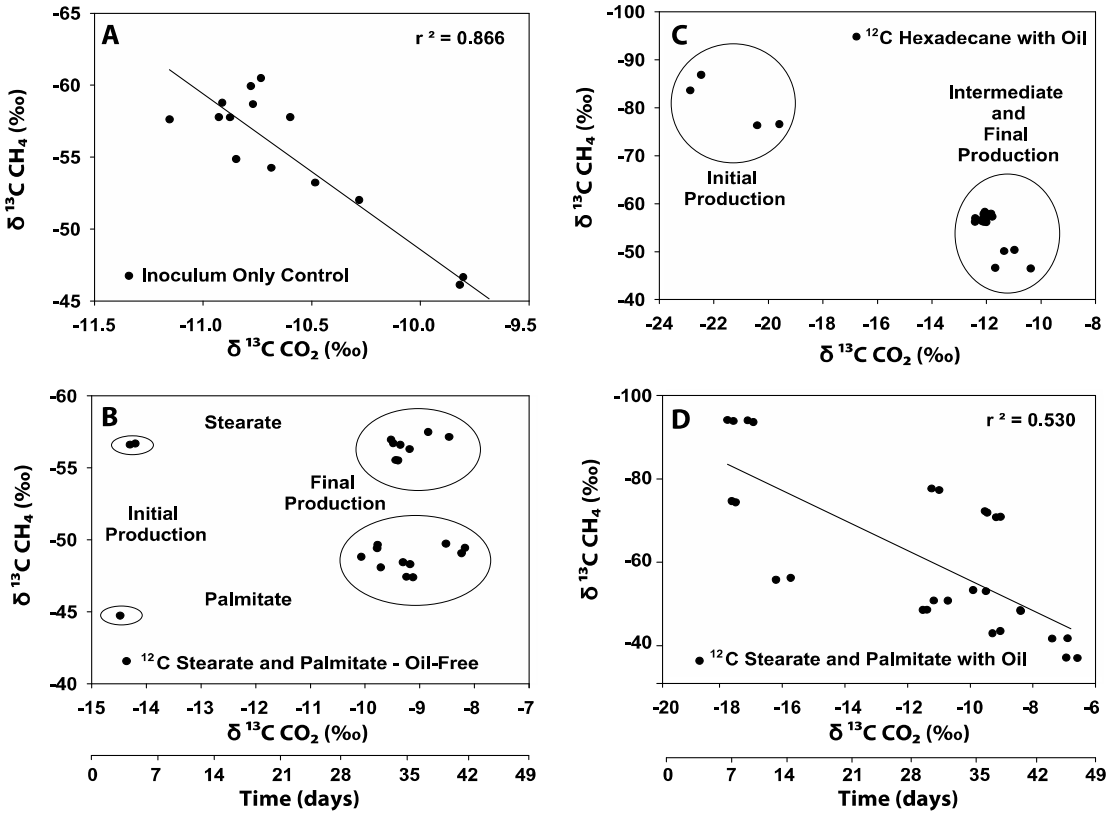

Figure 1: Plots of per mil (‰) $\delta^{13}C$ values for methane and carbon dioxide during the methanogenic degradation of fatty acids and *n*-hexadecane in the present and absence of residual oil-bearing sandstone core. All plots are shown for 49 days with primary values plotted closest to the y-axis. A) $\delta^{13}C$ (‰) of CH_4 vs. CO_2 for the inoculum only control. B) $\delta^{13}C$ (‰) of CH_4 vs. CO_2 for stearate- and palmitate-amended sterile quartz sand. C) $\delta^{13}C$ (‰) of CH_4 vs. CO_2 for hexadecane-amended residual oil-bearing core. D) $\delta^{13}C$ (‰) of CH_4 vs. CO_2 for stearate- and palmitate-amended residual oil bearing core. Coefficient of determination (R^2) values for linear regressions in boxes A and D are provided. Circles in boxes B and C represent 95% confidence intervals of the data.

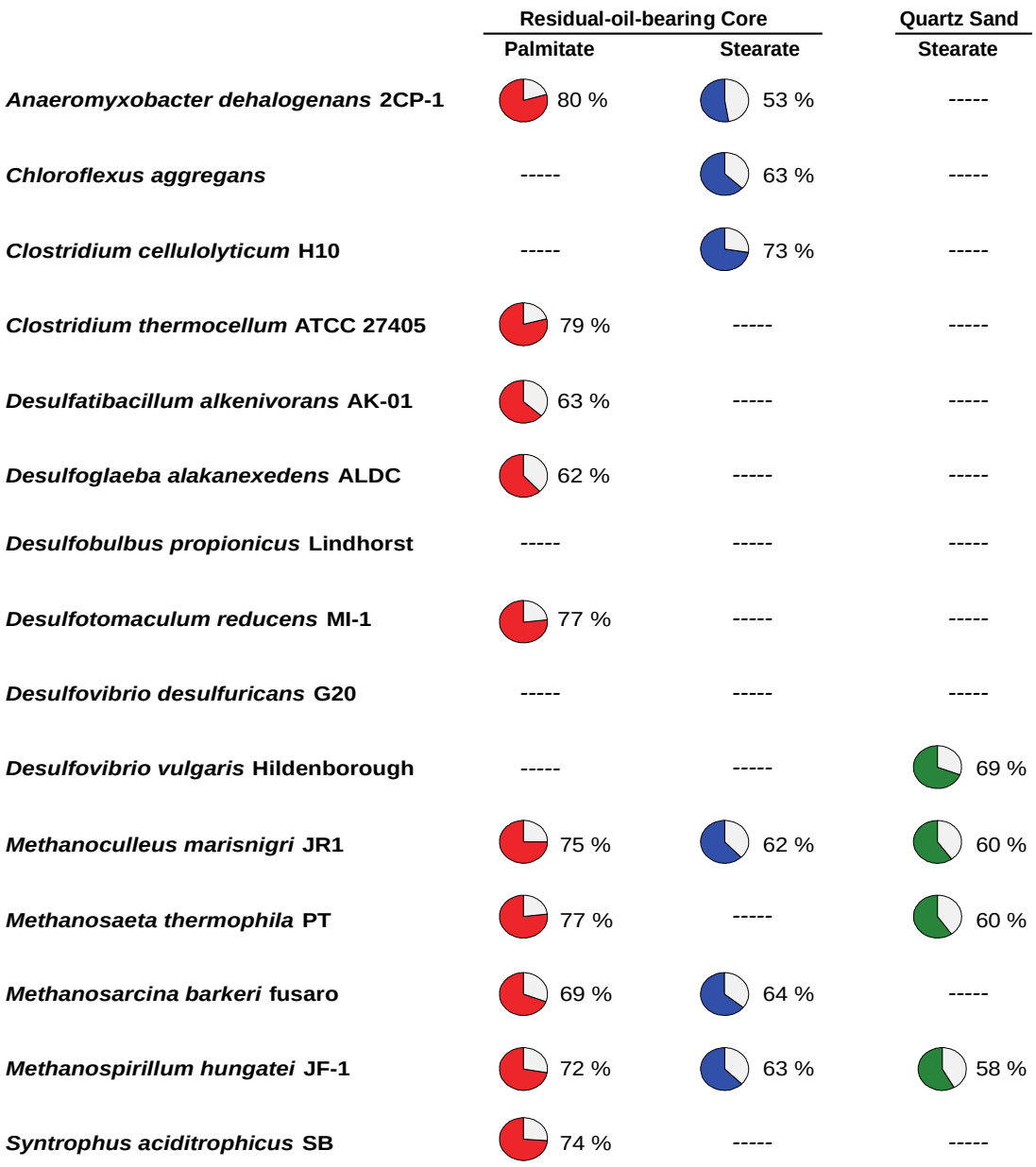

Figure 2: Incorporation of ^{13}C into the proteomes of different species in the microbial enrichment. The members of the community were previously identified from clone library analysis (33) and closest-relatives with completed genomes were used to build a metagenomic database of protein sequences for use during the proteomics portion of the study. All proteins identified for each species were grouped and a global ^{13}C incorporation value was calculated as previously described (28). The proteins yields from the palmitate-amended oil-free samples were too low and precluded analysis at appropriate significance levels.